

**Design Methodology and Experimental Investigation of a Multiple-Inlet BIPV/T System
in a Curtain Wall Facade Assembly and Roof Application**

Olesia Kruglov

A Thesis in the Department of
Building, Civil and Environmental Engineering

Presented in Partial Fulfillment of the Requirements
for the Degree of Master of Applied Science (Building Engineering) at

Concordia University
Montreal, Quebec, Canada

November 2018

© Olesia Kruglov 2018

CONCORDIA UNIVERSITY

CONCORDIA UNIVERSITY
School of Graduate Studies

This is to certify that the thesis prepared

By: Olesia Kruglov

Entitled: Design Methodology and Experimental Investigation of a Multiple-Inlet BIPV/T System in a Curtain Wall Facade Assembly and Roof Application

and submitted in partial fulfillment of the requirements for the degree of

Magistrate of Applied Science (Building Engineering)

complies with the regulations of the University and meets the accepted standards with respect to originality and quality.

Signed by the final examining committee:

<u>Dr. Ashutosh Bagchi</u>	Chair
<u>Dr. Andreas K. Athienitis</u>	Supervisor
<u>Dr. Hua Ge</u>	Supervisor
<u>Dr. Pragasen Pillay</u>	Examiner (External)
<u>Dr. Bruno Lee</u>	Examiner
<u>Dr. Ashutosh Bagchi</u>	Examiner

Approved by _____

Chair of Department or Graduate Program Director

Dean, Department of Building, Civil and Environmental Engineering

Date _____

Design Methodology and Experimental Investigation of a Multiple-Inlet BIPV/T System in a Curtain Wall Facade Assembly and Roof Application

Building-integrated photovoltaic (BIPV) technologies are becoming a competitive alternative to traditional claddings as the building industry looks toward renewables for local energy sources. An advancement of the BIPV is the building-integrated photovoltaic/thermal (BIPV/T) system, which harvests excess heat produced by the photovoltaic panels and transfers it to a medium for useful energy. For application on large scale facades, air-based BIPV/T systems can be used in low temperature applications. However, due to a lack of installation and maintenance guidelines as well as insufficient performance standardization, both technologies have yet to experience widespread implementation. Additionally, tools for determining potential energy generation during the early design phase are complex and not readily available.

This thesis provides a discussion, analysis and comparison of recent advancements in BIPV and BIPV/T systems in order to assess architectural and energy performance considerations for full facade integration. A BIPV/T design methodology was developed based on the investigation of three novel case studies involving both roof and facade applications. Issues of constructability, building envelope requirements, material compatibility, and maintenance were addressed. Subsequently, guidelines for a BIPV/T performance standard were suggested.

Linking this research to the established criteria of current building practices, a BIPV/T prototype was constructed, adopting a conventional curtain wall frame. Base characterization testing was conducted at the Solar Simulator and Environmental Chamber (SSEC) testing facility at Concordia University to assess the prototype's electrical and thermal performance. Three different flow rates, the use of single or multiple inlets, and two different transparencies of photovoltaic modules were investigated for their effect on system performance. Results from the preliminary testing showed that the use of multiple inlets may increase the thermal output by up to 18%, decrease the peak photovoltaic (PV) temperatures by up to 3°C, and marginally increase the electrical output. While the experiments were a first step in confirming prototype functionality and for model verification purposes, there is a need to further explore the optimization of this design and its application on building typologies through simulation.

Acknowledgements

I would like to thank my supervisor, Dr. Andreas Athienitis, for the unique opportunities he has provided me with and for showing me the significance of interdisciplinary collaboration. I am also grateful for the guidance and support of my co-supervisor, Dr. Hua Ge.

This work is part of the research under the Center for Zero Energy Buildings, and I would like to thank all of my talented colleagues who comprise this organization. I would like to thank Dr. Bruno Lee and his students for their collaboration on multiple projects throughout the years. I am especially grateful to Stratos Rounis, who has taught me so much and who has been my design and execution partner in most of the projects I have worked on during my time here. Thank you also to Vasken Dermardiros and Harry Vallianos for your valuable input on my work and your encouragement when I needed it most.

I would like to acknowledge the financial support from the Hydro-Quebec Industrial Research Chair, the Department of Building, Civil and Environmental Engineering at Concordia University and the IC-Impacts Research Center of Excellence. The scholarship awarded by the Power Corporation of Canada was much appreciated. Special thanks to Samuel Doyon-Bissonnette and Unicel Architectural for their collaboration to fabricate a prototype and for being attentive to our research needs.

Thank you, Dr. Jiwu Rao and Jaime Yeargans, for your time and resourcefulness during the experimental work and setup. Thank you, Lyne Dee, for your patience, and to the rest of the administrative team at the department.

I would like to thank my family and friends for their love and steadfast support from near and far, and to the late Wagdy Anis, without whom perhaps I may not have taken this journey.

List of Figures	vii
List of Tables	x
Nomenclature	xi
Symbols	xi
Abbreviations and Acronyms	xii
1. Introduction	1
1.1 Background.....	1
1.2 Problem Statement.....	4
1.3 Objectives	5
1.4 Overview	6
2. Literature Review and Comparative Analysis of Technologies.....	7
2.1 Background.....	7
2.2 BIPV Overview	10
2.3 BIPV/T Overview	13
2.4 Facade design	23
2.5 Integration with the facade	24
2.6 Existing Standards	31
2.7 Conclusions	34
3. Design Case Studies and a Methodology for BIPV/T.....	37
3.1 Introduction	37
3.2 Courthouse Building BIPV/T Facade.....	38
3.3 Solar Decathlon BIPV/T Roof.....	49
3.4 BIPV/T Roof Retrofits for Residential Low-Rises in India	53
3.5 Key Elements of Case Studies.....	62

3.6 Design Methodology	64
4. Multiple-Inlet BIPV/T Curtain Wall Prototype Development	70
4.1 Design Development	70
4.2 Construction.....	73
5. Experimental Testing In a Solar Simulator and Comparison with Model Predictions.....	76
5.1 Experimental Setup.....	76
5.2 Scope of Experiments	80
5.3 Experimental Results.....	83
6. Conclusion	90
6.1 Contributions	91
6.2 Recommended future work	92
References.....	94
Appendix A: Electrical, Solar Thermal and Building Standards	103
Appendix B: Photographs of Prototype Construction	108
Appendix C: Product Specification Sheets.....	110
Appendix D: Results of Experimental Work.....	113
Appendix E: Measurement Uncertainties	117

List of Figures

Figure 1.1: BIPV roof application (left) and solar collectors on the Meusburger Production Hall in Austria (right) (Weller et al. 2010; Zhang et al. 2015)	2
Figure 1.2: Solar energy distribution in BIPV/T system (Bambara 2012)	3
Figure 1.3: Global LCOE from utility-scale renewable power generation technologies, 2010 to 2017 (“Renewable Power Generation Costs in 2017” 2018).....	4
Figure 2.1: BIPV, STPV, BIPV/T (air based), and BIPV/T (water based) schematics (A. Athienitis et al. 2015)	8
Figure 2.2: Installed BAPV system (C. Peng, Huang, and Wu 2011).....	8
Figure 2.3: Layers of a PV module (Blieske and Stollwerck 2013)	9
Figure 2.4: STPV skylight (“Skylight with Transparent Photovoltaic Glass” 2018)	10
Figure 2.5: Diagram of an active air-based BIPV/T roof (Candanedo et al. 2010).....	16
Figure 2.6: Ecoterra house (Chen, Athienitis, and Galal 2010).....	18
Figure 2.7: Wood sub-framing for roof at factory (left) and BIPV/T finished module on-site (right) (Chen, Athienitis, and Galal 2010)	19
Figure 2.8: The BIPV/T roof of the Varennes library in Varennes, Quebec	19
Figure 2.9: The Varennes roof by type of BIPV. The naturally ventilated portion (yellow) has an air channel depth of 150mm, while the forced-fan vented portion (blue and green) has an air channel depth of 70 mm.....	20
Figure 2.10: BIPV/T facade on the JMSB building (left) and PV/UTC components in a concept diagram (right) (A. K. Athienitis et al. 2010)	21
Figure 2.11: Custom PV modules attached over UTC (left) and section diagram showing modules attached at top edge to horizontally corrugated UTC panels (right) (A. K. Athienitis et al. 2010)	22
Figure 3.1: Multiple-inlet BIPV/T concept.....	38
Figure 3.2: Stick built CW (left) and Unitized CW (right).....	39
Figure 3.3: Stick-built CW installation sequence (Rendering by S. Rounis)	40
Figure 3.4: Existing facade (left) and sample of unitized CW layout for re-clad (right)	41
Figure 3.5: South elevation with penthouse area in red box (left) and suggested module layout (right)	44

Figure 3.6: Module dimensions (“Solar Panel CS6X-P - Canadian Solar” 2018).....	44
Figure 3.7: STPV used as modules (left) and rendering of STPV and painted backpan (right)...	45
Figure 3.8: Structural attachment of the BIPV/T system (left) and horizontal tie-backs at inlet framing (right).....	46
Figure 3.9: Unit distribution for unitized system (left) and typical unitized details for the BIPV/T (right)	47
Figure 3.10: Components of a unit in a unitized system (left) and unit and horizontal cap prior to install (right).....	47
Figure 3.11: Actual south facade (left) and visualization of BIPV/T cladding at penthouse level of the facade (right).....	49
Figure 3.12: Configuration options for Decathlon roof and render of optimal design	50
Figure 3.13: Section through BIPV/T roof and skylight.....	51
Figure 3.14: Architectural details of the BIPV/T framing system.....	51
Figure 3.15: Exploded axonometric diagram of BIPV/T system layers and materials	52
Figure 3.16: Deep Performance Dwelling aerial view (left) and BIPV/T roof after completion (right) (Efstratios Dimitrios Rounis et al. 2017).....	53
Figure 3.17: Roof retrofit as solarium.....	54
Figure 3.18: Radiation and temperature maps of Chennai, India (“Global Solar Atlas” 2018) ...	55
Figure 3.19: Monthly averages for air temperatures in Chennai, India	56
Figure 3.20: Monthly total for GHI (left) and percentage of sky covered by clouds (right)	56
Figure 3.21: Building typologies in the state of Tamil Nadu (National Disaster Management Authority 2013).....	57
Figure 3.22: Building schematic and specific envelope properties (BEEP 2016).....	58
Figure 3.23: Various rooftop PV layouts and total coverage of BIPV/T system	58
Figure 3.24: Size of BIPV/T rooftop system	59
Figure 3.25: Available area under BIPV/T system for mechanical equipment	60
Figure 3.26: BIPV/T Plan view (left) and section through the system, framing and building structure (right)	60
Figure 3.27: Monthly electrical and thermal energy production for BIPV/T System 1	61
Figure 3.28: Air outlet temperature occurrence frequencies of the BIPV/T throughout the annual period, on an hourly basis	61

Figure 3.29: Thermal network diagram of a BIPV/T system in section (STPV option is possible) (T. Yang and Athienitis 2015)	67
Figure 3.30: Multiple-inlet CW BIPV/T system.....	69
Figure 4.1: Features of final prototype design include CW framing, multiple inlets and a metal extrusion for directing the air flow	71
Figure 4.2: Architectural elevation of prototype with final dimensions (left) and renderings of the metal extrusion at the middle air inlet (right)	72
Figure 4.3: 66-cell module with a 20% transparency (left) and 72-cell module with a 12% transparency (right).....	73
Figure 4.4: Openings for the manifold.....	74
Figure 4.5: Details of constructed prototype.....	75
Figure 5.1: Solar simulation laboratory (Left) and vertical position of prototype during testing (right) (“Labs & Equipment - Centre for Zero Energy Building Studies” 2018)	78
Figure 5.2: Location of thermocouples shown in elevation (left) and four sections (right)	78
Figure 5.3: Thermocouple setup inside of BIPV/T air cavity.....	78
Figure 5.4: Thermocouple heights in channel (left) and attachment method (right)	79
Figure 5.5: Photograph (left) and infrared images of prototype. The photo in the center shows a test in progress for the 72-cell, single-inlet configuration with a flow rate of 0.11 kg/s. The photo on the right shows a test in progress for the 66-cell, double-inlet configuration with a flow rate of 0.17 kg/s.....	86
Figure 5.6: Summary results for 66-cell (left) and 72-cell (right) configurations at NOCT conditions.....	89
Figure 6.1: Vertical manifold configuration that was tested (left) and horizontal manifold configuration as a future testing option (right)	92
Figure 6.2: BIPV/T prototype as part of a facade on an enclosed test hut for thermal testing.....	93

List of Tables

Table 2.1: Projects with installed BIPV	11
Table 2.2: BIPV related standards	33
Table 3.1: Advantages and disadvantages of CW systems.....	42
Table 3.2: Advantages and disadvantages of framed vs. frameless modules	43
Table 3.3: Summary of Case Studies	68
Table 3.4: Standards related to BIPV/T performance.....	68
Table 5.1: Details of the Instruments Used for Measurements.....	79
Table 5.2: Reynolds numbers for varying air flow rates inside of the air channel	81
Table 5.3: CHTC values for varying air flow rates inside of the channel at NOCT for the 72-cell single-inlet configuration	82
Table 5.4: Physical configurations of the prototype for testing.....	82
Table 5.5: Thermal efficiency of the BIPV/T prototype.....	85
Table 5.6: Air temperature rise within BIPV/T prototype air channel	86
Table 5.7: Maximum PV temperatures of the BIPV/T prototype.....	87
Table 5.8: Electrical efficiency of the BIPV/T prototype.....	88
Table A.1: PV/Electrical standards by issuing committee.....	103
Table A.2: Solar thermal standards by issuing committee	104
Table A.3: Building standards by issuing committee	104

Nomenclature

Symbols

A	Total surface area of the collector (m^2)
β_{PV}	PV module temperature coefficient ($0.45\%/^{\circ}C$)
c_p	Specific heat of the air ($J/kg^{\circ}C$)
E_{el}	Electrical power produced by the PVs (W)
G	Solar radiation (W/m^2)
\dot{m}	Mass flow rate of the air (kg/s)
η_{el}	PV electrical efficiency (%)
η_{stc}	PV electrical efficiency under standard testing conditions (%)
η_{th}	Thermal efficiency of the collector (%)
Q_{air}	Thermal energy of the air exiting the collector (W)
T_i	Temperature of the air at the inlet ($^{\circ}C$)
T_o	Temperature of the air at the outlet ($^{\circ}C$)
$T_{PV,S}$	Surface temperature of the PV ($^{\circ}C$)
T_{ref}	PV reference temperature ($^{\circ}C$)

Abbreviations and Acronyms

AC	Alternating current
ASHP	Air source heat pump
ASTM	American Society of Testing and Materials
BIPV	Building-integrated photovoltaic
BIPV/T	Building-integrated photovoltaic/thermal
BIST	Building-integrated solar thermal
COP	Coefficient of performance
CW	Curtain wall
DC	Direct current
EIFS	Exterior insulation and finish system
EN	European Standard
EPT	Energy payback time
EVA	Ethyl vinyl acetate
FF	Fill factor
GSHP	Ground source heat pump
HVAC	Heating, ventilation, and air conditioning
IEA	International Energy Agency
IEC	International Electrotechnical Commission
IR	Infrared
ISO	International Organization for Standardization
JMSB	John Molson School of Business

NFRC	National Fenestration Rating Council
NOCT	Nominal Operating Cell Temperature
PV	Photovoltaic
PV/T	Photovoltaic/thermal
PVB	Polyvinyl butyral
SHGC	Solar heat gain coefficient
SRCC	Solar Rating and Certification Corporation
SSEC	Solar Simulator and Environmental Chamber
SSG	Structural silicone glazed
STC	Standard testing conditions
STPV	Semi-transparent photovoltaic
UL	Underwriters Laboratories
UTC	Unglazed Transpired Collector
UV	Ultraviolet

Chapter 1

Introduction

1.1 Background

The building sector is currently responsible for more than 30% of the global energy consumption. Half of it is used for space heating and provided primarily by fossil fuels (IEA, 2017). To meet an emission trajectory that would limit the global temperature increase to 2°C by 2025, also known as the 2°C Scenario or 2DS, the International Energy Agency suggests a 32% increase in heat generation from renewable sources, which can be largely achieved with solar thermal heating (IEA, 2017).

Throughout history, facades have always been designed with the intent of making a statement about the building, influenced by status and symbolism. In the modern day, some architects choose to design it with traditional materials as a stance against submersion into the digital world (Farkas et al., 2009). Others take advantage of this and design facades that are illuminated or are a result of parametric modeling, showing complex forms and textures. However, a high-performing building envelope is a necessary feature, regardless of the statement. As the building sector moves away from fossil fuel use, the incorporation of solar technologies into the enclosure is an innovative solution to on-site renewable energy generation. Conscientious in its nature, this method of design also places priority on a high quality building envelope.

Every year, the earth receives 1.53×10^{18} KWh of solar radiation onto the surface of the atmosphere, or 1367 W/m^2 , making the sun the most abundant of all available energy sources on our planet (Reinhart, 2014). The world consumes energy at a rate much lower than this, averaging 1.57×10^{14} KWh a year. Systems that convert solar energy from the sun into electricity (photovoltaics, or PV) as well as heat (solar thermal technologies) are expected to hold the largest share of renewable energy production. It is predicted that by 2050, the PV electricity generation will be close in cost to that of conventional power (Peng et al., 2011). Facing space restriction and competition for land coverage against other industries such as agriculture, ground-mounted PV arrays have their own set of challenges. Current practices for PV applications directly on buildings include primarily racked roof systems, as well as building-integrated photovoltaics (BIPV). Solar

thermal technologies include collectors on roofs and unglazed transpired collector (UTC) walls. BIPV and solar thermal applications are shown in Figure 1.1.



Figure 1.1: BIPV roof application (left) and solar collectors on the Meusburger Production Hall in Austria (right) (Weller et al., 2010; Zhang et al., 2015)

When a typical crystalline photovoltaic panel receives energy from the sun in the form of radiation, approximately 15-20% of that is converted to electricity, another 5-10% is reflected, (this value is usually lower due to antireflective coatings) and the remaining 75-80% or so is converted to heat. This excess heat leads to degradation of the PV module, decreasing electrical efficiency by up to 0.53%/°C (varying by PV technology) and causing thermal stresses (Athienitis et al., 2015; Chow, 2010). PV panels should maintain low operating temperatures, (generally lower than 70°C) prioritizing the high quality energy generation of electricity (Tonui and Tripanagnostopoulos, 2006).

A building-integrated photovoltaic/thermal (BIPV/T) system combines production of electricity from the PV modules while removing much of the absorbed heat and directing it towards the building where it can be used, for example, to pre-heat the fresh air intake. Air, water or a glycol solution is typically used as the heat transfer fluid, and the concept of the system is derived from solar thermal collector technologies. As shown in Figure 1.2, for an incoming solar radiation level of 1000 W/m² incident on the outer face of the system, 10% (or 100 W/m²) is reflected, 15% (or 150 W/m²) is converted to electricity, giving the PV modules an electrical efficiency of 0.15, another 20% is lost to the interior and exterior from heat transfer, and the remaining 55% (or 550 W/m²) is collected as thermal energy. It should be noted that this is an optimistic scenario, and actual recovered heat is more typically in the range of 15% to 25%.

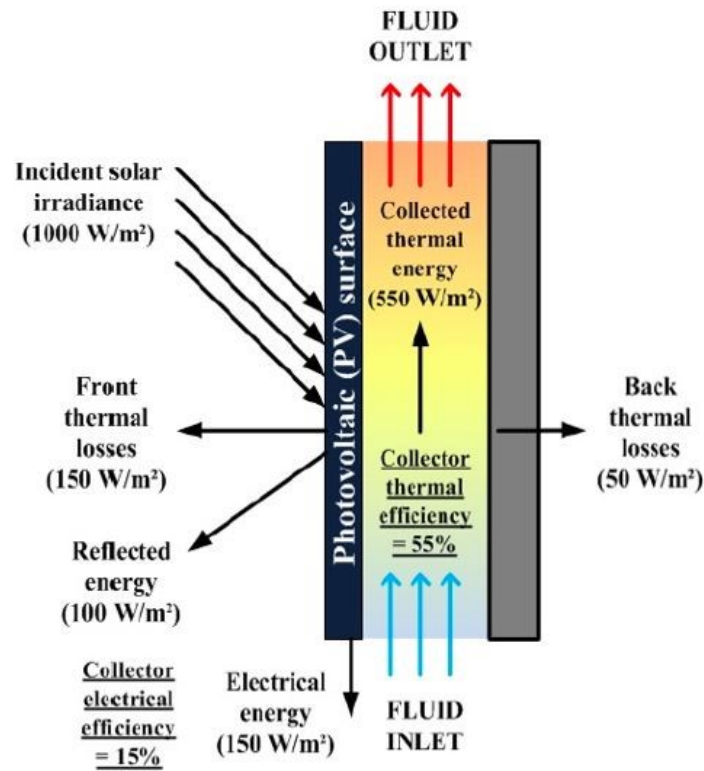


Figure 1.2: Solar energy distribution in BIPV/T system (Bambara, 2012)

Unfortunately, facade-integrated BIPV applications are much less prevalent in today's market of PV systems installed directly on buildings. Aside from roof PV racks, the actual integration of BIPV and BIPV/T systems still has many barriers. In the architectural world, smart, energy-efficient buildings play a large role in the contemporary and future designs, but deliberate and methodical BIPV design is not at the forefront of this movement. PV products are not developed with a consideration of social, cultural and aesthetic issues, resulting in their being neglected by architects and property owners (Farkas et al., 2009). Design and construction guidelines for both BIPV and BIPV/T are not fully established, and there do not exist any standards which address the dual nature of the BIPV/T as both a building envelope component and a PV system. Many of these solar technologies are developed one unique project at a time, and therefore primarily have custom building applications, hindering their use on a wider scale.

1.2 Problem Statement

The price of PV modules have been dropping following an exponential trend. In Renewable Power Generation Costs in 2017, a report published by the International Renewable Energy Agency (IRENA), the cost of PV electricity has dropped 73% since 2010, and now has a levelised cost of electricity (LCOE) of 0.10 USD per kWh with that of fossil fuels ranging from 0.05 USD to 0.17 USD (Figure 1.3).

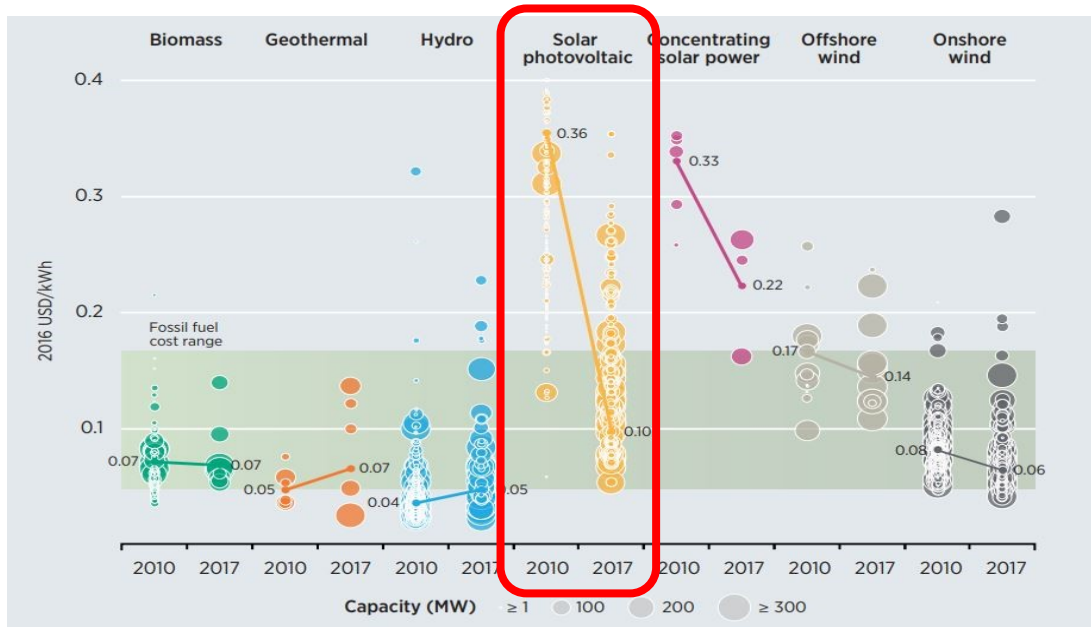


Figure 1.3: Global LCOE from utility-scale renewable power generation technologies, 2010 to 2017 (IRENA, 2018).

Another source, an outlook report by Bloomberg New Energy Finance, has estimated that the cost of solar has now matched that of coal in both the United States and Germany, and will do the same in India and China by 2021 (Shankleman and Warren, 2017). Global demand for PV power is predicted to be a record high of 113 GW in the year of 2018 (Hill, 2018). While still relatively uncommon compared to solar parks, BIPV systems are an established method of producing on-site electricity for buildings. With developments such as the BIPV/T, it is even possible to harvest the excess heat from the PV modules for useful energy gains, guaranteeing that they do not overheat and suffer performance loss. Research has shown advancements in optimizing the electrical and thermal performance of BIPV/T systems through comprehensive modeling and experimentation (Yang and Athienitis, 2016a).

Conventional claddings for commercial and industrial buildings, unlike PV products, do not follow a technology price trend. Some of the materials used in these assemblies have increased in price due to limited availability. The step to replace these claddings with BIPV and BIPV/T systems is an obvious one in terms of both cost and the overarching need for renewable energy production. Despite this argument, most professionals in the building industry do not readily design with PV. The reason for this is that accurate building integration is still quite undefined, especially for emerging technologies such as BIPV/T. The key to expanding the use and application of BIPV/T systems is to make them a competitive alternative to other cladding systems. In addition to providing electricity and useful heat, which has already been proven as a benefit, a BIPV/T system must outperform conventional facades in terms of thermal insulation, moisture resistance, durability, constructability and architectural options for color, texture, sizing, cost and more. With the assistance of clear guidelines and established standards, architects and builders can start designing with BIPV and BIPV/T not as an energy producing necessity, but as an architectural choice over conventional building elements, ultimately rendering them obsolete.

1.3 Objectives

This thesis aims to address the background, technological advancements, design, testing and construction of BIPV/T systems from the point of view of both architects and building envelope specialists. Based on this information, the objective is to develop an open-loop, air-based BIPV/T cladding system that uses a conventional curtain-wall design. The reason to use air as the fluid medium is that there is no leakage or freezing, and both maintenance costs and the weight of the system are significantly reduced. Open-loop systems operate at lower temperatures than closed-loop systems, improving durability and PV performance.

The system should have an optimal design for electrical and thermal performance and fulfill the requirements of a building envelope. Air-based BIPV/T systems are best suited for large, uninterrupted opaque facade areas, which are commonly found on commercial buildings. The curtain wall (CW) facade assembly is frequently seen on such building typologies and is therefore used in this design.

On a broader scale, the goal is to extend the idea of the curtain-wall BIPV/T system as an advantageous cladding choice for designers rather than presenting them with a customized feature which is primarily perceived as a source of renewable energy.

1.4 Overview

Chapter 1 provides a background on the BIPV/T concept, the problem statement and main objectives of the work, and the scope of this thesis.

Chapter 2 presents a literature review of BIPV and BIPV/T systems, focusing on information gaps related to building integration. The chapter also covers current practices and advancements in building claddings, and addresses the state of both PV and building standards. The research, experiments and projects are discussed, including architectural considerations.

Based on the findings in Chapter 2, Chapter 3 highlights the key aspects of BIPV/T system performance as well as most relevant requirements for building claddings. Based on these main points, a BIPV/T cladding design is conceived and applied to several projects at a schematic level and the early design phase. Finally, considerations for a unified standard for BIPV/T claddings are proposed.

Chapter 4 examines the design development and construction of a curtain wall BIPV/T prototype resulting from the iterations presented in Chapter 3. Attention is directed at the practical challenges of constructability and assembly of the cladding.

Chapter 5 documents the experimental testing of the BIPV/T prototype carried out under controlled laboratory conditions in a solar simulator. The results for the series of base characterization tests are included.

Chapter 6 summarizes the research findings, proposes guidelines for the design and construction of BIPV/T claddings, and provides recommendations for future work in this field.

Chapter 2

Literature Review and Comparative Analysis of Technologies

This chapter presents a review of BIPV and BIPV/T technologies and what is missing in terms of a systematic building integration approach. Current practices and advancements for building claddings, specifically curtain wall (CW) facades, are discussed and an overview of standards for both PVs and building enclosures is given.

2.1 Background

Systems which utilize solar radiation for the purpose of reducing energy needs in a building can be passive or active. Systems such as thermal storage walls and solar chimneys do not generate energy and are used as passive solar design strategies. Active technologies generate renewable energy and include building-integrated solar thermal (BIST) systems, building-integrated photovoltaic (BIPV) systems, and building-integrated photovoltaic thermal (BIPV/T) systems (Quesada et al., 2012).

Solar thermal systems absorb and convert solar radiation to thermal energy, which can then be used for space heating or domestic hot water applications. One example is the unglazed transpired collector (UTC), which has a dark porous cladding that draws in air and heats it with the absorbed solar radiation. UTCs are well suited for preheating air for building ventilation systems, and with fan assistance can reach thermal efficiencies of 60% or more (Athienitis et al., 2010). Another developed technology is a flat plate collector, which consists of an absorber plate with tubing. The absorber receives incident radiation, converting it to thermal energy, and transfers it to a fluid medium inside the tubing (Athienitis et al., 2015).

BIPV systems generate local electricity and can be applied to any part of the building exterior, most commonly on the roof and facades. These systems have multiple roles in that they also replace the cladding components, becoming the barrier between the interior space and outdoor environment. When a BIPV application also has solar thermal functionality, it is considered as a BIPV/T. A system that has some transparency and allows light to pass through is called semi-transparent PV (STPV). Figure 2.1 shows schematics of these technologies.

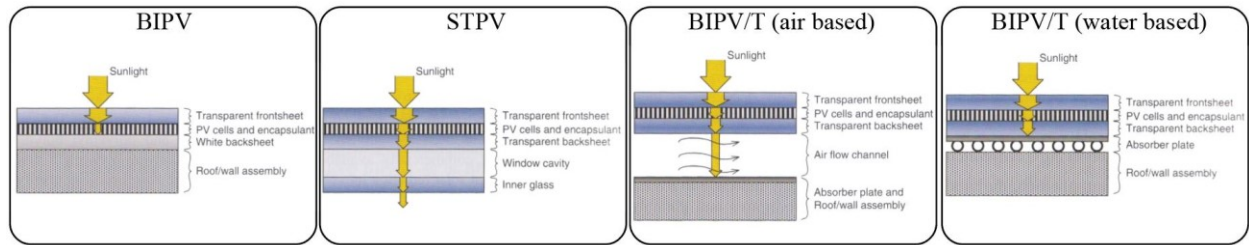


Figure 2.1: BIPV, STPV, BIPV/T (air based), and BIPV/T (water based) schematics (Athienitis et al., 2015)

Building-applied PV (BAPV) systems are similar to the BIPV concept in that they are also located on a building, but they do not replace the envelope or structural components. Instead, they are usually installed with typical framing that is used for conventional modules, most commonly as rack-mounted arrays (Figure 2.2). The framing is mechanically fastened to the structural members of the roof, creating perforations in the building envelope if needed. In comparison to BIPV, BAPV systems are redundant by design and have the sole purpose of producing electricity. They will not be discussed in this study.



Figure 2.2: Installed BAPV system (Peng et al., 2011)

2.1.1 Photovoltaic Technology

Silicon is the most common material used to make PV cells. It is processed with phosphorous and boron, which are semi-conductors. Light arriving from the sun in the form of solar radiation frees the electrons in these charged materials, allowing them to flow from the negative phosphorous to the positive boron. This produces a current, which is then harvested using a metal grid that covers the cell.

Of the materials to make PV cells, monocrystalline, polycrystalline and amorphous silicon is more popular than materials such as gallium arsenide (GaAs), cadmium telluride (CdTe), copper indium diselenide (CIS) and copper indium gallium selenide (CIGS). Monocrystalline silicon cells, made from the purest silicon, have the highest efficiency but are also high in cost. Polycrystalline cells, like monocrystalline, are categorized as wafer-based PV technologies (as opposed to amorphous and the non-silicon materials previously mentioned, all of which are thin-film), but are lower in price. Thin-film PVs were expected to increase in production, however wafer-based technologies were 92% of total PV production in 2014 (Scognamiglio, 2017). PV cells are connected in series to form strings, and a PV module usually has several rows of them. When the strings are connected in parallel, they form arrays. These arrays transfer the electricity to components which convert it from DC to AC electricity (Jelle et al., 2012).

A PV module consists of cells sandwiched between layers to protect them from the external environment. At the front, or the side directly facing the sun, and therefore exposed to the outdoors, there is a highly transparent cover made of glass or polymer. The back layer, or interior layer, is typically a polymer, but glass is also used (Figure 2.3). Between the cells and the front and backsheet is a material which acts as the direct encapsulant, typically ethylene vinyl acetate (EVA). The complete layered system is often held together at the perimeter with an aluminum frame for structural strength to resist snow and other loads and to reduce deflection that may cause cell cracks.

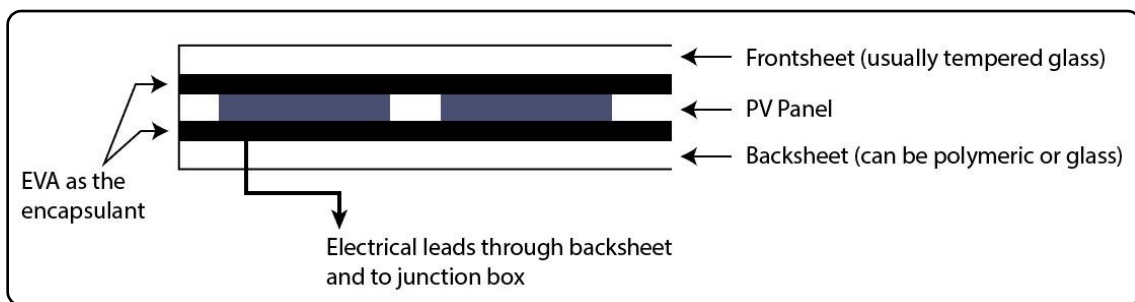


Figure 2.3: Layers of a PV module (Blieske and Stollwerck, 2013)

Warranties for PVs vary by manufacturer and range from 10 to 25 years for approximately 90% to 80% of the original energy output (Jelle et al., 2012). In terms of durability, tests conducted on 25-year-old modules showed that they were supplying 75% of their original output, even though they had visible signs of ageing (browning effects, cell corrosion). The annual average degradation

is less than 0.5% (Melorose et al., 2015). PVs can last well beyond 25 years, but rapid deployment of new and improved technologies in the market make evaluation of their use beyond this duration irrelevant.

One of the most important factors that affects the performance of PV technologies is the PV cell temperature. The electrical efficiency of the modules decreases as the cell temperature increases, and this can be as much as -0.53% for a change of 1°C. This means that a temperature increase of a PV module by 20°C can reduce the electrical production by 10% (Athienitis et al., 2015).

2.2 BIPV Overview

BIPVs function as both the outer layer and weather barrier of the building enclosure, as well as an energy generating device, reducing the cost of cladding material and labor as well as the electricity needs of the building. Considered a key factor in the future success of PV technology development, there are four main options for building integration with opaque modules: sloped roofs, flat roofs, facades, and shading systems (Jelle et al., 2012). Semi-transparent PV (STPV) and transparent PV technologies are a developing field and are gaining attention in the field of fenestration. Most commonly, STPV modules consist of opaque PV cells spaced apart to allow a fraction of the solar radiation to pass through, making them especially useful where reduced or filtered sunlight is desired. Replacing a glazing product that is fritted or tinted, STPVs can reduce solar heat gain while producing electricity (Kapsis, 2016). STPV technologies can be applied to windows, curtain walls and skylights (Figure 2.4). There are also thin film technologies that have been developed for transparent STPV applications but they have much lower efficiencies than opaque ones.

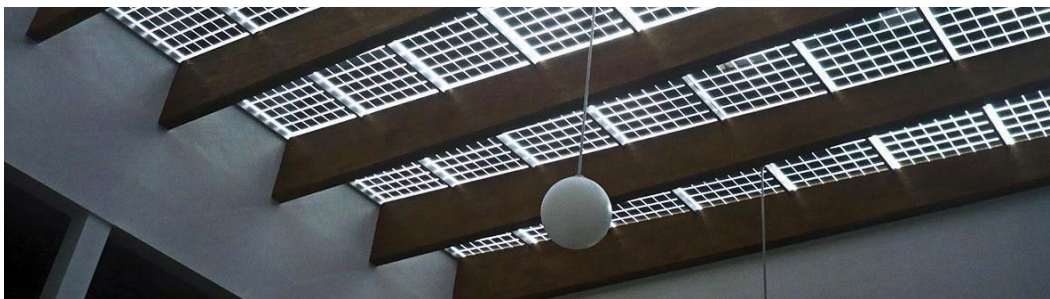




Figure 2.4: STPV skylight (“Skylight with Transparent Photovoltaic Glass,” n.d.)

The available BIPV products are typically categorized as tiles, foils, modules and glazings. Most module products are used for facades, while foils and tiles are more popular as roof applications due to their light weight and flexibility. Tiles can be arranged to resemble standard roofing tiles, and can therefore be a good option for retrofits. Many are premade and assembled with insulation (Jelle et al., 2012).

A less obvious but critical benefit of BIPV installations is their ability to produce electricity in a distributed manner to communities, reducing the peak energy demand from the grid (Athienitis et al., 2015). Table 2.1 shows several examples of conceptual or realized projects, which implement BIPV systems as part of their design.

Table 2.1: Projects with installed BIPV

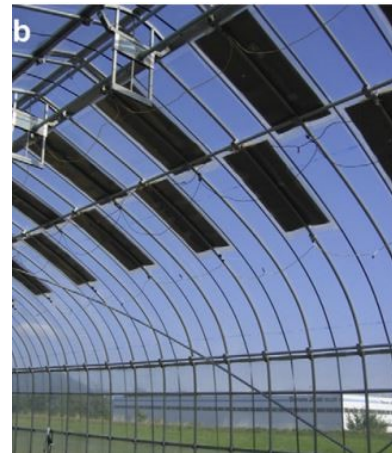
Location	Description	Image
SUNY Albany campus Albany, NY USA	A building on the SUNY Albany campus in upstate New York has the Kawneer 1600 Powerwall system with a size of 15 kWp. The Kawneer 1600 Powerwall is a variation of the traditional Kawneer 1600 CW system with the addition of amorphous silicon thin film PVs in glass laminates. A skylight version of this is the 1600 Power Slope.	
4 Times Square New York, NY USA	PV modules replace conventional spandrel glass in the south and east facades at 4 Times Square in New York City. With 4 different sizes of modules, they correspond to the spandrel sizes established earlier in the process by the architects. The Photovoltaic Manufacturing Facility located in Fairfield, CA has PV glass laminates as curtain wall spandrels, skylights and awnings (Eiffert and Kiss, 2000).	

(Eiffert and Kiss, 2000)

(Eiffert and Kiss, 2000)

Matsue, Japan

A 2010 study assessed the spatial distribution of sunlight energy in east-west oriented single-span greenhouse equipped with a PV array covering 12.9% of the roof area, which had a Gothic-arch style geometry. The checkerboard PV module arrangement improved the balance of the sunlight's spatial distribution inside of the greenhouse. The generation of electrical energy by the PV cells was an aid in producing sustainable greenhouse crop.



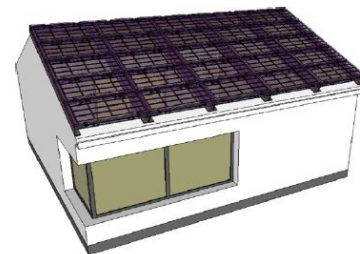
(Yano et al., 2010)

University of Almeria, Almeria, Spain

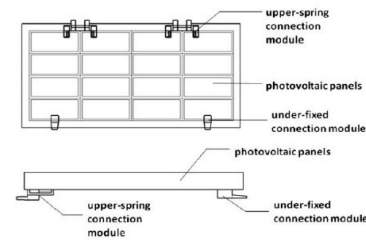
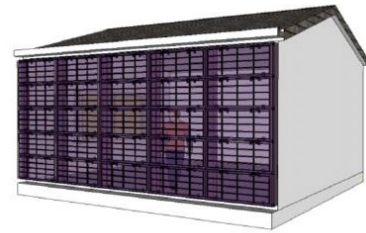
An experiment in southern Spain involved monitoring a greenhouse, which had an integrated PV system built onto it. The work confirmed the feasibility of using PV modules in cladded areas of the greenhouse as a means to assist with reduction of fossil fuel consumption for the farms in the Almeria province. By covering approximately 10% of the cladding with thin-film modules, the greenhouse produced 8.25 kWh/m² of electrical energy (Pe, 2012).

Jiangsu Province, China

A novel design is proposed by a team in China to address the shortcomings of a typical BIPV mounting system, which often consists of aluminum plates holding down the panels and intermediaries and bolts to fasten this to the existing frame or facade. The design proposed focuses on the importance of easy



replacement of the PV modules within the framing system. The figures show the facade and roof concept (top and middle) and the structural components (bottom).



(Peng et al., 2011)

2.3 BIPV/T Overview

The BIPV/T is a development of the photovoltaic/thermal (PV/T) system, which is discussed in terms of performance improvements to the thermal output.

2.3.1 PV/T Systems

On sunny days, the temperatures of PV panels can reach up to 35°C above the ambient air (Yang and Athienitis, 2012). PV/T systems collect some of the heat generated by the PV cells, maintaining them at relatively low temperatures. Using a fluid medium, part of the heat can then be recovered for various applications. In this way, the generation of electricity is combined with the application of useful heat. The concept is similar to a flat plate solar collector, except that the absorber is replaced with PV cells. PV/T systems were originally developed in the 1970s (Wolf, 1976; Florshuetz, 1979), the focus being on the thermal efficiency, since the efficiency of the PV cells was still considerably low (~6%) and these systems were intended for small scale residential applications. In the following decades, there has been a lot of research on ways to enhance the thermal output of PV/T systems including studies on optimal geometric features and flow rates (Bambrook and Sproul, 2012; Kaiser et al., 2014), the use of added glazing and double pass channels (Baljit et al., 2016; Hegazy, 2000; Tiwari et al., 2006), as well as the use of added elements inside the coolant channel to enhance heat transfer to the coolant (Hussain et al., 2015;

Kumar and Rosen, 2011; Tonui and Tripanagnostopoulos, 2006; Yang and Athienitis, 2014a) among others.

One study aimed to improve the thermal efficiency of a PV/T system by inserting a hexagonal honeycomb heat exchanger made from a thin aluminum sheet into the air channel. Experimental testing showed that the thermal efficiency was improved by up to 60% and the electrical efficiency improved by 1%, which indicates that this kind of system would be best used for space heating or solar drying (Hussain et al., 2015).

Most common types of PV/T systems are as follows:

- Water-based systems, which use water as the fluid medium for transfer of heat from the PV panels. Due to the thermal properties of water, there is a higher heat exchange efficiency and thus these systems are best suited for climates which have high levels of solar irradiation and high ambient temperatures.
- Concentrator systems, which use reflectors to increase the radiation intensity on the PV cells. The PV system will need less area, but the high temperatures inside of the collector will reduce the PV efficiency. Applications for such systems would be intended for high temperatures and usually include a tracking system to follow the sun path.
- Air-based systems, which use air as the fluid medium. In cold climates, where ambient temperatures can be very low, these systems would be better applicable than the previously mentioned. More specifically, there are two types of air-based systems:
 - Passive air systems: these use the effect of buoyancy or stack effect and a natural air flow is created, cooling the PV panels
 - Active air systems: The air flow in these systems is mechanically assisted, and this can be an open-loop or closed-loop configuration

Depending on the temperature of the fluid medium exiting the BIPV/T, the system can be classified as high-temperature (fluid medium over 60°C) or low-temperature (fluid medium below 60°C) (Athienitis et al., 2015).

2.3.2 BIPV/T Systems

Similarly to the benefits of a BIPV, the advantages of integrating a PV/T system with the building envelope include an increase in the cost-effectiveness of the installation, the replacement of common building materials and a better architectural result (Yang and Athienitis, 2016a).

BIPV/T systems supply buildings with both electrical and thermal energy, and are usually connected to systems such as heat pumps or heat recovery units to utilize the heat generated. Like the PV/T, the BIPV/T concept originated in the 1970s, but the technology didn't become realized until the 1990s. The system is different from stand-alone PV and PV/T systems in that it is heavily influenced by the building design and requirements. Types of building integrations include replacing roofing elements on existing flat or low-slope roofs, taking the place of ventilated facades (the PV panels act as the exterior cladding), rainscreen claddings and also, CW systems.

Using air as the heat transfer medium facilitates BIPV/T applications on roofs, facades, windows and skylights. There are passive systems, which rely on buoyancy, and active systems. The active system, which uses a fan to draw in air from the exterior, is considered open-loop and runs at lower temperatures than closed-loop air systems. In such cases, higher thermal efficiency is usually achieved, and the PV performance and durability is also improved (Yang and Athienitis, 2016a). The result from the thermal portion is that there is pre-heated fresh air for the building to utilize. A key advantage of open-loop air systems as compared to liquid systems is that there is no need for maintenance of the building envelope associated with possible leakage of the heat transfer liquid or its periodic replacement.

In an active system, depending on cell type, approximately 15% - 20% of the incoming solar radiation is converted to electricity, another 5-10% is reflected, and the remaining 75-80% is converted to heat and removed by radiative exchange with the sky, convection with outdoor air, radiative exchange with the channel surfaces or through convection with a fan-induced air flow inside the channel (Figure 2.5). BIPV/T systems aim to utilize the last two heat transfer methods to remove much of the excess heat from the PV panels and transfer it to the air in the channel.

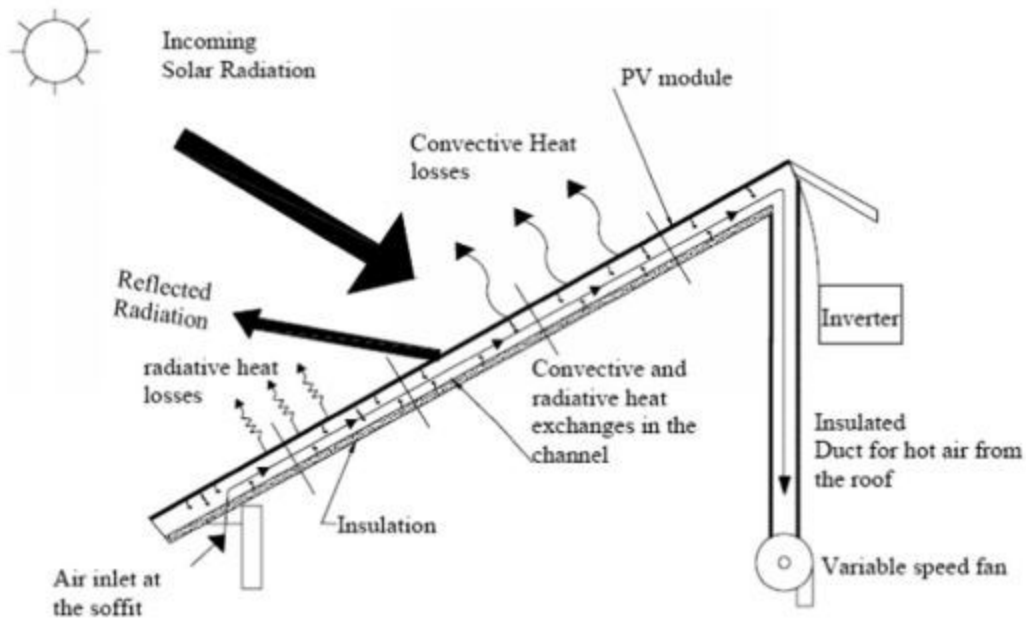


Figure 2.5: Diagram of an active air-based BIPV/T roof (Candanedo et al., 2010)

For applications on large-scale commercial or industrial buildings, selecting an air-based BIPV/T system has several advantages. Air-based systems are lightweight and eliminate the risk of leakage, which would be a problem with fluid mediums. As a consequence of this, they generally require less maintenance. However, air has a low heat capacity, and this is the major downside to the air-based system. Because of this, natural convection is often not enough to cool the PV panels adequately to maintain optimal electrical efficiency. Using a fan to assist the airflow may provide sufficient cooling of the PV panels, and this gives the opportunity to collect part of the excess heat for additional use. With the assistance of thermal enhancements, which increase the heat transfer from the system to the air medium, lower PV temperatures would be expected. This does not apply to methods which reduce thermal loss to the environment.

Although heat pumps are among the most common technology to be used with PVs, utilizing the heated air from an air-based BIPV/T can present challenges. In a theoretical investigation, the performance of an air source heat pump (ASHP) was studied in two modes; one using ambient air directly, and the other using the heated air from a BIPV/T. The results suggested that during some parts of the year, the coefficient of performance (COP) of the ASHP was higher when coupled with the BIPV/T system (Hailu et al., 2015). ASHP is one of the most efficient technologies for supplying buildings with hot water or with the heating and cooling. Also, ASHP

can achieve higher COP values than ground source heat pumps (GSHP) at certain outdoor temperatures (Safa et al., 2015), signifying that hot air from BIPV/T systems can be used quite efficiently.

One important factor to consider when assessing the overall energy production of a BIPV/T system is that most commercially available ASHPs with a COP of 4 produce four units of thermal energy for every one unit of electricity produced by a PV module (Owen and Kennedy, 2009). This highlights the value of electricity over thermal energy production.

2.3.3 BIPV/T Demonstration Projects and Prototypes

Several demonstration projects are mentioned below which include BIPV/T applications. Unique challenges and solutions in the design and construction of each project are discussed.

The Ecoterra house is shown in Figure 2.6. The upper portion of the roof is a BIPV/T assembly consisting of 21 amorphous silicon PV modules. The roof section is 10.4 m wide and 6.2m in length (sloped dimension). It is an air-based open-loop system (the air channel depth is 3.8 cm) which uses a variable speed fan. The thermal energy produced by the BIPV/T can be used for domestic hot water (DHW) heating, space heating or for the clothes dryer. As shown in the diagram on the right of Figure , the BIPV/T is also connected to a ventilated concrete slab (VCS). Based on the outlet temperatures, a control system directs to the air to one of these locations:

- Dryer (if needed) can utilize BIPV/T air if it is 15°C or higher (and has a relative humidity less than 50%)
- The VCS, which is typically at 17°C or 18°C, can be heated with outlet air that is 21°C or higher
- If the outlet air is warmer than the water in the DHW storage tank by at least 5°C, it can be directed there

In monitored data, the BIPV/T system demonstrated a 20% thermal efficiency by using multiple applications for the heated air. Compared to the national average, the system reduced the annual space heating energy by 5% (Chen et al., 2010).

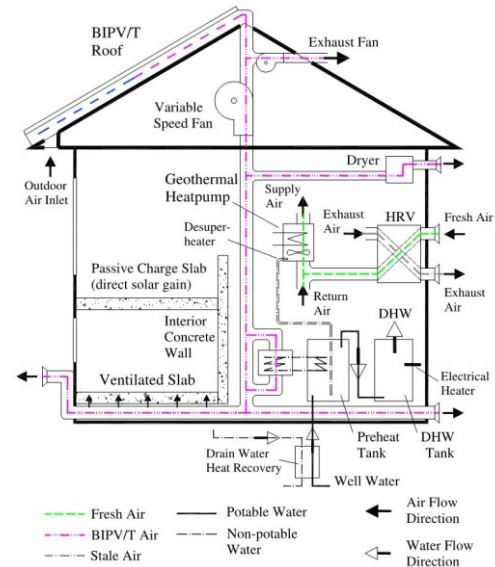


Figure 2.6: Ecoterra house (Chen et al., 2010)

The BIPV/T roof was pre-fabricated in a factory, which ensured high quality of assembly. Special attention was paid to the air tightness and thermal insulation of the assembly, and the manifold was built with consideration for uniform flow and balanced pressure drops. Figure 2.7 shows the initial wood frame prior to metal roofing (left picture) and the finished roof after it was delivered on-site (right). The PV modules were attached to metal roofing with adhesive, and mechanically fastened at the roof ridge with a cap and screws (Chen et al., 2010). The continuity provided by the PV modules serves to maintain water tightness and have an aesthetic effect.

Although the buildings' energy consumption is already low at approximately 9419 kWh/year, the energy produced from the BIPV/T roof is expected to lower this to approximately 5000 kWh/year, which is only 10% of the national average. Two advantages of this design were based on the following choices:

- Pre-fabrication of the entire roof assembly in quality-controlled shop conditions
- The use of amorphous PV modules, which resulted in lower electrical generation as opposed to more commonly used PV technologies, but lowered the cost of construction



Figure 2.7: Wood sub-framing for roof at factory (left) and BIPV/T finished module on-site (right) (Chen et al., 2010)

In the Varennes Library in Quebec, the design of a net-zero energy building with a BIPV/T roof occurred through an integrated design process (IDP) which saw the collaboration of government and academic researchers with the architectural team and industry partners (Figure 2.8). The building achieved LEED Gold certification in 2016. The early design choices were influenced by the need to size for a 110 to 120 kW PV system on the roof, based on energy consumption predictions, and a building geometry that allows for deep penetration of daylighting (resulting in a building depth of 6 m to 10 m) as well as natural ventilation. The slope of the roof with PV modules would be 40° due south for optimal electrical production and reduction of snow accumulation. Part of the roof was designed to be a BIPV/T system, and together with a GSHP, would reduce heating energy use and export excess heat to assist with heating of the neighborhood public swimming pool.



Figure 2.8: The BIPV/T roof of the Varennes library in Varennes, Quebec

The roof is a 110.5 kW BIPV system, covering a total of 711 m² (Figure 2.9). Of this area, 428m² is naturally vented and 280 m² has fan-assisted ventilation. Only 173m² of the fan-assisted portion of the roof is a BIPV/T system, bringing the heated air into the building to the fresh-air intake. The fan was designed to maintain an air velocity of 1 m/s for effective heat transfer without significant pressure loss. On a typical sunny day in the winter, the BIPV/T can bring in about 220 kWh of thermal energy. In the summer months, the air is exhausted to the outdoors due to lack of heating needs.

There are ten 10 kW inverters. Monitoring the system showed that daily electrical production reached only 80 to 90 kW peaks (occurring in May and June) with losses due to conversion and wiring of the modules. Additionally, up to three of the ten inverters were not functioning correctly, likely due to a higher production than they were designed for (Dermardiros, n.d.).

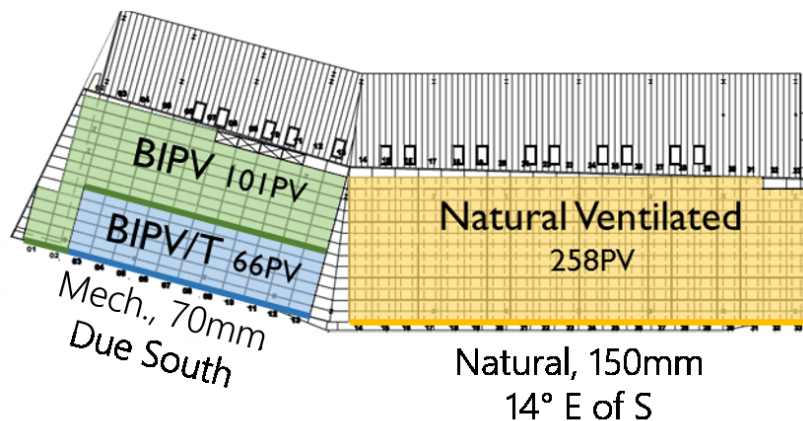


Figure 2.9: The Varennes roof by type of BIPV. The naturally ventilated portion (yellow) has an air channel depth of 150mm, while the forced-fan vented portion (blue and green) has an air channel depth of 70 mm.

The library has an energy use intensity (EUI) of 6.51 kWh/ft²/year, and with the addition of the energy produced by renewable sources, the net EUI is reduced to 1.35 kWh/ft²/year. Since there are no batteries to store the electricity produced by the roof, it is sold to the grid or to customers who need to charge their electric vehicles (the library has a charging station). One of the challenges in managing energy in a building such as this is that feeding electricity back to the

grid when production is high does not necessarily match with times of the day when there is a peak in consumption (considered to be 6:00am to 9:00am and 5:00pm to 9:00pm).

The air-based BIPV/T facade at the penthouse level of the John Molson School of Business (JMSB) in Montreal, Canada is a custom design in response to architectural requirements for visible uniformity (Figure 2.10). The system has 384 PV modules covering 70% of the UTC cladding behind them. The modules are connected to five inverters. The UTC has a dark porous cladding which draws in air and heats it with the absorbed solar radiation. UTCs have thermal efficiencies as high as 60% on their own, but when incorporated into a BIPV/T, the value of the electricity generated (at least four times more than heat, as mentioned in the previous section, 2.3.2) gives the overall system a higher combined efficiency even if the addition of PV initially lowers the thermal efficiency. Energy production for this BIPV/T includes 25 kW of electricity, 75 kW of heat for fresh air ventilation preheating and has a peak solar energy utilization of 55% (Athienitis et al., 2010).

Since Montreal has a cold climate and sunny winters where peak values for incident solar irradiance on south-facing surfaces often range up to 1100 W/m^2 , the use of a BIPV/T on such a facade for fresh air preheating seems advantageous. At the JMSB, the facade was placed intentionally at the level of the mechanical room, reducing the distance for the preheated air to travel to the HVAC system, thereby reducing ducting material.

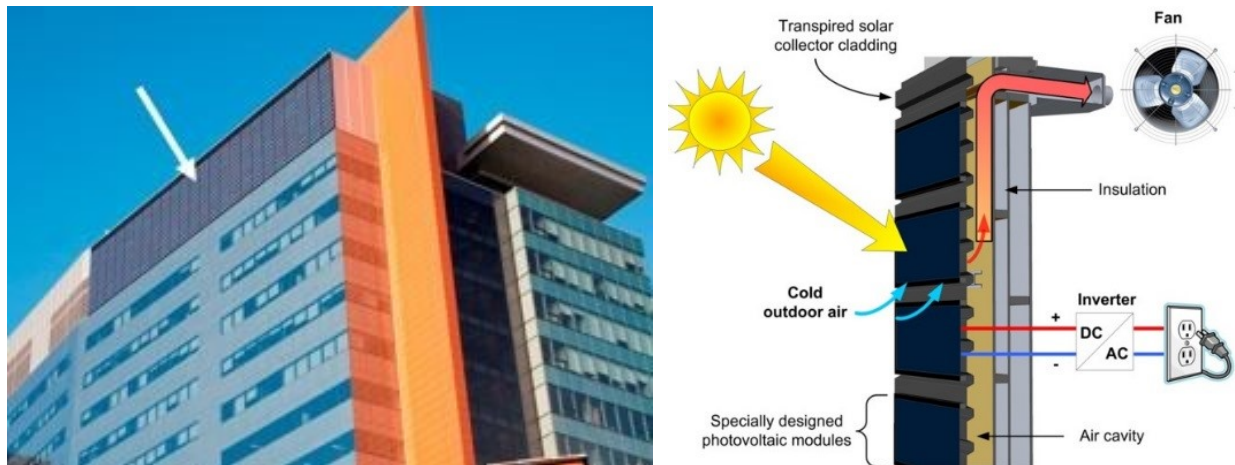


Figure 2.10: BIPV/T facade on the JMSB building (left) and PV/UTC components in a concept diagram (right)
(Athienitis et al., 2010)

The energy generation of the system was dependent on design factors such as panel dimensions, absorptance of the framing, thermal properties of the structure, design of the array (vertical stratification can cause non-uniform array temperatures, and this depends on the series or parallel connections of the array), and porosity and corrugation orientation of the UTC cladding. The system was dimensioned to replicate the existing curtain wall configuration, extending the aesthetic look of the facade without disrupting the verticality. Mounted on the UTC cladding with special clamps to reduce heated air from escaping once inside the air channel, the PV modules have black framing for increased absorptance (and to match the existing facade) and a height to width aspect ratio which encourages transfer and temperature stratification reduction (Figure 2.11, left). Both the size of the modules and the UTC cladding was subject to limitation by industry availability, and since a horizontal corrugation pattern was preferred for the UTC, (reduction of heat losses, induced turbulence) the PV modules were vertically spaced at 90mm accordingly (Figure 2.11, right). At the top of the facade, a section of the UTC cladding was not covered by PVs. This was to assist with cooling of the system by encouraging additional buoyancy of the air (Athienitis et al., 2010).

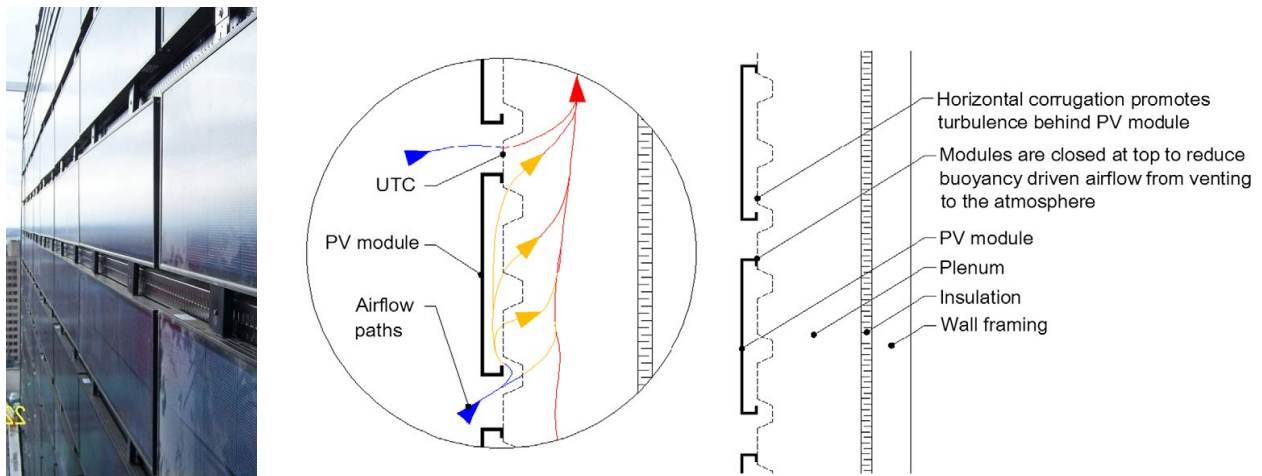


Figure 2.11: Custom PV modules attached over UTC (left) and section diagram showing modules attached at top edge to horizontally corrugated UTC panels (right) (Athienitis et al., 2010)

The design and construction of the BIPV/T system on the JMSB penthouse facade demonstrates several important lessons for future designs of this technology. Without a proper energy analysis, it is unclear if the thermal energy generated is useful in months when heating is not required. In such cases, integrating the system with additional applications, such as in the

Ecoterra house, is favorable. The primary purpose of the UTC component is to maintain the performance of the PV modules, so as long as the operation of the fan does not consume more energy than it saves, it is a beneficial addition to the design.

Experiments have been conducted at the prototype level to improve efficiency of BIPV/T systems. A design was proposed to use multiple air inlets instead of one inlet for a large-scale installation of a BIPV/T system. Results from modeling showed a 5% increase in thermal efficiency, and a reduction in peak PV temperatures by 1.5°C. The study suggested that the PV temperatures could be reduced by up to 5°C to 10°C for longer spans of the BIPV/T, such as 5 or 6 meters (Yang and Athienitis, 2014b). Bigaila developed a new design for a BIPV/T solar air collector prototype for facade retrofit with the emphasis on simplifying the integration into the building envelope. Testing was then conducted on an open-loop multiple inlet building-integrated PV/thermal unglazed air collector (Bigaila et al., 2015).

2.4 Facade design

To be able to consider BIPV systems as facade assemblies, it is valuable to have an understanding of conventional claddings that may be replaced with the newer technology. Typical facade assemblies include the following (Mike Carter, C.E.T. and Roman Stangl, 2016).

- Masonry wall systems: Typically, these are masonry units (i.e. brick or concrete masonry units) and mortar constructions. They can be structural or veneers which act as the cladding. These systems usually require insulation, moisture management and an air space behind them.
- Panelized metal wall systems: Usually fabricated from aluminum, copper, stainless steel or other composite materials, these systems are metal sheets which are ship-lapped with other panels. The thickness is usually around 1mm and require framing to be held in place. Insulation may or may not be included in the panel system, and depending on the type of joints, a backup air and moisture barrier may be required.
- Precast concrete wall systems: Most often, precast concrete is used as a cladding and connected to the building structure with anchors or supports. Typically, an insulated stud back-up wall is used for precast panels. Sandwiched precast panels, however, do not need a structural back-up wall.

- Thin stone wall systems: Stone panels with a thickness of ranging from ¾” to 2” are fabricated, typically from granite, limestone or less commonly, sandstone. The panels are supported with anchors and other metal components connecting to the structure, and require insulation as well as an air and moisture barrier or a drainage cavity.
- Exterior insulation and finish systems (EIFS): Painted plaster boards, typically consisting of synthetic lamina, covering rigid insulation comprise EIFS claddings. These panels, along with the joints between, typically comprise the barrier system of the facade.
- CW systems: Aluminum (or other) framed wall that contains in-fills of glass, metal panels or thin stone (as the one mentioned above). Typically, these systems do not carry the floor or roof loads. There are two primary types of CW systems: stick-built and unitized. Those suitable for BIPV and BIPV/T systems are discussed further in Section 3.2.1

2.5 Integration with the facade

As previously mentioned, there are four main options for building integration: sloped roofs, flat roofs, facades, and shading systems. South facing sloped roofs are favorable because of direct angle to the sun. For facades, the typical ways to integrate include ventilated facades with the PV panels as the external cladding or the rainscreen, and as window elements, often including semi-transparent photovoltaics (STPV) (Yang and Athienitis, 2016b). STPV modules use clear front and back sheets, usually a type of plastic or glass, and have silicon cells spaced apart enough to transmit light through the clear portion. For ventilated and non-ventilated facades, an air gap under or behind the PV modules is critical to incorporate since a temperature increase decreases electrical performance of the cells, especially for mono- and polycrystalline modules. The PV modules also have to deal with physical issues such as heat and moisture transfer, high and low exterior temperatures, rapid temperature changes, freezing and thawing in colder climates, and wind and snow loads (Jelle et al., 2012). In the IEA-PVPS report from 2000, the criteria for a successful BIPV/T system includes: a pleasing, natural integration, good color composition, continuity of the building and facade concept, and finally innovative engineered design.

Using a BIPV/T facade may have a positive effect on the thermal performance of the envelope by reducing the cooling load. This can happen because solar radiation is not transmitted but instead is converted to electrical energy, the physical addition of the PV/T elements can increase the envelope insulation, and because some of the heat is removed with the cooling medium

(Yang and Athienitis, 2016b). Several monitoring experiments support this. In one study, infrared imaging was used to record daytime ceiling temperatures under rooftop BIPV arrays, and it was found that they were 2.5 Kelvin (K) cooler than ceiling under the same type of roof but exposed to the sun (Dominguez et al., 2011). Another study indicated that a BIPV/T facade can reduce the temperature oscillation amplitude within the wall, resulting in higher wall temperatures on a winter day (Chow et al., 2007). An investigation showed that a BIPV wall reduced daytime heat gain by 69% and nighttime heat loss by 32% during winter months (Peng et al., 2013).

2.5.1 Installation and Maintenance Methods

A monthly maintenance schedule is recommended for checking and recording electric output, while on an annual basis, a visual inspection and cleaning of the PV panels is suggested. While inverters were previously considered one of the more common electrical problems, design is now more reliable. Electrical problems like open circuits and connection corrosion are of more concern. Soiling maintenance includes manual removal of lichen, dirt accumulation at lower edge of modules (especially those at lower inclinations), which can be addressed by adding laminates that help with water run-off (Roberts and Guariento, 2015).

Modules are normally linked as daisy chains, with cables looping from one module onto the other. If these cables are exposed to exterior water or moisture conditions, as seen in a rainscreen cladding, the components along with the junction box need to be carefully selected for this. Nonetheless, for a practical application with minimal cost and voltage drop, cabling should be as short as possible. Applications with STPV panels must acknowledge visibility concerns.

Rainscreens, often used as replacements for existing or out-of-date envelopes are a good method of incorporating BIPV or BIPV/T systems. The inner layers of the facade include the air and/or vapor barrier and stay dry. The exterior layer must shield the inner layers from contact with large amounts of water, and must ventilate the layers of the wall. This is one of the reasons a rainscreen concept works well for BIPV/T systems. There are two types of rainscreen systems that are relevant to BIPV/T. A face-drained and back-ventilated system, where water comes into contact with the joints without restriction, and a pressure-equalized system, with controlled water penetration due to small openings on the exterior that restrict water shedding to the exterior layer. The difference between face-drained and pressure-equalized systems is that the latter is compartmentalized for each glazing unit. Typical materials for rainscreen systems include stone,

terracotta and concrete panels. These panels are connected back to the primary structure using bolts, studs or cladding rails. To prevent uplift due to wind loads, there are lateral mechanical fixings locking the panels into place, although this is primarily utilized in roofing applications (Roberts and Guariento, 2015).

For existing facades/claddings, little modification would take place to add or incorporate PV panels. Ventilating the cladding would circulate air behind the panels and keep their operating temperatures lower. For a standard rainscreen with lightweight metal panels, the PV panels could easily replace the metal panels. The existing panels could be modified into a frame that the PVs could fit into.

The wiring of the junction box is something that must be considered. The wires should be located behind the rainscreen layer and out of the “wet zone”. They can be guided along the vertical tracks that are used for mounting the panels. At the base or the top of cladding system, they can be brought together and drawn inside of the cladding to reduce the number of penetrations. One of the best options to integrate PV panels into existing claddings is the pressure-equalized rainscreen, as it already has the air gap behind the outer layer to be able to ventilate the panels. It’s up to the designer whether to keep all of the wiring external and make one penetration through the weather barrier, or to bring the wiring in at regular intervals and create multiple penetrations, which will keep wiring safe from external conditions. To make this decision, space requirements, access and weather performance must be considered. One way to bring down the cost of the system is to use standard PV sizes, but this will limit the grid sizing of the facade (Roberts and Guariento, 2015).

In terms of maintenance and replacement, one way to keep the panels clean is running water down the face, but this will only work to a certain degree. The cleaning schedule can be the same as for glazing claddings. Replacement strategies for the PV panels can be similar to large CW units, since swing stages can only support up to 250 kg. Since almost all of the PV components can be replaced from the outside, replacement should be fairly easy. This can be done by unlocking the brackets for individual modules. Once one or a series of modules is dismantled, there is access to the wiring (Roberts and Guariento, 2015).

PV panels can be integrated into the vision or the spandrel area of a facade. PV can be integrated into IGUs by serving as the outer lite of a clear, double-glazed unit, laminated onto a carrier glass. The laminated layer would include heat-treated glazing to avoid breakage due to

thermal stress. In a shadow box, STPV can be used to create the perception of depth with some light penetration. However, when designing the shadow box, care must be taken not to shade the PV layer. Heat can build up inside the spandrel or shadow box, so this will require a heat-treated outer layer. For spandrels, the PV can be incorporated into the outer layer of a sandwich panel.

Two types of glazing can be used. Dry glazing means that the system is held together by wedge gaskets, with exposed split mullion and transom profiles. This is a mechanical system with pressure plates. Wet glazing is the use of structural silicone to bond the glass to the aluminum frame. Structural silicone glazed (SSG) systems do not require pressure plates on the exterior, allowing for a fully flush design of the glazing. Structural silicone should be applied under carefully controlled factory conditions, and replacement of these units is not easy. A hybrid of these two glazing types includes using structural silicone sealant where the glass is bonded to the aluminum sub-frame, and if replacement is necessary, the mechanical fixings are unlocked to release the aluminum carrier frame, which is then unscrewed. Any sealant replacement happens in the shop (Roberts and Guariento, 2015). It is important for the silicone sealant not to come into contact with acrylic spacers of the modules, or the laminate films, which have EVA or PVB layers. The insulation for the cabling also must not come into contact with the silicone (Melorose et al., 2015).

Any single or double-glazed units can be replaced by clear or opaque, single or double-glazed PV modules. All of the penetrations of the PV wiring through the framing members or weather seals can be therefore sealed in factory conditions with a high level of quality control. Specifically, for PV panel systems, 4-sided SSG systems are not recommended as the panels are heavier than typical glass. It should be noted that the silicone sealant of the weather seals should not come into contact with the acrylic spacers of the laminate films (such as EVA and PVB) used in the modules. The cabling which runs along the glass edges of the modules must be routed out of the modules and through joints into the framing supporting them. The caps on the exterior pressure plates should not self-shade the PV cells, and should be kept to a shallow design. One way to decrease this shading effect is to apply structural sealant between the PV glazed units in a flush manner (Roberts and Guariento, 2015).

2.5.2 Challenges

Despite development of various system improvements and a handful of physical demonstrations, there are many current barriers which prevent widespread industry application of BIPV/Ts. Such barriers include inconsistent integration into building design, unclear performance assessment and predictions, cost-benefit analysis, a lack of BIPV/T-specific standards and codes, and constructability issues (R. J. Yang, 2015).

For both BIPV and BIPV/T systems, understanding of long-term durability is limited and mostly undocumented. Studying one installed BIPV system at the Politecnico di Milano University over a period of 13 years of continuous operation has shown how external factors like available solar radiation, long-term ultraviolet (UV) exposure, shadowing, and dust accumulation affect the system performance. The length of operation is approximately half that of a typical PV system lifespan. Methods for assessing PV module performance consisted of visual inspections, use of infrared (IR) thermography, measurements of the I-V parameters and an analysis of the actual performance decay over the observed time. The visual inspection showed slight yellowing, minor delamination, and occasional cracking of PV cells. A soiling analysis showed that the rack typically reaches saturation, or full dirt coverage, after 30-50 days, however high-tilt modules usually have a soiling rate of less than 3%. An economic analysis of operation and maintenance costs noted repairs of the inverter and monitoring systems, one deep cleaning with payback time equaling to approximately 12 years. Due to early design considerations for PV system design including back ventilation of the PV modules and high quality components, no significant decrease in overall system performance was observed, while the modules remained in good shape despite minor deterioration (Aste et al., 2016).

For BIPV/T systems, durability is especially important with regards to larger scale systems like CW facades as opposed to small, stand-alone systems. Depending on the type of technology, PV modules will generally operate between -20°C and 65°C , sometimes reaching 110°C , and addressing such high temperatures becomes significantly more critical in larger installations (Blieske and Stollwerck, 2013). Replacement of single modules becomes more challenging and natural ventilation or cooling is necessary in case of system failure.

Addressing the risks associated with BIPV applications involves assessing the building stages from concept design to operation and maintenance. One of the main reasons that BIPV

implementation has not developed at a larger scale is that the many of these risks are not well understood or identified by architects, manufacturers and most importantly, stakeholders. There is a lack of documentation of these risks and challenges, although an effort to make progress in this subject has been met with enthusiasm by industry professionals (R. J. Yang, 2015).

Some of the issues encountered during the design stage include lack of easy access to external fixings and wiring, little or no post-installation requirements, and lack of designers' knowledge in choosing an efficient PV string layout that conforms to the building geometry and functionality. The data which is needed to design the layout includes formation of composite frequency distribution of hourly radiation along with an analysis of the descriptive statistics parameters, and finally an optimization of these statistics. The resulting information can be used to calculate inverter size. When designing the structural system, there is uncertainty about which load bearing elements of the facade or roof will be shared or replaced. Building self-shading will account for approximately 5% - 10% in the decrease of the electrical output, which needs a shading analysis during early design.

During installation, limited availability of mounting systems reduces architectural solutions for elements such as large bolts and holding plates securing the PV panels. Furthermore, the framing of the PV modules is difficult to hide with conventional mounts. If water-tightness is not observed and water infiltration occurs, condensation can occur inside the system. A well thought-out design utilizing simulation tools to analyze the effects of wind driven rain can prevent/address this.

After installation is complete and the BIPV system is operational, there are requirements for successful long-term energy production, many of which are currently unresolved. There is a general need for performance monitoring systems, warranties for the full system, and definitive maintenance procedures for PV protection and cleaning, as well as inspections of the silicone waterproofing sealants (R. J. Yang, 2015).

2.5.3 Costs and Economics

Implementing a PV system has a large cost of construction, but costs are minimal during the operating phase. All capital costs related to the PV system are as follows:

- Modules and inverters delivered on-site

- Labor of installation
- Installation materials, including wiring and mounting
- All aspects related to the site work, such as land acquisition and preparation
- Environmental permitting and connection to the grid.

For BIPV systems, certain costs can be subtracted from these, such as those tied to replacement of building materials and the additional functions of the PV components (Goodrich et al., 2012). It should be noted that building surfaces often do not have an optimal tilt for maximum incident radiation, which reduces the annual electricity generation. If the system is not properly vented, the decrease in performance due to high PV temperatures will also have an effect on this.

The lifetime of most buildings is more than 50 years. The warranty for PV modules is typically 25 years, and when taking into account the rapid development of new solar cell technologies which are decreasing in cost but increasing in efficiency, easily replacing modules in a BIPV system becomes very important (Peng et al., 2011). This frequent upgrade in technology can present a problem in manufacturing and sales, as was the case in China between 2010 and 2014. In an effort to address air pollution, the government subsidized PV companies to manufacture panels, which they did and in large quantities. This caused PV prices to drop rapidly between 2009 and 2011 and companies in other countries went bankrupt. The overproduced panels ended up in warehouses as projects struggled to keep up with the supply, while new technologies were developed. These panels became obsolete since installing older, weaker panels is more expensive than newer ones and installation costs are usually based on a per-watt basis (Y. Yang, 2015).

In market reports, power generated from BIPV is only 1% to 3% of all PV installations. Not a lot of countries are providing support for BIPV development and implementation, according to an analysis from the IEA PVPS Task 1 (Scognamiglio, 2017). Feed-in tariff systems can play a role in promoting architectural integration.

In northern regions, proper building insulation will benefit a building more than the savings from renewable energy generation. However, the specific cost of insulating is actually

higher (Eicker et al., 2015). Installing conventional cladding materials, such as steel or glass, is only lower by 2% - 5% as compared to installing BIPV systems (Eiffert, 2003).

In a 2017 survey of BIPV products, approximately 200 international products are commercially available for roofs and facades, with rooftop applications being the largest segment in the market (Zanetti et al., 2017).

2.5.4 Architectural Aspects

Amorphous silicon tiles can be made to look like tiles in BIPV roofs, STPVs can be used in facades or glass ceilings for the visual effect. The choice to make the technology blend in with the existing enclosure design or to make it stand out to show the BIPV concept is a choice of the designer (Jelle et al., 2012).

Thin film cells have a homogeneous surface and there is no restriction on cell size. One concept to integrate these is to use them with a structural substrate such as corrugated metal sheeting. Wafer based cells can vary in shape and be quadratic, round, or take on other geometries. Monocrystalline cells have a homogenous surface, but the blue and grey silicon crystals are visible in polycrystalline cells. Special anti-reflection coatings can give the cells colors other than blue, such as red, brown, green or magenta (Farkas et al., 2009). Continuity with existing roofing elements is done by using the same forms and mounting methods, but this doesn't provide an aesthetical solution. Furthermore, roof elements such as gable endings, ridges, skylights and chimneys disrupt the harmony of the overall look when the PV components do not match in color and texture.

2.6 Existing Standards

A number of standards exist for PV systems, and more recently, several BIPV standards have become available primarily in Europe (Scott and Zielnik, 2009). Standards discussed in the following sections are separated by system type, covering solar thermal, PV and building envelope applications. Standards from the following organizations are included:

- International Organization for Standardization (ISO) is a global standard
- European Standard (EN) is primarily used in European countries
- Solar Rating and Certification Corporation (SRCC) standards are used in the United States
- Canadian Standards Organization (CAN/CSA) is a series of Canadian standards

- International Electrotechnical Commission (IEC) is a global standard
- American Society for Testing and Materials (ASTM) provides international standards
- Institute of Electrical and Electronics Engineers (IEEE) standards are used globally
- Underwriters Laboratories (UL) standards primarily cover North America
- National Fenestration Rating Council (NFRC) provides the US with performance standards

2.6.1 Standards for PVs and Solar Thermal Collectors

Parameters that are typically evaluated for PVs include solar cell efficiency, open circuit voltage and potential, short circuit electrical current, max power point, fill factor (FF), band gap, and quantum yield. These values are typically achieved by manufacturers using standard test conditions (STC), and nominal operating cell temperature (NOCT) conditions (Jelle et al., 2012). Conventional PV testing (from IEC and UL standards) consists of qualification tests which are performed on new modules and do not take into account consideration of weather-aged products. Most standards relevant to PV performance, installation and additional components, such as inverters, are listed in Appendix A (Table , Table).

Some of the frequently mentioned standards include IEC 61215 for design qualification and type approval for crystalline silicon PV modules (and now includes thin-film modules) (IEC, 2016a), IEC 61730 for PV module safety qualifications (IEC, 2016b), and EN 60904 for PV device characteristic measurements (IEC, 2006).

2.6.2 Standards for facades

Building standards relevant to this research are organized by issuing committee in Appendix A (Table). Building codes which reference the standards listed and discussed include :

- International Building Code (IBC)
- International Residential Code (IRC)
- International Fire Code (IFC)
- EN 1990, EN 1991, EN 1993, EN 1999

2.6.3 Standards for BIPV

Requirements for BIPV standards arise from safety, quality and durability issues related to circuits and inverters. Architectural and building codes typically include elements which would impose requirements on BIPVs as construction materials, such as fire resistance and safety,

structural stability including wind and hail resistance, wind driven rain (especially in regions with heavy rain), energy economy, protection against debris and organic pollutants, noise protection, energy economy, heat retention, means of egress. Newer PV technologies, such as silicon thin-film or non-silicon cell material, do not have the same data as traditionally framed PVs.

One of the bigger gaps in existing standards is that they are limited only to reliability testing, without focusing on durability and long-term performance. It is also important for BIPV standards to conform not only to building standards but also building manufacturer product codes. Long-term durability testing is needed. For example, the IBC has established BIPV systems as roofing materials, so it is necessary to also establish it as a structural system for facade applications. The construction industry and the PV industry incorporate different units and metrics, making the unification process even more difficult (Scott and Zielnik, 2009). One of the existing BIPV standards, EN 50583-1 includes that the PV must be a construction product with functions defined in the European Construction Product Regulation CPR 305/2011 (Scognamiglio, 2017). The EN 50583 standards reference standards applied to the BIPV from both the electrical side and the building side, and these standards are noted in the tables of Appendix A with an asterisk (*).

The roofing standard AC 365 references building codes IBC, IRC and IFC, and includes provisions for wind resistance, wind-driven rain, and accelerated weathering. Table 2.2 shows the current standards established for BIPV systems:

Table 2.2: BIPV related standards

Issuing Committee	Name	Description and Remarks
ICC	AC 365	Acceptance Criteria for Building-Integrated Photovoltaic (BIPV) Roof Covering Systems (ICC-ES, 2015) <ul style="list-style-type: none"> • Includes requirements for wind driven rain testing in accordance with Florida Building Code TAS 100-95 • Humidity tests in accordance with UL 1703, Section 36 (Flat plate PV modules and panels)
ISO	ISO 19467	Thermal performance of windows and doors – Determination of solar heat gain coefficient using solar simulator <ul style="list-style-type: none"> • Determination of SHGC using solar simulator • Annex F: measuring method and example of measurement of active solar fenestration systems

		<ul style="list-style-type: none"> • Under ISO/TC 180 Solar Energy committee (“ISO/TC 180 - Solar energy,” 1980) • Mentions integration with active solar fenestration systems such as BIST or BIPV
<i>EN</i>	EN 50583-1	Photovoltaics in buildings – Part 1: BIPV modules (BSI, 2016a)
	EN 50583-2	Photovoltaics in buildings – Part 2: BIPV systems (BSI, 2016b)

In terms of ongoing publications, Standard ISO 18178 “Laminated solar photovoltaic glass for use in buildings” under development and expected for end of 2018 (ISO, 2018). The IEC Technical Committee 82, or IEC TC 82, is devoted to solar PV energy systems and also has a standard under development that is relevant: IEC 63092 – Photovoltaics in buildings (Part 1: Modules and Part 2: Systems) with an expected publication date in 2019 (IEC, 2018). IEA Task 15, “Enabling Framework for the Acceleration of BIPV,” is also ongoing and consists of several subtasks which include building a BIPV product database, identifying BIPV business models, implementing BIPV specifications internationally, and documenting the environmental benefits of these products (IEA, 2018).

Although some progress has been made for BIPV standards, there are no existing standards for BIPV/T (Yang and Athienitis, 2016b). All new technologies go through an evolutionary period in the building industry, going under trial and through experimentation. Farkas makes a good analogy with concrete, which has been around for over 2000 years and is currently one of the most common building and infrastructure materials. However, for concrete to reach this trusted status, scientists experimented and studied its characteristics for many years in the 20th century (Farkas et al., 2009). BIPV and BIPV/T technologies can follow the same path, with proper attention and education of building owners, architects, and engineers.

2.7 Conclusions

Systems which utilize solar radiation for the purpose of reducing energy needs in a building can be passive or active. Active technologies include BIST, BIPV and BIPV/T systems. BAPV systems are similar to the BIPV concept in that they are also located on a building, but they do not replace the envelope or structural components. PV cells are most commonly made from silicon. Polycrystalline cells are categorized as wafer-based PV technologies and are lower in price than

most of the other technologies. A PV module consists of the silicon cells contained within an encapsulant which is sandwiched between a frontsheet (typically glass) and a backsheet (glass or polymer) and held together at the perimeter with an aluminum frame for structural strength. PV module warranties are typically 25 years. The temperature of the PV is of great importance. The electrical efficiency of the modules decreases as the cell temperature increases.

There are four main options for building integration with opaque modules: sloped roofs, flat roofs, facades, and shading systems. STPV modules can be used in fenestration and shading. PV/T systems collect some of the heat generated by PV cells, maintaining them at relatively low temperatures. Water based, concentrator types, and air based PV/T systems exist. Air-based systems can be passive or active, with the active systems being open-loop or closed-loop. BIPV/T systems supply buildings with both electrical and thermal energy, and are usually connected to systems such as heat pumps or heat recovery units to utilize the heat generated. Types of building integrations include replacing roofing elements on existing flat or low-slope roofs, taking the place of ventilated facades, rainscreen claddings and also, CW systems.

Air-based BIPV/T systems are lightweight and eliminate the risk of leakage which would be a problem with fluid mediums. As a consequence of this, they generally require less maintenance. However, natural convection is often not enough to cool the PV panels adequately to maintain optimal electrical efficiency and the use of a fan to assist airflow is required. This gives the opportunity to collect part of the excess heat for additional use. Many thermal enhancements have been studied to aid in this. BIPV/T systems are preferred to solar thermal systems for most applications, due to the better quality of electrical energy over thermal.

Several existing BIPV/T projects include the Ecoterra house, the Varennes library, and the JMSB building. The Ecoterra has good integration of the various systems but uses amorphous silicon PV modules and therefore does not produce as much electricity as with a polycrystalline technology. The Varennes library has a only a small portion of the BIPV roof as a BIPV/T, and the excess hot air is often exhausted to the environment instead of being utilized. The JMSB BIPV/T facade is a custom design, making it difficult to reproduce or apply to other project profiles.

Facade assemblies that could be replaced with BIPV and BIPV/T systems include masonry walls, panelized metal wall systems, precast concrete walls, thin stone walls, EIFS, and CW

systems (which includes rainscreens). Two types of rainscreen systems that are relevant to BIPV/T integration are face-drained and back-ventilated systems. The latter can also be pressure-equalized. Integrated PV modules also have to deal with physical issues such as heat and moisture transfer, high and low exterior temperatures, rapid temperature changes, freezing and thawing in colder climates, and wind and snow loads. Installation and maintenance considerations include wiring and cabling methods, sealant compatibility, and regular visual inspections.

Some of the challenges of BIPV design include ensuring proper ventilation to increase operating life, dealing with limited availability of mounting systems and the need for performance monitoring systems, warranties for the full system, and definitive maintenance procedures for PV protection and cleaning. While implementing a PV system has a large cost of construction, the costs are minimal during the operating phase. Installing conventional cladding materials, such as steel or glass, is only lower by 2% - 5% as compared to installing BIPV systems

A number of standards exist for PV systems, and more recently, several BIPV standards have become available primarily in Europe, with North America still lacking any building standard for these systems. Requirements for BIPV standards arise from safety, quality and durability issues related to circuits and inverters. Architectural and building codes typically include elements which would impose requirements on BIPVs as construction materials. One of the bigger gaps in existing standards is that they are limited only to reliability testing, without focusing on durability and long-term performance. It is also important for BIPV standards to conform to building manufacturer product codes. Currently, standards EN 50583:1 BIPV Products and 50583:2 BIPV Systems are the only known documents that address both PV and building performance. There are no known standards for BIPV/T systems.

There is a strong need to develop a best practice guide for BIPV/T systems. Instead of using custom designs for each unique project, there needs to be a focus on generic assemblies and conventional building product use for integration. Simple and accessible simulation tools should be developed for rapid, iterative BIPV/T early design phases by architectural teams. Standards, especially in North America, must be compiled for BIPV/T performance requirements.

Chapter 3

Design Case Studies and a Methodology for BIPV/T

This chapter includes three case studies for BIPV/T applications based on the accumulated knowledge about the existing development of this technology (previously discussed in the literature review). Each case study has a unique set of needs, for which further research on the specific project was required. These individual studies helped to compile a set of design considerations and performance requirements which then formed the groundwork of a methodology for BIPV/T design.

3.1 Introduction

Design considerations for a BIPV/T system are derived from requirements of the energy production system and the facade assembly. Architectural and structural aspects, along with constructability and durability requirements affect the PV system size, layout and method of connection. Meanwhile, limitations to the PV system create constraints for the architectural design of the facade. In the following sections, three case studies address main factors that must be considered for a successful BIPV/T design. Figure 3.1 shows the primary concept of the multiple-inlet BIPV/T that is used when describing these criteria. The panels are shown slightly overlapping to provide protection against the wind-driven rain, however the focus is on the multiple inlets, air cavity and insulated portion of the system. Results from modeling and then experimental testing show an increase in thermal efficiency as well as reduction of peak PV temperatures in a BIPV/T system if using multiple inlets (Yang and Athienitis, 2014b). This improvement is expected to have a greater effect in systems with longer spans (heights) over shorter systems such as prototypes.

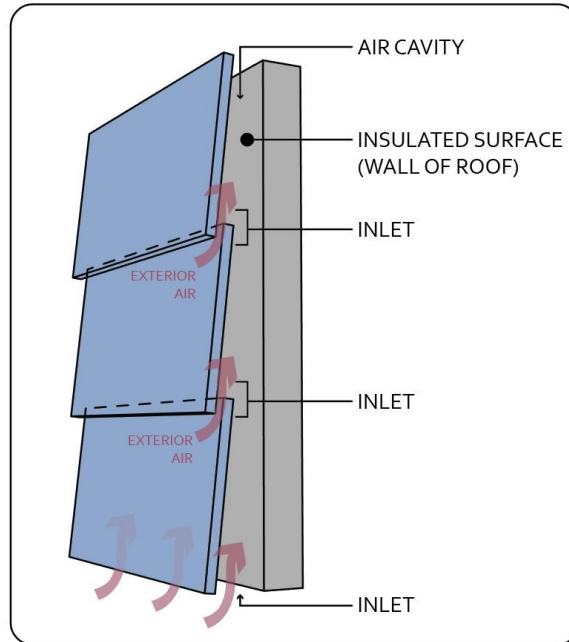


Figure 3.1: Multiple-inlet BIPV/T concept

The inlet profile is designed with the intent to direct the air behind the panels in a way that maximizes the amount of heat gained from each panel. Inlet sizing is optimized based on maximum outside temperature, maximum thermal efficiency of the system or a combination of the two. A mesh can be included in the inlet opening to protect the air cavity from insects and debris.

3.2 Courthouse Building BIPV/T Facade

This section describes the process of designing a BIPV/T facade for the Courthouse building retrofit project. However, a study of cladding suitable to architecturally integrate the PV system needed to be conducted first.

3.2.1 Facades

A curtain wall (CW) framing assembly is one of the better solutions for designing large scale, air-based BIPV/T systems, but it is important to consider the types of CW systems, depending on the uniqueness of the project. The two types of systems discussed are stick-built and unitized (Figure 3.2).

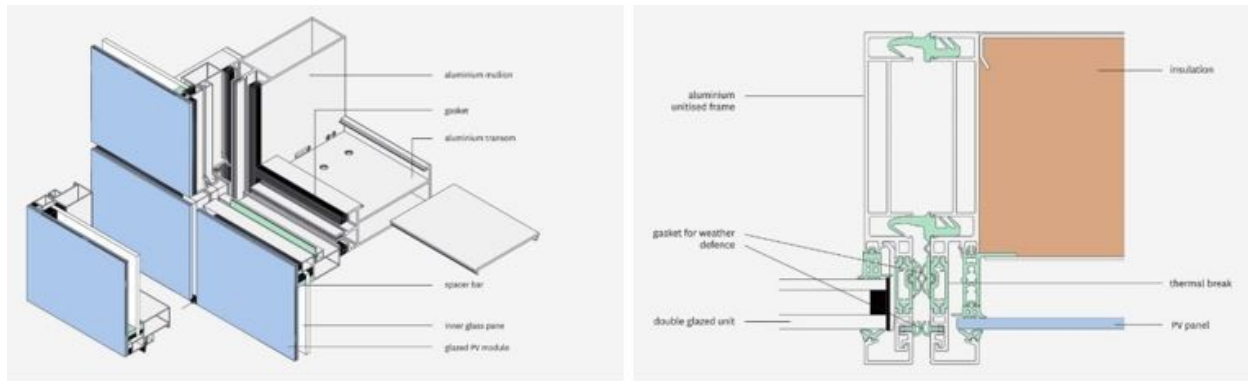


Figure 3.2: Stick built CW (left) and Unitized CW (right)

The stick-built system is a common method for CW assembly, in which assembly occurs in the field. Parts can be individually packaged and delivered, and resulting in a lower shipping cost. Less specialized training is required, since parts are not custom and the installers are more familiar with generic systems. Material distribution on site is easier, and construction sequencing is more flexible. However, there are also several downsides to this type of installation. There is less quality control, since field installation of sealants and other materials is subject to outdoor conditions, also limiting timeframe of construction throughout the year. There is generally a longer installation time and some costs are associated with an increase of labor intensity. There is less chance for custom shape integration in the design, limiting designers' choices. In-plane movement of joints is more likely to occur during and after installation.

Figure 3.3 shows a basic stick-built installation sequence for a curtain wall. The sequence starts with the placement of the vertical framing, followed by the horizontal framing to complete the structural components. The profile of the horizontal framing would have to be more shallow than the vertical to ensure an uninterrupted air channel. Following, the back-pan and insulation would be installed, creating a continuous inner surface for the air channel. Finally, the glazing is placed at the outer face of the system. For a BIPV/T system, PV panels would replace the glazing layer, and the interior channel would be dimensioned for sufficient air flow behind the PV panels.

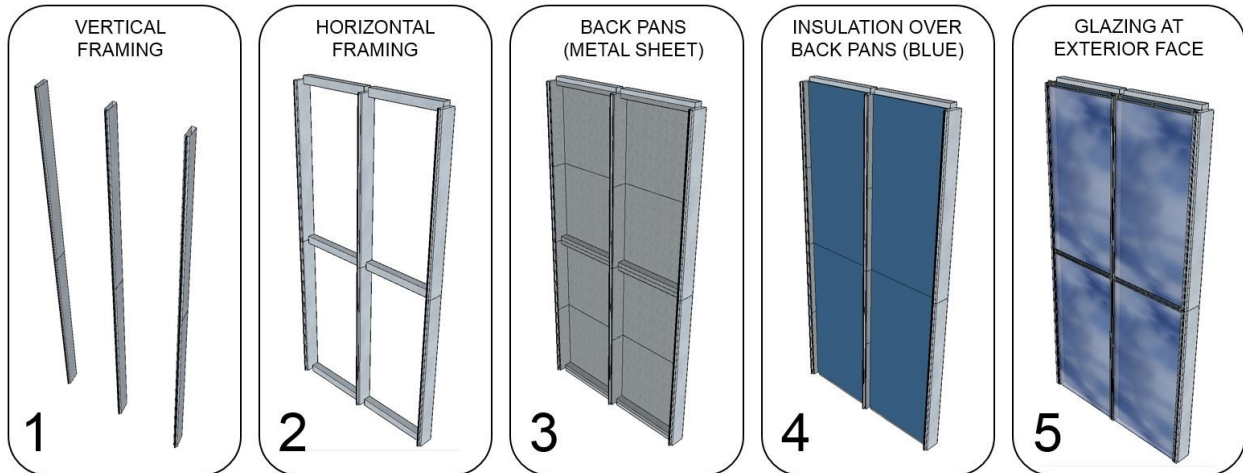


Figure 3.3: Stick-built CW installation sequence (Rendering by S. Rounis)

For a BIPV/T system, the transition from a stick-built design to a unitized design can be relatively easy. Unitized systems are generally considered more expensive and therefore less common applications than stick-built systems, but they have their own advantages. Most of the assembly occurs in the shop, which increases quality control while decreasing the chance of defective parts. Once these panels are shipped to the site, there is a much faster erection and enclosure phase.

The design allows for more customizable extrusions as well as accommodation of in-plane movements. The disadvantages to this type of system include higher shipping costs, a much more rigid construction sequence, extra training of the installers for the custom parts, and a larger error in alignment tolerance during the final assembly due to the design. Although the particular BIPV/T design mentioned in this paper was constructed using the stick-built approach, it is just as easy to incorporate the PV panels and insulation into a unitized system as most of the components are interchangeable.

Unitized systems are typically story-height and start at 1.5 meters in width, but can go up to 9 meters wide. The panels contain all of the necessary elements as the exterior building fabric, and are considered to be the basic building block by providing the following elements: external weathering, insulation, vapor barrier, structural framing, fire protection, vision panels, and an internal finish. The non-vision areas are usually covered with metal or natural stone. The vision areas are typically double- or triple-glazed units. Installation does not necessarily require a crane,

but can be done from the floor slabs of the building. The cost for unitized systems is in the mid to high range. The structural framing of the panel is intended to carry the full weight of the panel and all superimposed loads such as wind. Raceways in the extrusions allow for pre-formed EPDM or silicone gasketing, and the external face forms the primary weather barrier. The units are gravity loaded at each of the floor levels and can accommodate some live load deflection, usually not more than 10 to 12 mm (Roberts and Guariento, 2015). Figure 3.4 shows a layout for a unitized system utilized in a retrofit.

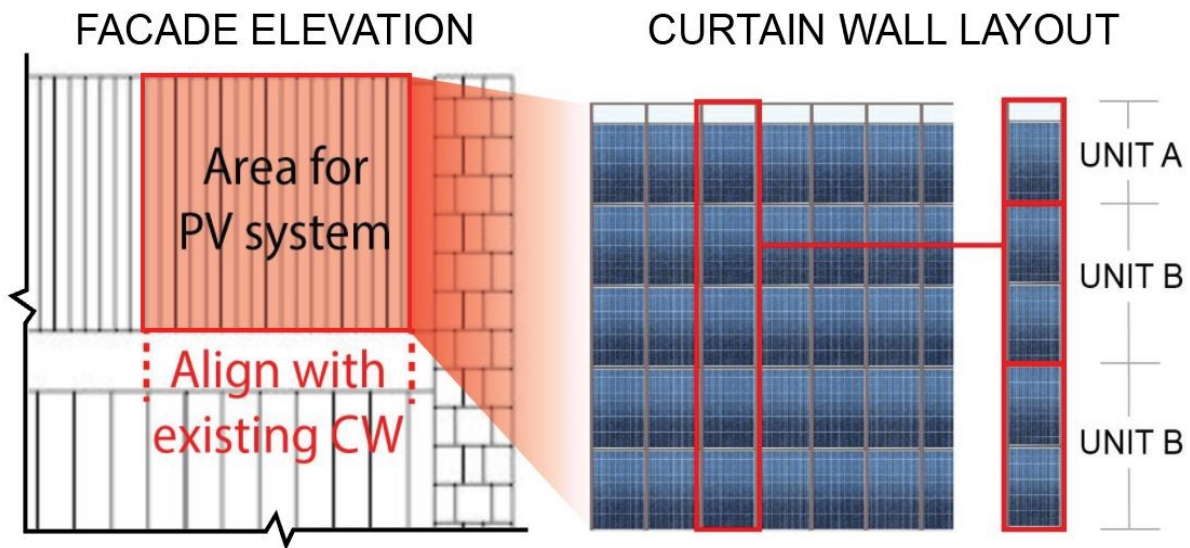
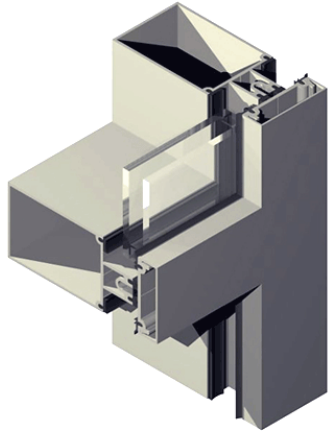
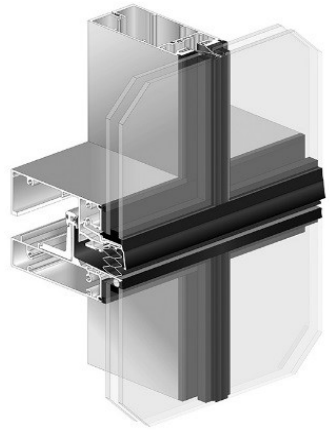


Figure 3.4: Existing facade (left) and sample of unitized CW layout for re-clad (right)



Structural framing significantly affects the design of the curtain wall. Sizing and quality of the floor slabs, as well as dimensions and spacing of the beams will affect whether the system may be hung or placed on top of the slab. If the system is unitized, there will be a size limitation to the vertical span of each unit. Due to the weight of BIPV panels, it is also important to consider whether the system will be captured on all four sides, or if two sides will be glazed in with silicone sealant. Table 3.1 summarizes the advantages and disadvantages of each type of CW system:

Table 3.1: Advantages and disadvantages of CW systems

CW Type	Advantages	Disadvantages	Typical Frame Detail
Stick Built	<p>Easy to transport</p> <p>Lower shipping cost</p> <p>Less training/ specialization</p> <p>Easier material distribution on site</p> <p>Flexible erection sequence</p>	<p>Less quality control</p> <p>Field installation (sealants, other materials subject to outdoor conditions)</p> <p>Longer install time/more labor intensive</p> <p>Less chance for custom shapes</p> <p>In-plane movement joints</p>	 <p><i>Unicel, Stick built</i> (“Unicel Architectural Manufacturers of aluminum and glazing products,” n.d.)</p>
Unitized	<p>Faster erection and enclosure phase</p> <p>Most of the assembly fabricated in the shop: better quality control</p> <p>Customizable extrusions</p> <p>Design for accommodation of in-plane movements</p>	<p>High shipping cost</p> <p>Fixed sequence</p> <p>Requires extra training for install</p> <p>Larger change error in tolerance during final assembly</p>	 <p><i>Kawneer 2500 UT, 4 Sided SSG</i> (“Products: 2500 UT Unitwall System - Kawneer North America,” n.d.)</p>

Framed and frameless PV modules have advantages and disadvantages in terms of acting as a building envelope element. Table 3.2 below summarizes these points:

Table 3.2: Advantages and disadvantages of framed vs. frameless modules

PV Module	Sample Module Images (“Solar Panel CS6X-P - Canadian Solar,” n.d.)	Specs	Advantages	Disadvantages
Framed	 <p data-bbox="448 957 678 1031">Canadian Solar CS6X-P</p>	<p data-bbox="706 506 927 537">1954 x 982 x 40 mm</p> <p data-bbox="706 552 927 583">Weight: 22kg</p> <p data-bbox="706 598 927 667">Front cover: 3.2mm tempered glass</p>	<p data-bbox="951 506 1172 537">Lighter</p> <p data-bbox="951 552 1172 621">Better stability at inlet location</p> <p data-bbox="951 636 1172 716">No need to protect at perimeter</p>	<p data-bbox="1198 506 1419 667">Thicker panel, less flexibility for installation within glazing pocket</p> <p data-bbox="1198 682 1419 762">Location of j-box is fixed</p> <p data-bbox="1198 777 1419 898">The Tedlar back sheet is permeable to humidity</p> <p data-bbox="1198 913 1419 1171">If the frame is removed, the panel has the strength of a single sheet of glass and loses all certification</p>
Frameless	 <p data-bbox="448 1738 678 1808">Canadian Solar CS6X-P-FG</p>	<p data-bbox="706 1241 927 1272">1968 x 992 x 5.8mm</p> <p data-bbox="706 1287 927 1356">(without J-box or corner protection)</p> <p data-bbox="706 1371 927 1440">1972 x 993 x 10 mm (without J-box)</p> <p data-bbox="706 1455 927 1486">Weight: 27.5 kg</p> <p data-bbox="706 1501 927 1633">Front & back cover: 2.5mm heat strengthened glass</p>	<p data-bbox="951 1241 1172 1310">Glazing pocket could fit wiring</p> <p data-bbox="951 1325 1172 1486">Comfortable for installers to use as typical glass/IGU unit</p> <p data-bbox="951 1501 1172 1818">If STPV possible, can design with regular back glass for a cheaper option Glass-glass is better against humidity, is impermeable</p>	<p data-bbox="1198 1241 1419 1493">Heavier because of the double glass STPV design would depend on company’s ability to do it</p> <p data-bbox="1198 1507 1419 1587">Location of j-box is fixed</p>

3.2.2 BIPV/T Façade on the Courthouse Building

The following project presents the design iterations for the implementation of a BIPV/T facade as part of a retrofit for the Municipal Court Building in downtown Montreal. The system is intended to be installed on the south facade, at the mechanical penthouse. The goal is to maintain a semi-conditioned space behind the new cladding, similar to the functionality of the original facade. Figure 3.5 shows the layout of PV panels over the area of existing metal panels currently covering the south facade of the penthouse. The total area of coverage is approximately 850m².

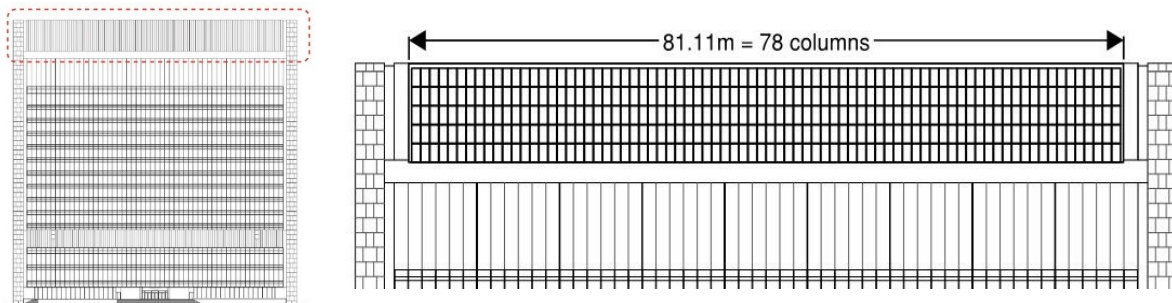


Figure 3.5: South elevation with penthouse area in red box (left) and suggested module layout (right)

The dimensions of the module used in the layout design is shown in Figure 3.6. The horizontal spacing between the panels is 3.54 cm and the vertical spacing is 2 cm. The final layout consists of 78 columns across, each with 5 panels stacked vertically.



- Canadian Solar model CS6X-P-FG
- Dimensions: 1972 mm x 996 mm x 10 mm (without junction box)
- Dimensions: 1968mm x 992 mm x 5.8 mm (without junction box or corner protection)

Figure 3.6: Module dimensions (“Solar Panel CS6X-P - Canadian Solar,” n.d.)

For this project, the existing conditions shaped the design of the BIPV/T system to be implemented. The current facade, which is comprised of corrugated metal paneling, will be removed and the existing structure assessed for reuse. The new cladding system will separate the exterior conditions from an interior unconditioned space which houses mechanical equipment.

This allows for less stringent air infiltration and water penetration requirements. In terms of thermal performance of the facade, the primary concern is to insulate the air cavity inside of the BIPV/T system which transfers the heated air to the HVAC system. Some protection of the inside space against the outdoor elements would result from the new system, but it is not the ultimate goal of the design.

The BIPV/T concept for this application is based on an open-loop system. The outside air is drawn from multiple inlets in the facade, which are optimally sized to obtain as much solar heat as possible from the PV panels on the exterior surface of the facade. Removing heat from the PV panels aids in maintaining their high efficiency. The size of each inlet is approximately 1% of the area of the PV panel. The specific design goals for this project are the following:

- BIPV/T system with multiple air inlets, an insulated cavity and a manifold at the top of the assembly
- Rainscreen approach for reduced stringency of envelope requirements
- Curtain wall approach with metal framing to replicate existing cladding
- STPV incorporation
- Aesthetically pleasing design to unify new system with existing facade

In order to assist with maintaining a unified look of the facade, using STPV modules was proposed. A STPV with a transmittance of 10% still allows for 90% of the incoming solar radiation to be absorbed, while the remainder passes through the module and heats the back surface of the air cavity, which can be painted to match the existing color of the facade curtain wall framing. These details are shown in Figure 3.7.

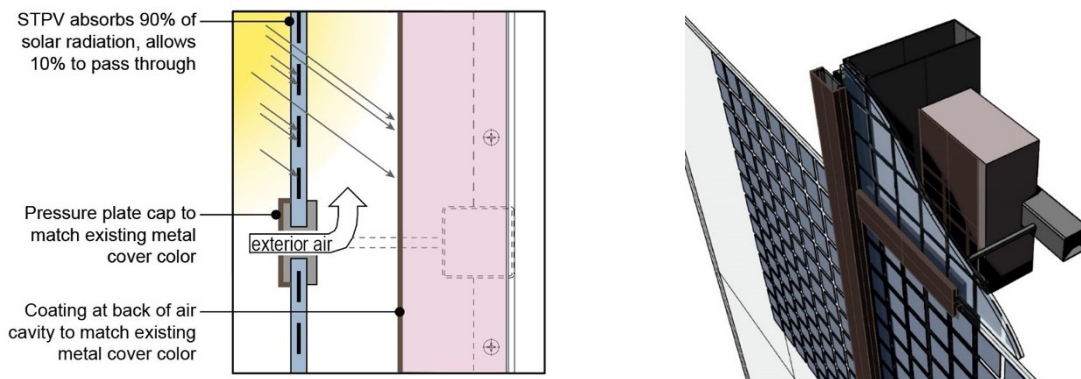


Figure 3.7: STPV used as modules (left) and rendering of STPV and painted backpan (right)

One major impact to the design is the structural framing. The sizing and quality of the floor slabs, spacing and dimension of the beams, as well as the removal of the steel framing will affect whether the system may be hung or placed on top of the floor slabs. The current design shows the curtain wall framing attached outboard of the floor and ceiling slabs, with a dead load attachment proposed at the roof slab, lateral bracing at the floor slab and additional steel supports diagonal to the middle of the wall. The secondary structural consideration is that of each individual panel (or set of panels) to the vertical framing. While the vertical framing will contain the panels within the glazing pocket as a typical curtain wall system, the horizontal mullions will be a custom shape and attachment. The typical horizontal mullion will be scaled back to allow room for the air cavity and insulation, and with the use of rods, attached to the front inlet caps. This is shown in Figure 3.8.

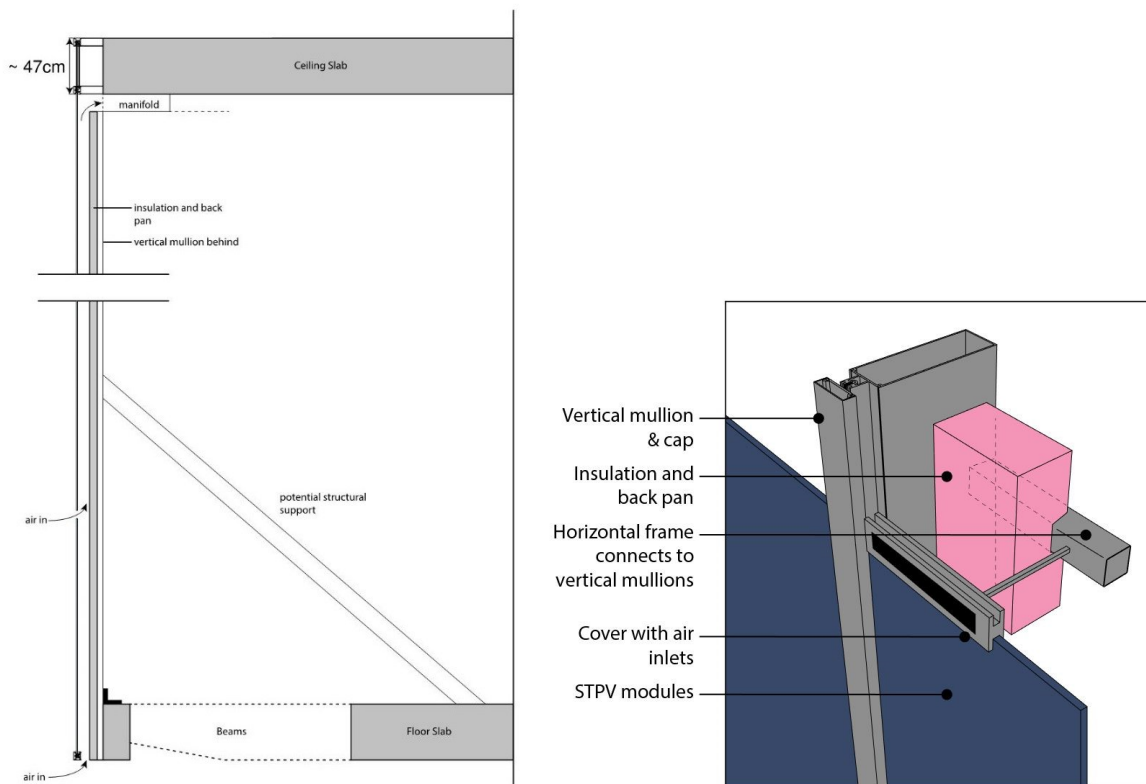


Figure 3.8: Structural attachment of the BIPV/T system (left) and horizontal tie-backs at inlet framing (right)

One important decision in the design process was the selection of the curtain wall system type to be used; stick-built or unitized. For this specific layout, if a unitized system is selected, it is expected that each unit will be 2 to 3 modules tall and separated by the vertical mullions. This configuration as well as unitized details for the BIPV/T module are shown in Figure 3.9.

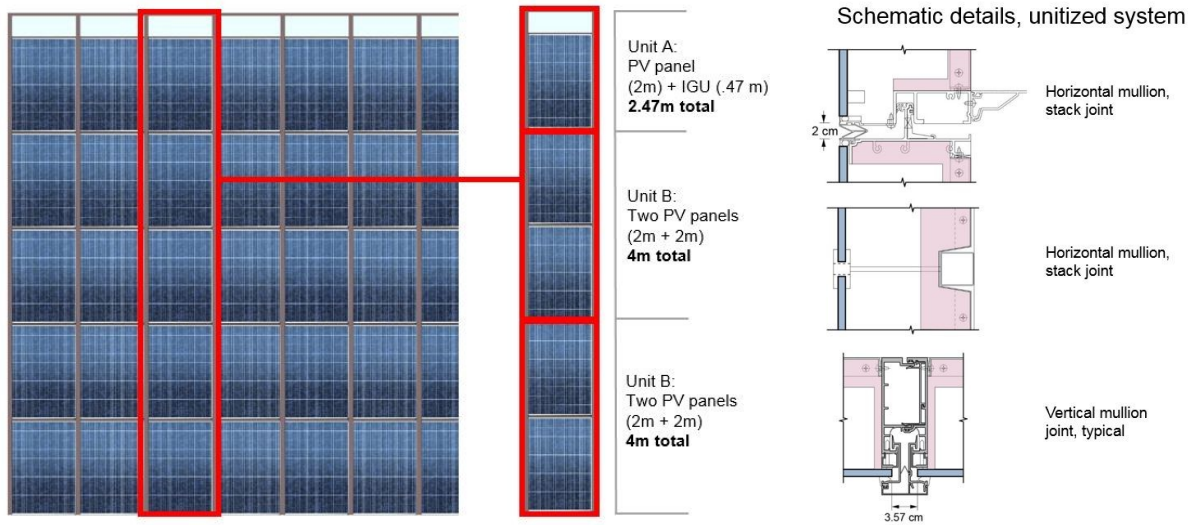


Figure 3.9: Unit distribution for unitized system (left) and typical unitized details for the BIPV/T (right)

Both framed and frameless PV panels were considered for this design. In the end, frameless panels were chosen. Figure 3.10 shows the components of the frameless proposed unit and how the assembled product would be installed on site:

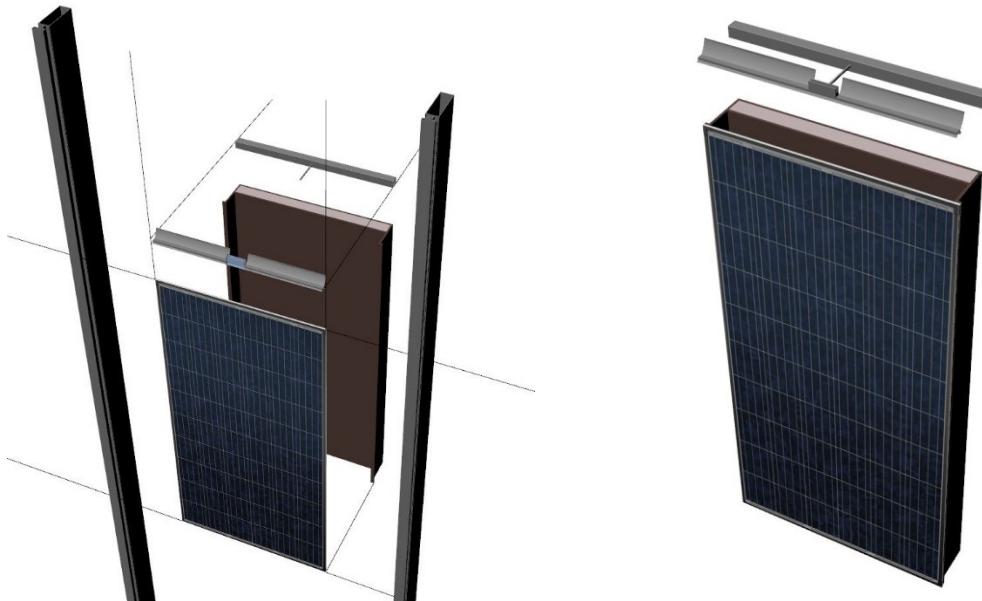


Figure 3.10: Components of a unit in a unitized system (left) and unit and horizontal cap prior to install (right)

Some of the considerations and challenges that were encountered during the development of this project include:

- Ability of the curtain wall manufacturer to produce custom extrusions and fabrication of units in their shop
- Options for lowering the overall project costs by replacing the proposed mineral wool insulation with styrofoam (maintaining an R-5 performance), framing without thermal breaks, and a module without an airtight back pan
- Minimizing the shadow on the PV cells by reducing the thickness of the pressure plates and caps
- The option of perforated screens in the air inlets as a dual purpose; to mitigate the amount of debris that collects inside of the air cavity and also to keep out birds and insects, which is a common problem with perforated claddings
- If the unit fabricated in the shop includes the PV module, air cavity, insulation and back-pan, a method to access the back of each cell and the wiring needed to be developed for maintenance once the system is installed
- The panels are connected vertically in series according to the design, so if there is a disruption in energy production, only five of the panels in one column are disconnected and reviewed. The purpose of this is to facilitate troubleshooting and access to panels.
- The advantages and disadvantages of using STPV modules instead of regular opaque modules
- The advantages and disadvantages of framed and frameless modules for this particular installation

The three optimization goals of this project were:

1. Engineering of the system performance, including electrical and thermal efficiencies
2. Structural integrity using the existing materials and framing
3. Facade aesthetics to unify the BIPV/T technology with the building's current style

In conclusion, there were several developments that were the focus as the design of the BIPV/T progressed. The use of heat transfer enhancement mechanisms, such as wire mesh inside of the air cavity for improved thermal efficiency of the system, is one factor. Another is the level of airtightness agreed upon for the system, one that is financially responsible without compromising thermal efficiency. The team planned to move forward with the design of a unitized system for the curtain wall since it has the most benefits and falls in line with the bigger goal of

developing a unit flexible for various applications on facades. Several companies were reviewed which would be able to supply the PV panels. One of the major components of the design development was the plan to build and test a prototype of several units connected. The prototype would be scaled down to an approximate height of 3 meters to be tested in the solar simulator. There was also a plan to test it in the rain penetration chamber. Several other tasks involved in moving forward included taking field measurements for an accurate curtain wall framing design and unit layout. Photographs were obtained of the building during daytime and nighttime for rendering and visualization purposes (Figure 3.11).



Figure 3.11: Actual south facade (left) and visualization of BIPV/T cladding at penthouse level of the facade (right)

3.3 Solar Decathlon BIPV/T Roof

3.3.1 Roofs

Curtain wall BIPV/T systems also have the potential to be applied to low-slope roofs as new roofing systems, or as retrofits. Although a low slope keeps the traditional flat roof look, a slope close to latitude is preferred for optimal electrical and thermal performance. The design developed for the Solar Decathlon reflects these aspects.

3.3.2 Solar Decathlon

For the 2018 Solar Decathlon China competition, a team of students and professors from Concordia University and McGill University conceptualized a residential home with a BIPV/T roof system, the design of which was based on building energy needs. The design of a BIPV/T

system on the south roof is an improvement beyond the original intent of a typical sawtooth PV array. Due to the requirement of a skylight, and to conform to the maximum allowed building width, several configurations of PV panels were studied in terms of capacity, skylight placement and framing system (Figure 3.12).

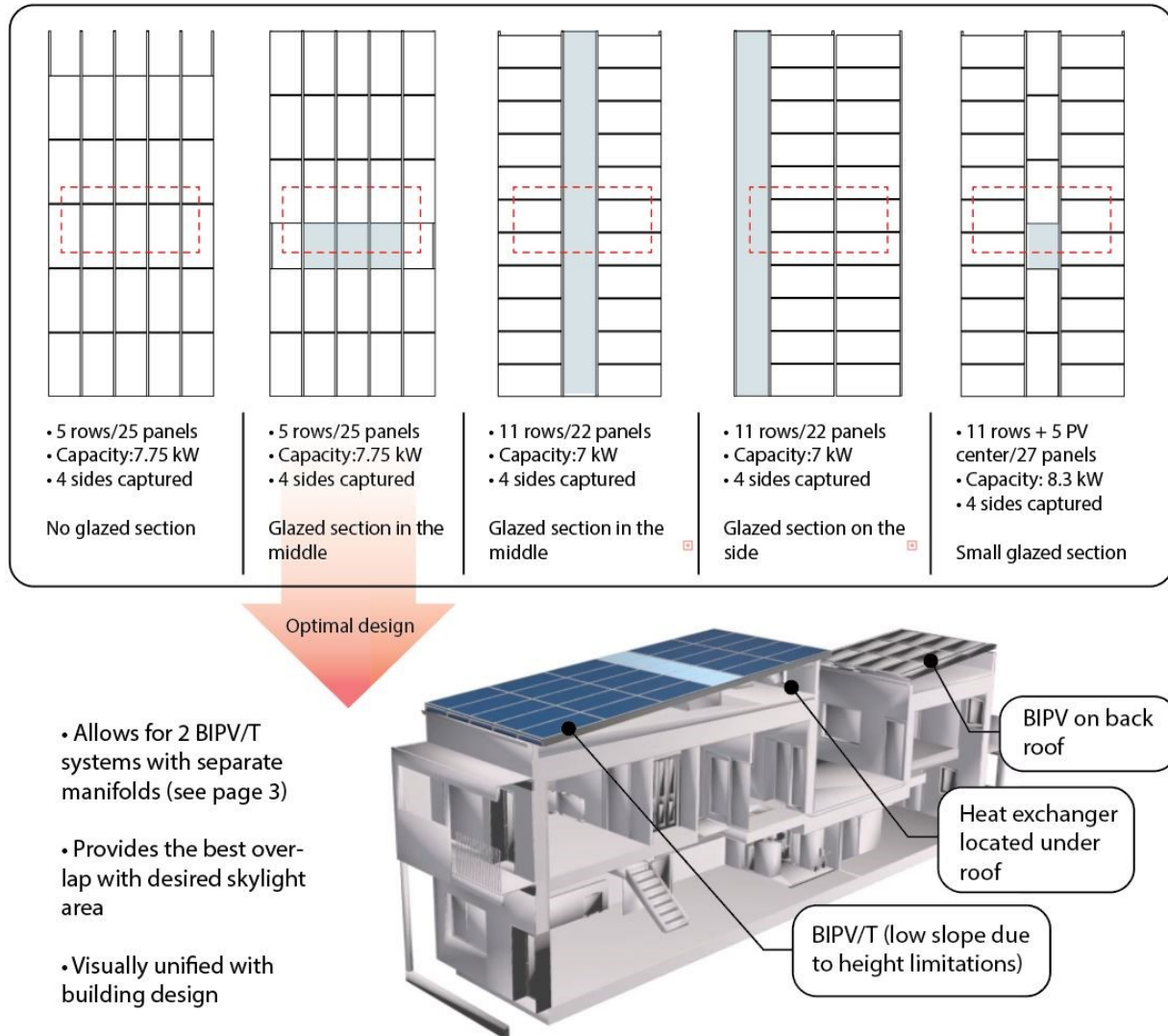


Figure 3.12: Configuration options for Decathlon roof and rendering of final design.

The BIPV/T roof is divided into two sections by the skylight in the middle, which allows daylight to enter the second floor corridor through a light well (Figure 3.13). The original concept had the goal of keeping the skylight operable to allow for ventilation, and the BIPV/T would be two separate systems; one to the front of the skylight and one towards the back. Each of these systems would have an individual, uninterrupted air channel. This division into two systems is

beneficial for the PV production because it keeps the air channels short, maintaining relatively low air temperatures inside. Further modeling was carried out to determine outlet temperatures.

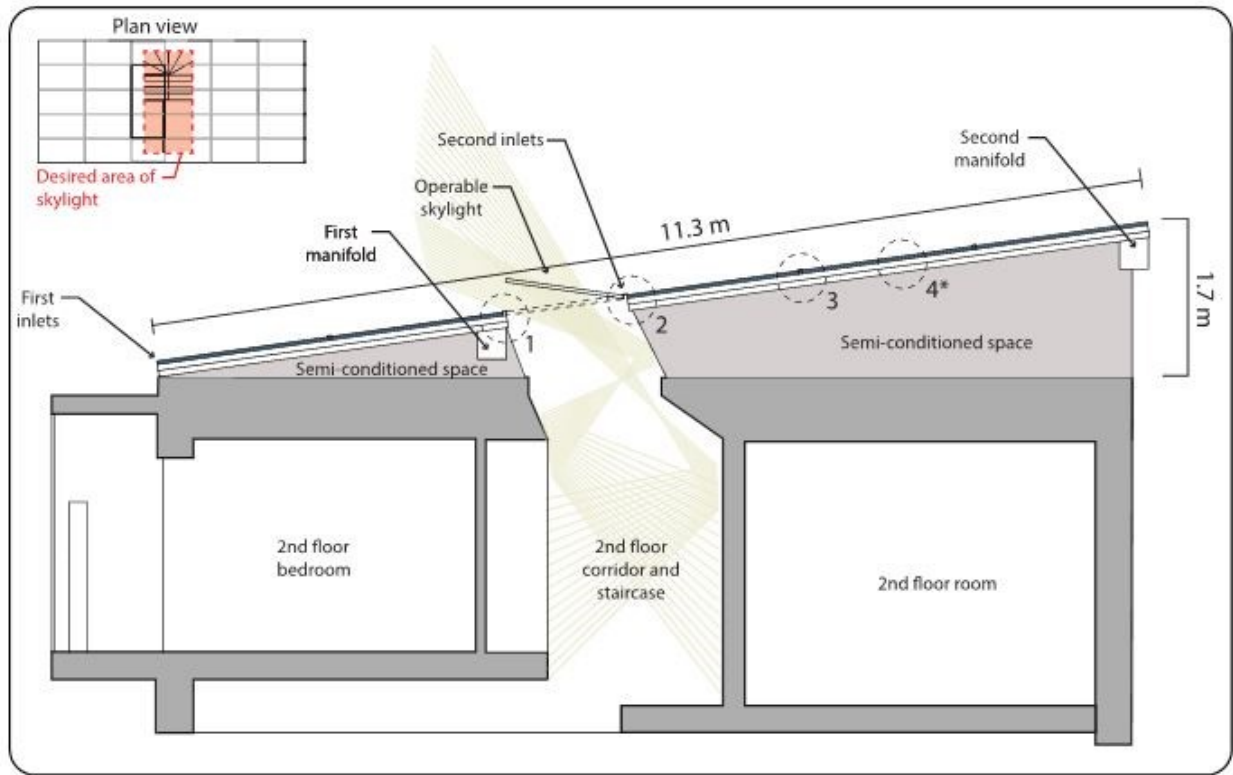


Figure 3.13: Section through BIPV/T roof and skylight

The details in Figure 3.14 show design resolutions for the framing system. Detail 1 shows an extrusion profile that addresses incidental rainwater drainage when the skylight is open. Detail 2 shows a horizontal detail at an air inlet, where a custom extrusion is shaped to direct the incoming air towards the back of the PV panel as well as collect water and pass it to the vertical mullions for drainage. Detail 3 describes a typical horizontal detail, in which the framing purlin will act as a “fin” to further mix the air in the channel for increased thermal efficiency.

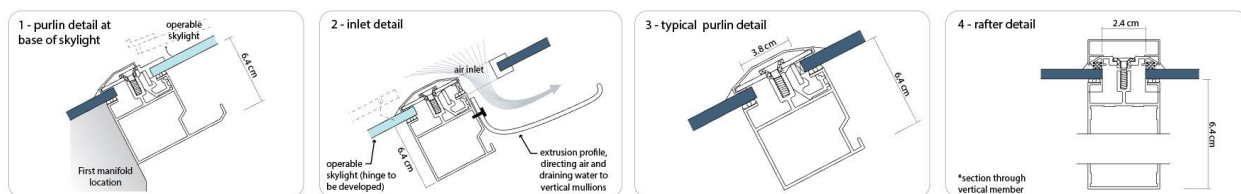


Figure 3.14: Architectural details of the BIPV/T framing system

The PV panels are 1954 mm in length and 982 mm in width. The framing system accommodates for the expansion of the panels and auxiliary materials, but these types of aspects are always verified with curtain wall manufacturers. The profile of the caps covering the pressure plates can be adjusted to reduce self-shading. The manifold connected to the upper ends of the air channels transfers the heated air to an air-to-water heat exchanger, and equipment location, size and placement was later clarified by the Decathlon team. The space under the panels and insulation is to be semi-conditioned. Figure 3.15 shows a schematic of the individual materials and layers of the BIPV/T system.

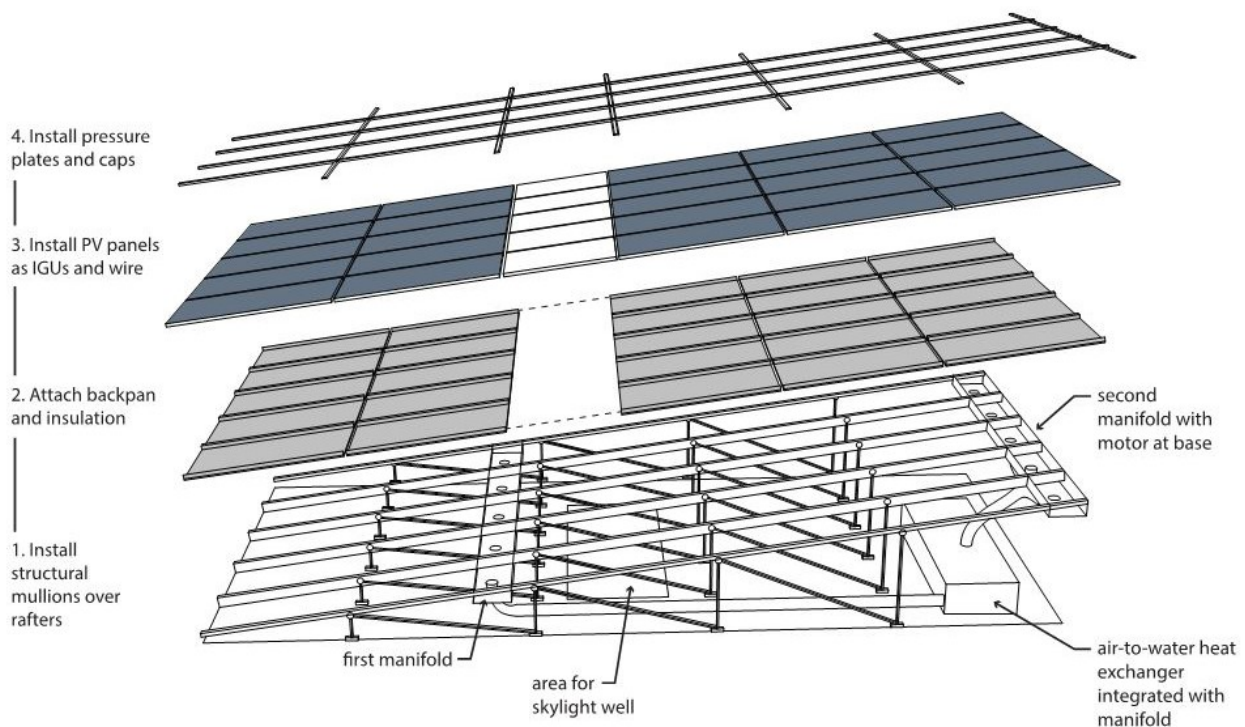


Figure 3.15: Exploded axonometric diagram of original BIPV/T system layers and materials. The final design had a continuous channel and one manifold at the back end.

The building was constructed during the summer of 2018 as part of the Solar Decathlon competition held in Dezhou, China. Photographs of the Deep Performance Dwelling (the name given to the project by the team) and the installed BIPV/T roof are shown in Figure 3.16. The final slope of both roofs was 5° due to height constraints for the building. A tilt of 40° would have been optimal for maximizing incident solar radiation as well as reducing snow accumulation.



Figure 3.16: Deep Performance Dwelling aerial view (left) and BIPV/T roof after completion (right) (Rounis et al., 2017)

The BIPV/T roof provides its thermal energy to a water-to-water heat pump in order to reduce the temperature difference between the two tanks. The manifold at the end of the BIPV/T draws from each air channel through two take-offs and connects to one main duct leading to an air-to-water heat exchanger, which is then connected to the water-to-water heat pump (Rounis et al., 2017).

3.4 BIPV/T Roof Retrofits for Residential Low-Rises in India

The IC-Impacts collaborative project was an opportunity to study BIPV/T applications for rooftop retrofits in residential sectors of India. The India-Canada Centre for Innovative Multidisciplinary Partnerships to Accelerate Community Transformation and Sustainability (IC-Impacts) is a center of excellence, which focuses on research to improve sustainability within Canadian and Indian communities. The goal of this particular research is to identify optimal configurations of building technologies suitable for the local climate and to aim for the design of a net-zero energy building by utilizing local energy generation from renewable sources. Specifically, the project involves the design and modeling of a low-rise residential building in the city of Chennai, India.

3.4.1 BIPV/T Retrofit Concept

With the percentage of new building construction lowering in relation to the existing building stock, retrofits are becoming an attractive option for many property owners, both commercial and residential. BIPV/T systems can be designed for retrofits, especially with CW assembly components. The option for over-cladding or recladding allows for commonly used construction practices, and gives the possibility to turn semi-conditioned spaces or unused spaces

into fully enclosed conditioned spaces, with the insulating benefit of BIPV/T systems (Figure 3.17).

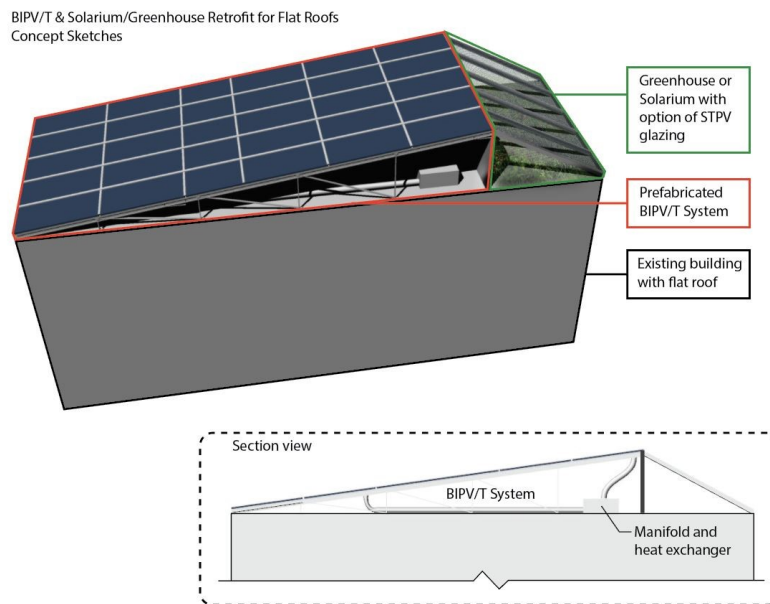


Figure 3.17: Roof retrofit as solarium

3.4.2 IC-Impacts Project

India is one of the top energy consuming countries in the world, after China, the United States and Russia. However, the country's per capita electricity consumption is less than one third of the world average. In acknowledgement of this as well as the rapid rise of technologies used to harness solar energy, the Indian government has recently initiated policies to encourage the use of photovoltaic (PV) and building-integrated photovoltaic (BIPV) systems for local energy production. While the country does get as many as 300 days of sunshine a year, it is densely populated with little land available for solar parks. Because of this limited land availability and largely accessible unused roof space, rooftop PV systems are especially garnering attention (Shukla et al., 2018).

The Indian government has set goals to produce 100 GW of solar energy by the year 2022, and 40% of this will come from rooftops, which is now the fastest growing technology in the clean energy sector, and is cheaper than commercial and industrial power in India (The World Bank, 2017). The current issue is that while the rooftop projects for commercial buildings are rapidly

advancing, solar for residential buildings is falling behind due to large upfront costs and net-metering programs (Un, 2017).

Net-zero energy buildings, while using a variety of passive methods to decrease energy use, also need active energy production, which is often achieved by including solar energy as part of the design. This project conceptualizes a BIPV/T cladding for the building which is more efficient than a typical rooftop system and replaces some of the building cladding components, lowering the critical up-front cost of material and installation. Since India is one of the leading producers of aluminum, it would be acceptable to use aluminum curtain wall framing to contain the PV panels.

Chennai is located in the southern part of India, in the state of Tamil Nadu. At the geographical coordinates 13°N, 90°E, this coastal city is close to the equator and has a warm-humid climate. As shown in Figure 3.18, the annual global horizontal irradiation is 1,957 kWh/m², while the average air temperature is over 28°C. The annual direct normal irradiation is 1,377 kWh/m² and the annual diffuse horizontal irradiation is 935 kWh/m².

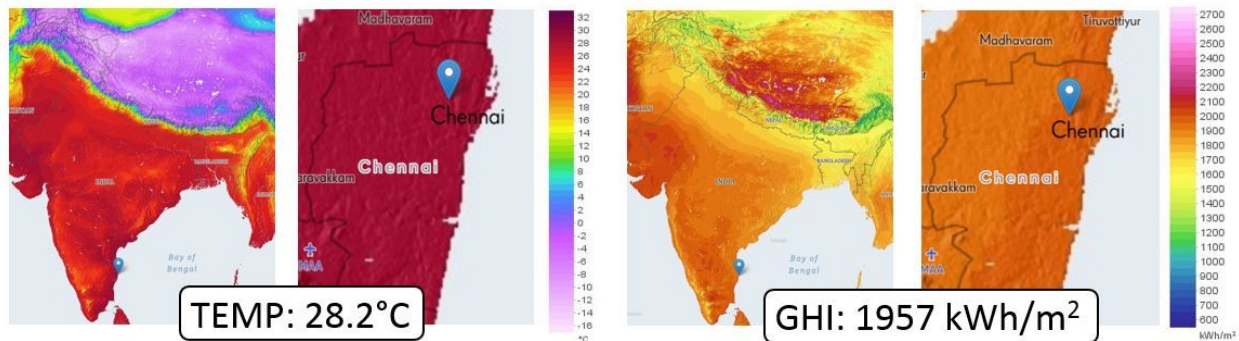


Figure 3.18: Radiation and temperature maps of Chennai, India (The World Bank, n.d.)

Average air temperatures for Chennai vary between 24°C in the winter months and up to 32°C in the summer, making this a cooling dominated climate (Figure 3.19).

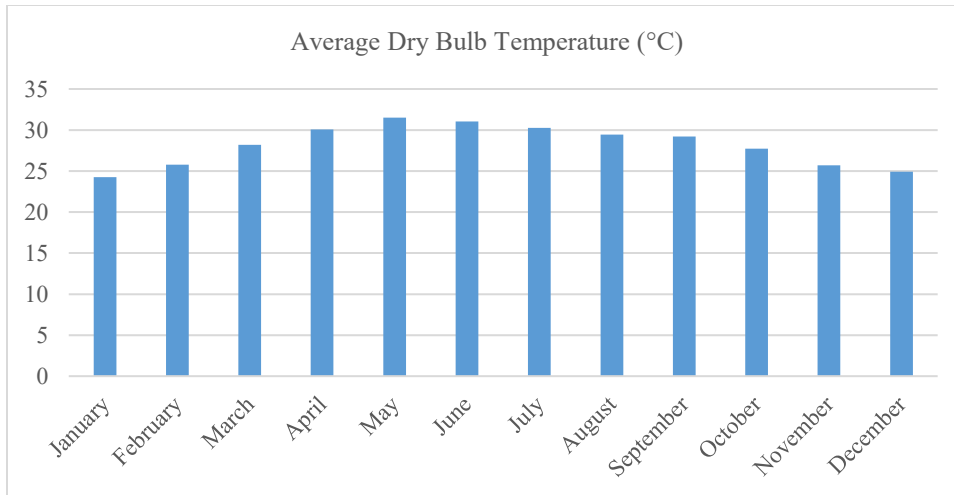


Figure 3.19: Monthly averages for air temperatures in Chennai, India

For a location such as Chennai, a PV system would need a low slope to maximize incident radiation. A 13° slope is favorable, but a lower slope would also be beneficial, due to dominating diffuse radiation. This is due to higher cloud cover in the summer months during the monsoon season. The global horizontal irradiation (GHI) follows a typical pattern throughout the year (Figure 3.20).

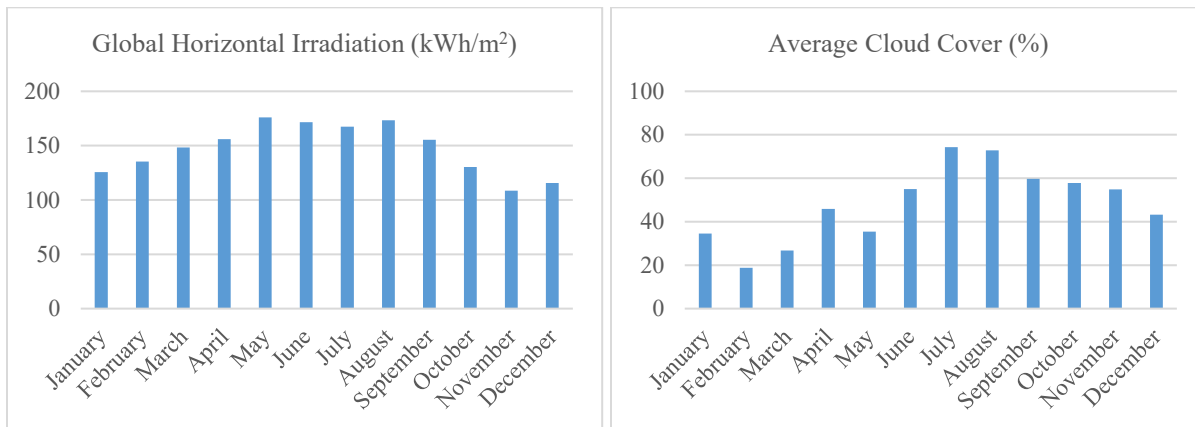


Figure 3.20: Monthly total for GHI (left) and percentage of sky covered by clouds (right)

Building typologies of the state of Tamil Nadu were studied for patterns in existing residential structures. Among the most common are reinforced concrete structures with unreinforced masonry infill walls. The buildings are often aligned at the front street facade and have narrow plots on which they sit. Several representative buildings are shown in Figure 3.21.



Figure 3.21: Building typologies in the state of Tamil Nadu (National Disaster Management Authority, 2013)

Initially for the study, four apartment buildings were selected as representative samples from both Nagpur, which has a composite climate, and Mumbai, which has a warm and humid climate. Specific to the city of Chennai, India, two types of building typologies were reviewed. One is a typical low-rise, 4-story building consisting of four apartments and retail or parking spaces on the ground level. Each floor is 55 m² by 45 m². The available rooftop area is 220m² and the western half of the south wall has no windows. The second typology is a 3-story single family home with parking on the ground floor. An energy analysis was performed on the first typology. The building envelope properties for energy analysis were selected based on BEEP (2016) Design Guidelines for Energy-Efficient Multi-Story Residential Buildings: Warm-Humid Climate (BEEP, 2016). Results show an average annual energy use intensity of 156 kWh/m². Only a base case building has been modeled (Figure 3.22). Improved insulation with a roof RSI of at least 1, double-glazed windows, and an airtight building design will significantly lower the energy use. The energy model is based on ideal control with an assumed constant cooling coefficient of performance (COP) of 2.5 for the heat pump.

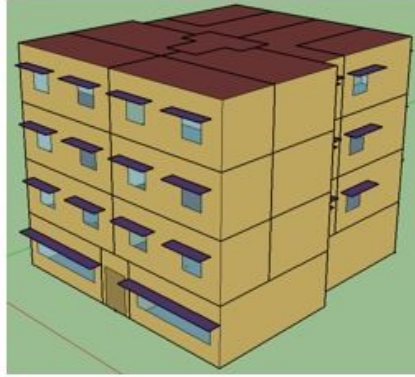


Figure 3.22: Building schematic of base case design (BEEP, 2016)

For this building design, the application of BIPV/T could extend not just across the roof but also over 97m² of the south wall. Different layouts were studied for rooftop PV applications and the BIPV/T layout was determined to not only have maximum area but also receive the most annual radiation (Figure 3.23). Preliminary calculations showed that for the design shown in the bottom right of Figure , the annual AC energy production would be approximately 46,781 kWh for a system sloped at 13° with both roof and wall coverage. However, it was decided to use only the roof portion available for BIPV/T system.

B

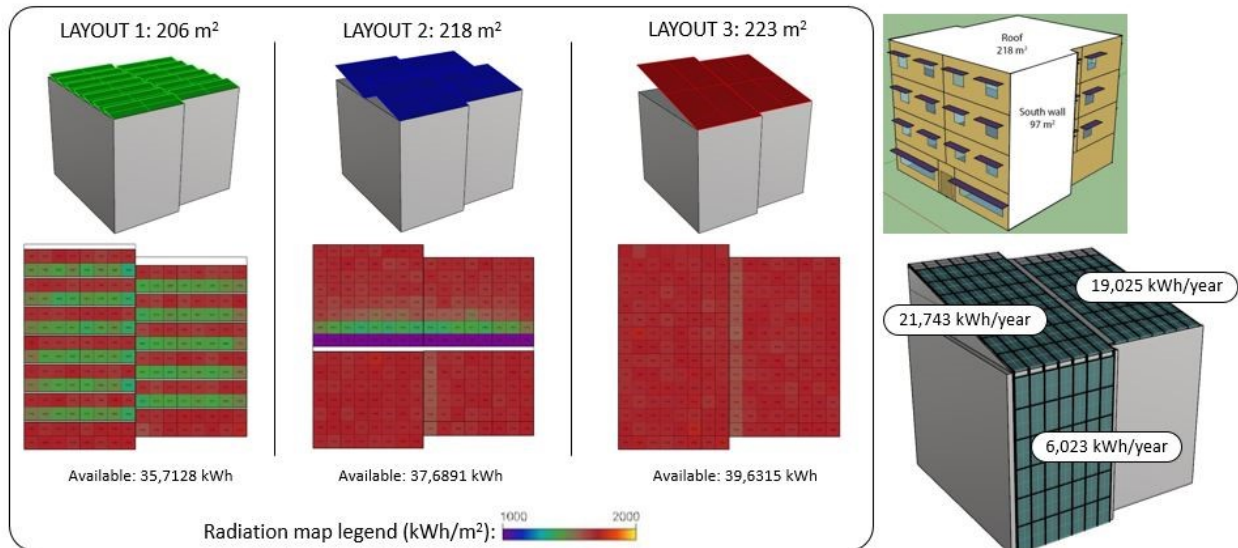


Figure 3.23: Various rooftop PV layouts and total coverage of BIPV/T system

A typical reinforced concrete building frame requires a lightweight BIPV/T framing system with simple attachment methods at the roof. The project features a low-sloped BIPV/T roof of approximately 13° which is optimal for near equatorial latitudes. The design includes an insulated air channel, allowing air to flow through it and cool the PV panels, which serve as the outer layer of the cladding. A manifold collects the preheated air from the air channel(s) to be utilized depending on the coupling with the HVAC system. Figure 3.24 shows the layout and capacity of the designed BIPV/T system.

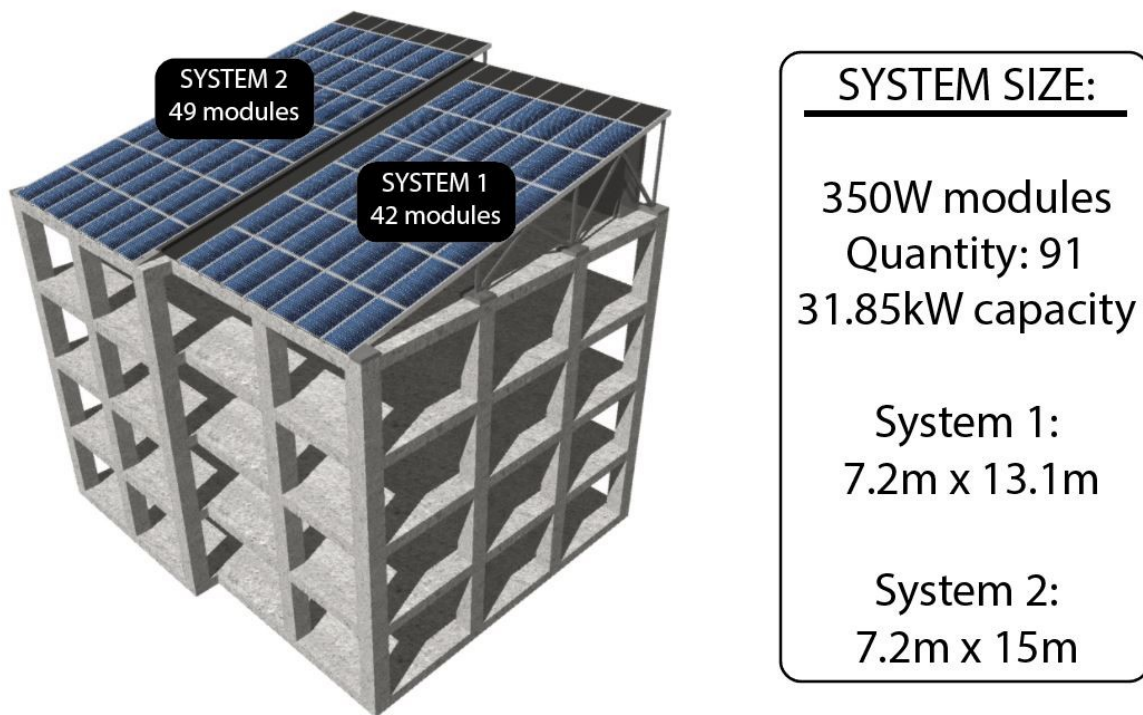


Figure 3.24: Size of BIPV/T rooftop system

The housing for the water storage tank (which takes up approximately 20% of the rooftop), air collecting manifold and heat exchanger must all be positioned in a way that it does not interfere with the continuity of the BIPV/T system. Available area for the mechanical equipment was determined under the system (Figure 3.25). Due to the hot climate, any resulting hot air from the system will best be used in a vapor absorption refrigeration system since the building needs to be cooled far more than heated.

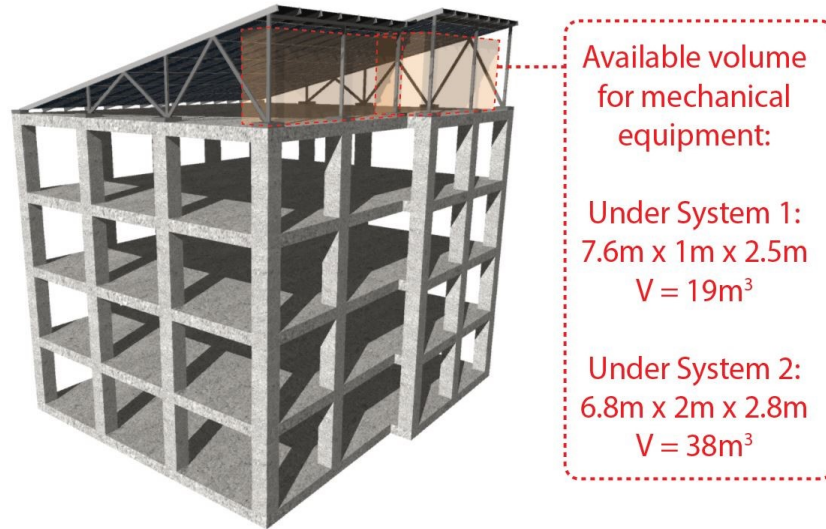


Figure 3.25: Available area under BIPV/T system for mechanical equipment

Figure 3.26 shows an architectural section through the BIPV/T roof, indicating a simple framing attachment to the reinforced concrete building frame. The sides of the system would be open to allow for some air movement as closing this space with paneling would increase the temperatures between the BIPV/T system and the roof.

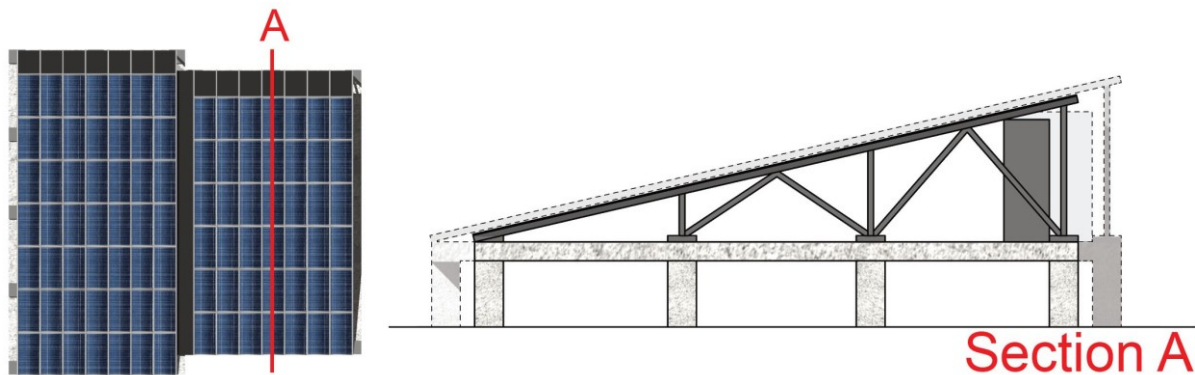


Figure 3.26: BIPV/T Plan view (left) and section through the system, framing and building structure (right)

Performance calculations were performed based on a dynamic model designed for a BIPV/T facade, vertical and inclined (Athienitis et al., 2018; Rounis et al., 2016). For System 1, which is approximately half of the entire roof system, an annual electrical production of 20,362 kWh/year and an annual thermal production of 22,115 kWh/year is expected (Figure 3.27).

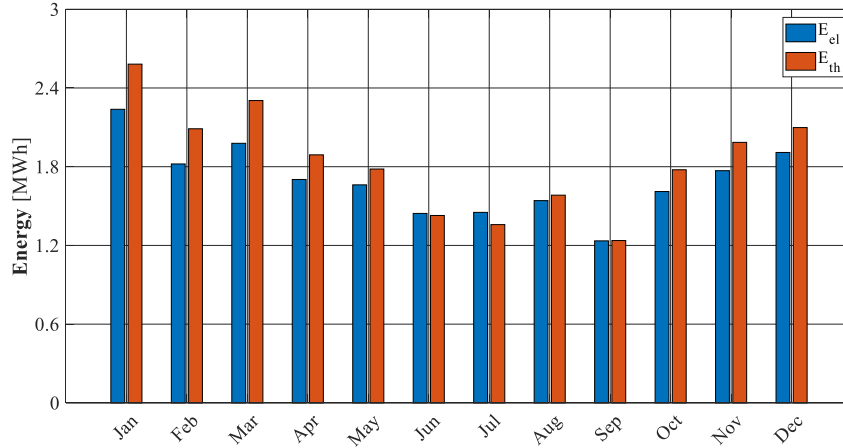


Figure 3.27: Monthly electrical and thermal energy production for BIPV/T System 1

The frequency of air outlet temperature occurrences is shown in Figure 3.28 for various temperature intervals. This represents the hours that outlet temperature is within a certain bracket out of the total hours (8760) throughout the year. While there is a large frequency of outlet temperatures in the lower ranges (16°C - 20°C, 21°C - 25°C), this is occurring during the hours when there is no incident solar radiation and the BIPV/T system is not operating. What is relevant is the number of hours when the outlet air is above 50°C. The heat extracted from air of this temperature can be used in a thermally driven cooling system. However, it is important to reduce building energy loads by passive design strategies prior to implementing energy generating technologies such as BIPV/T.

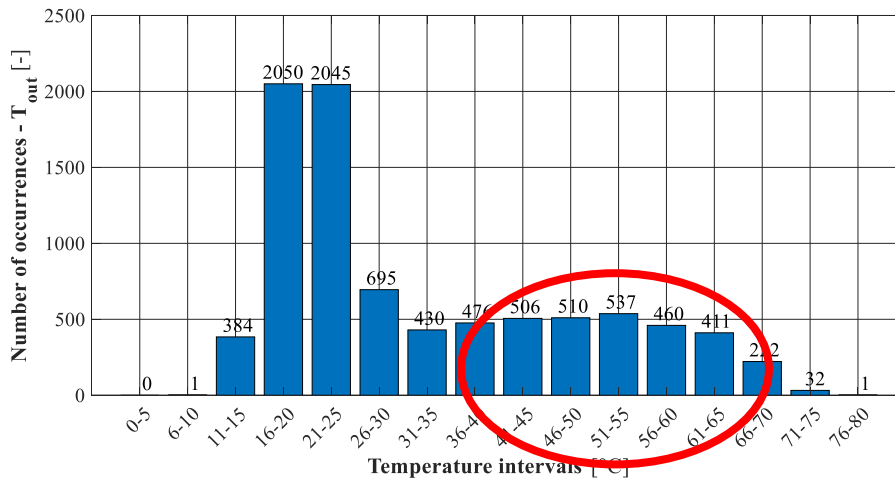


Figure 3.28: Air outlet temperature occurrence frequencies of the BIPV/T throughout the annual period, on an hourly basis


3.5 Key Elements of Case Studies


Key parameters, criteria and constraints of the three case studies are discussed in Table 3.3. The commonalities of these projects include:

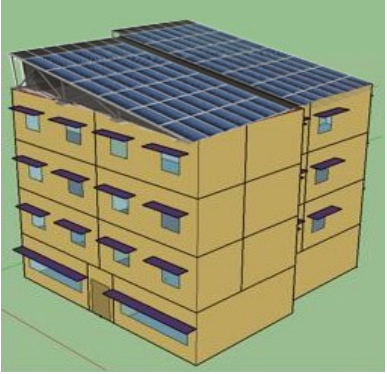
- Production of electricity and preheated air
- Retrofits onto existing buildings (Courthouse, IC-Impacts)
- Low slope roof applications (Decathlon, IC-Impacts)
- Standardized curtain wall framing incorporating the PV modules as glazing
- Locating manifold and heat exchanger directly under the system (Decathlon, IC-Impacts)

It is important to note that although the IC-Impacts roof design has a low slope, it is due to the latitude of the project location, and not the height limit. The Solar Decathlon design, however, is low slope exactly because of the height limit. The skylight featured in the Decathlon displays the novel ability to have a continuous BIPV/T system with glazing, whereas in previous built projects, such as the Varennes library, it was not feasible to incorporate such components. This project also considered a gutter design, which although not realized in the final construction, brings to light the importance of detailing that applies to both conventional and innovative works.

Table 3.3: Summary of Case Studies

Case Study	Key parameters	Criteria and Constraints	Schematics/Photos
Courthouse Façade Retrofit	Location: Montreal, Quebec, CA Climate: Very cold, humid BIPV/T slope: 90°	<ul style="list-style-type: none"> • Retrofit: conform to original façade dimensions • CW framing painted to match existing façade colors • Location directly at mechanical penthouse simplifies manifold ducting 	

Solar Decathlon Roof	Location: Dezhou, China Climate: Cold, humid BIPV/T slope: 5°	<ul style="list-style-type: none"> • Low slope due to building height restrictions • CW framing • Custom manifold sized to fit under roof along with heat exchanger 	
-----------------------------	---	--	---

IC-Impacts	Location: Chennai, India Climate: Hot, humid BIPV/T slope: 13°	<ul style="list-style-type: none"> • Challenge of utilizing preheated air from BIPV/T • CW framing, lightweight • Reduction of heating loads on roof is important • No height limit 	
-------------------	--	---	---

3.6 Design Methodology

According to the Whole Building Design Guide, the steps for designing a BIPV system include consideration of energy-conscious design practices, a choice between a stand-alone and utility-interactive PV system, review of daily electricity use to shift the peak load, providing adequate ventilation of the PVs, consideration of PVs as shading devices following a daylight analysis, designing the system for a local climate and environment (and addressing site planning and orientation issues that may affect this), and reducing the building envelope or other on-site loads (Mike Carter, C.E.T. and Roman Stangl, 2016). For a BIPV/T system, there is also the added consideration of fan use for drawing in air, placement in relation to electrical service areas, and integration with heat recovery systems.

In the bigger scope of designing net zero energy buildings (NZEBS), an integrated approach to all system design is critical. Equally important to designing with renewable energy sources is designing with an energy efficient method. Energy generated by renewables does not necessarily match grid production and can cause load instability when excess electricity is returned (Dermardiros, n.d.). While using batteries for electrical storage is a good option, it is expensive and not always sufficient. Exporting electricity to the grid should be done in conjunction with assessment of peak hours for both energy use and grid demand.

3.6.1 Building Envelope Requirements (Facade Requirements)

Common building typologies and established building envelope techniques guide the BIPV/T design from an architectural standpoint. It is important to consider that as a building material, the PV system must be considered for primary functions of the building envelope including dead, live and other loads, compatibility with other facade materials, thermal insulation performance, air and water resistance, fire safety characteristics, and soundproofing. The insulation of the air cavity of the BIPV/T system should be adjusted to meet thermal and code requirements such as assembly test method NFPA 285 (NFPA, 2012). Due to the size and continuity of the air cavity of this type of system, non-combustible insulation such as stone wool or mineral wool can be used, as well as fire stops at floor edges, to address the concern of vertical and lateral fire propagation on the exterior cladding (Lstiburek, 2017). Also, since the BIPV/T is not producing heat at night, the insulation must be at minimum sufficient as part of a passive wall assembly. This is even more important for systems which rely on the PV glazing thermal

performance, which is known to have a higher U-value than single glazing (Scognamiglio, 2017). Other aspects, such as water management, drainage, and insect and bird protection which are especially important to a rainscreen facade, must work in parallel with any electrical/thermal optimizations designed for the air channel.

For the purpose of conventional facade constructability, the installation sequencing and accessibility for maintenance after the system is in place are important. In terms of constraints from the industry, the design is susceptible to PV and PV framing technology limitations, manufacturing availability, and architectural as well as aesthetic aspects (color, texture, finish, visual conformance to other facade appearances) that come to the forefront during design development phases of projects.

3.6.2 PV System – Performance Requirements (Electrical and Thermal Efficiency)

For a BIPV/T system, the electrical efficiency of the system is of primary importance. This is because electrical output produces a higher quality energy than the thermal output. Thermal efficiency is also important and can be enhanced and optimized with methods to increase thermal extraction. Parameters such as building orientation and wall area geometries are less flexible and will affect BIPV/T layout and sizing and system shading, determining the electrical output. Various PV technologies, such as mono-crystalline silicon or poly-crystalline silicon, will also have an impact on electrical efficiency.

For a given BIPV/T roof length, the temperatures of the PV modules and the air at the outlet will be dependent on solar irradiance, the wind speed and ambient temperature of the environment, and the air velocity inside of the channel (Chen et al., 2010). Cooling of the PV through natural ventilation is typically inefficient as it only occurs through buoyancy or wind, while mechanical cooling with the use of a fan to draw air in must consider the net electrical efficiency after fan energy use is considered. For this, fan optimizations which involve calculating the fan speed and air pressure drop can be employed. Fan consumption is typically not more than 5% of the energy recovered from a BIPV/T system (Athienitis et al., 2010).

Design of the manifold to collect air is an optimization problem of reducing space, pressure drop in the air channel and fan energy consumption. As was shown in the JMSB building, location in relation to the HVAC system is very important. Collected air can be used with heat recovery

ventilators, water heating in an air-to-water heat exchanger, or directly for space heating. Depending on proximity to one of these applications, duct sizing and location will be determined.

For electrical efficiency, the effect of PV surface temperatures is reflected in the following equation:

$$\eta_{el} = \eta_{stc}(1 - \beta_{PV}(T_{PV,S} - T_{ref})) \quad (3.1)$$

where

η_{el} (%), PV electrical efficiency;

η_{stc} (%), PV electrical efficiency under standard testing conditions;

β_{PV} (0.45%/°C), PV module temperature coefficient for poly-Si (Athienitis et al., 2015);

$T_{PV,S}$ (°C), surface temperature of the PV and

T_{ref} (°C), PV reference temperature (25°C at STC).

This, in turn, affects many aspects of BIPV/T design to focus on reducing the PV temperatures. Even the location of the project in terms of the built environment can have an effect. In a 2006 study, it was determined that due to urban pollution and consequent reduced radiation on PV surfaces, the PV temperature conversion efficiency is actually improved (Tian et al., 2007).

Besides reducing the PV temperatures, other factors are also important to consider. Frame shadowing, even of a small frame, can significantly decrease the electrical efficiency. In a study on the effects of frame shadows on BIPV/T systems, a 39.3% decrease in electrical efficiency was found as a worst case scenario (Wang et al., 2017).

Figure 3.29 shows a diagram of a thermal network model for a BIPV/T system. The components included in this model are: the PV module, the air channel, the insulation at the back of the channel, and the ambient environment which surrounds the BIPV/T. Energy balance equations determine the interactions between these components to characterize a steady state condition.

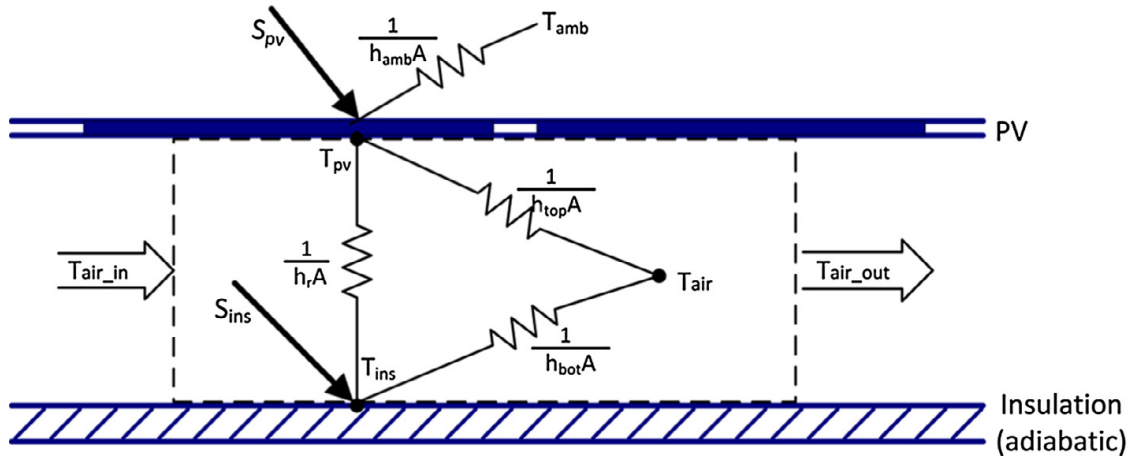


Figure 3.29: Thermal network diagram of a BIPV/T system in section (STPV option is possible) (Yang and Athienitis, 2015)

The total thermal energy extracted by the air flowing through the BIPV/T channel extracts heat from both front and back surfaces:

$$Q_{air} = \dot{m}c_p(T_o - T_i) \quad (3.2)$$

where

Q_{air} (W), thermal energy recovered by the circulating air;

\dot{m} (kg/s), mass flow rate of the air;

c_p (J/kg°C), specific heat of the air;

T_o (°C), Temperature of the air at the outlet and

T_i (°C), Temperature of the air at the inlet.

The thermal performance of the system can be enhanced by various techniques, such as double glazing, use of fins, and other methods discussed in the introduction. However, unlike for a solar thermal collector, these optimization and enhancement techniques should be chosen based on the acceptable upper threshold for PV surface temperatures, system durability and taking into account the intended purpose of the system, which may be a heat exchanger, a heat pump, direct integration of the pre-heated air to the air conditioning system in the winter months, or for domestic hot water heating during warm summer months. The selection of the flow rate as well as the heat

transfer characteristics of the back surface of the air channel can highly impact the performance of the system (Zogou and Stapountzis, 2012).

3.6.3 Standards for BIPV/T Performance

One of the biggest challenges to BIPV/T production is the lack of a unified performance standard. There are currently standards for electric performance of PV panels, air and liquid solar/thermal collector performance, even BIPV performance, but no standard exists for the performance of a PV/T system. Table 3.4 lists some of the existing standards related to PV and BIPV technologies.

Building on some of the existing standards, such as the more recent EN 50583, adding requirements from building envelope testing standards (for air infiltration, water penetration, and thermal performance) and extracting useful correlations from the experimental data, a set of guidelines can be developed for a BIPV/T standard. The system needs to be considered for its passive energy performance as a building envelope component, noting characteristics like the U-value, solar factor and solar heat gain coefficient (SHGC).

It is important to note that the design and optimization of the system’s thermal performance should not be arbitrary and should consider the intended use of the preheated air (heat pump boost, direct preheated fresh air supply, drying, desiccant cooling etc.), which would dictate the requirements for flow rate and outlet air temperature. These requirements, along with the upper limits for maximum PV temperatures, as well as the pumping energy consumption will provide the frame for the performance design of the system.

Table 3.4: Standards related to BIPV/T performance

PV standards	
EN 61215	Crystalline Silicon Terrestrial PV Modules
EN 61730	Photovoltaic Module Safety Qualification
UL 1703	Flat-Plate Photovoltaic Modules and Panels
UL 4703	Outline for Photovoltaic Wire
BIPV standards	
AC 365	BIPV roof covering systems
EN 50583-1	Photovoltaics in Buildings: BIPV modules
EN 50583-2	Photovoltaics in Buildings: BIPV systems

Suggestions for BIPV system comprehensive testing include testing for electrical performance, thermal performance and seasonal variation, ventilation performance, visual effect, maintenance criteria, wind resistance, wind-driven rain, and accelerated weathering (R. J. Yang, 2015).

3.6.4 Design concept

Performance enhancements for the BIPV/T cladding, construction limitations and architectural effects were key drivers through the case study design iterations. Figure 3.30 shows a concept render of a multiple-inlet CW system with horizontally oriented PV modules as the outer layer. This concept is the basis for the prototype described in Chapter 4.



Figure 3.30: Multiple-inlet CW BIPV/T system

Chapter 4

Multiple-Inlet BIPV/T Curtain Wall Prototype Development

The design requirements presented in Chapter 3 are considered for the development of a BIPV/T prototype for performance testing under laboratory conditions. The following chapter describes the design development and construction of the prototype, addressing some of the challenges during the construction and assembly process.

4.1 Design Development

The design of the BIPV/T prototype has two main objectives, which have both agreeing and conflicting aspects:

1. The prototype is designed to facilitate integration and assembly as a curtain wall facade, a conventional and established method for commercial building enclosures.
2. It must accommodate for constraints created by the experimental testing needs and capabilities.

Figure 4.1 shows the features of the prototype design. The PV panels serve as the rainscreen layer of the facade, followed by the air cavity and then the insulation layer, which is intended to create a near adiabatic boundary for the air channel but also serves as the envelope thermal barrier. The insulation can be selected to match the building code requirements for thermal resistance, which may affect the depth of the framing. A dark-colored absorber sheet, made of a thin sheet of painted metal, covers the insulation and absorbs any radiation that passes through the PV panels, if they are semi-transparent.

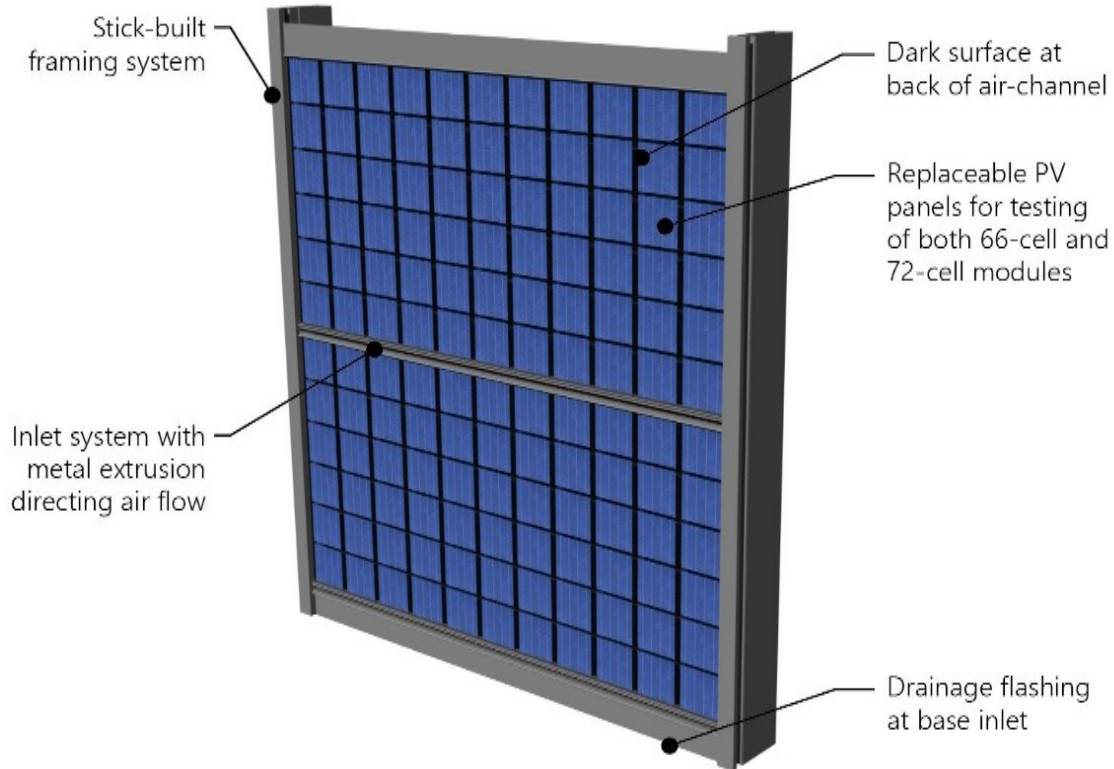


Figure 4.1: Features of final prototype design include CW framing, multiple inlets and a metal extrusion for directing the air flow

While this prototype concept was initially derived from the requirements and considerations in Chapter 3, some adjustments were made as the final iteration was prepared for fabrication and construction. Although the original design was a 3 panel system that spanned a typical floor to ceiling height, the prototype had to be smaller due to laboratory size limitations. Furthermore, the system designed is intended to be part of a larger facade system, at least one story in height, and not as a stand-alone section. For this reason, it is important to note that the particular configuration presented is not optimized for channel aspect ratio and flow rate of a 2-panel system.

The performance of multiple-inlet BIPV/T systems has been previously investigated (Rounis et al., 2016; Yang and Athienitis, 2015). In this study, there are two air inlets, one at the base that is almost the full depth of the channel, and one that is located between the two PV panels. The purpose of the middle inlet is to reduce the surface temperature of the upper panel by adding a cool stream of air to the air already flowing inside from the bottom inlet. This second intake of fresh air should break the thermal boundary layer and boost the heat extraction from the upper PV panel, ultimately enhancing the electrical and thermal performance of the system. A metal

extrusion was designed to be placed directly behind the middle inlet, the full width of the prototype. This serves a dual purpose, preventing rainwater from entering into the air cavity, and improving heat transfer from the upper PV to the air inside of the channel by directing it closer to the back of the PV surface (Figure 4.2).

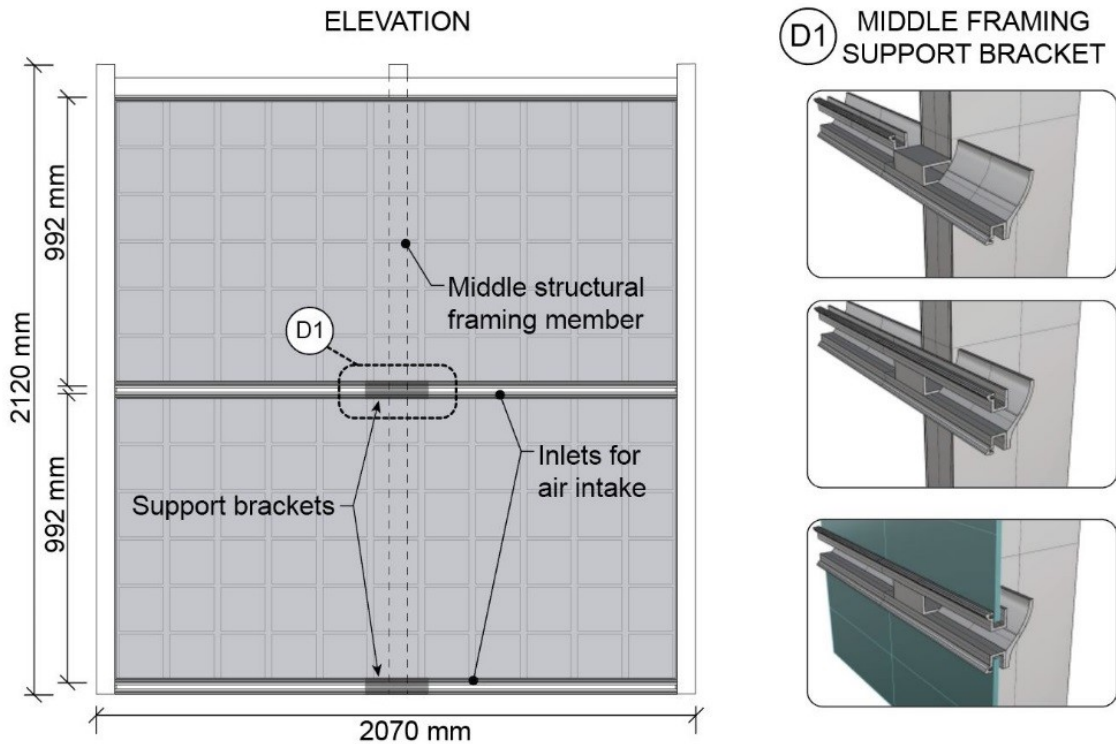


Figure 4.2: Architectural elevation of prototype with final dimensions (left) and renderings of the metal extrusion at the middle air inlet (right)

Two separate sets of glass-on-glass semi-transparent PV modules were custom fabricated by Canadian Solar for the prototype. One pair of modules has 66 cells on each panel with a spacing of 23 mm between the cells, and the other pair of modules has 72 cells on each panel, with a spacing of 10 mm between the cells. Thus, the two sets have different transparencies (20% transparency for the 66-cell modules and 12% for the 72-cell modules). The two types of modules are illustrated in Figure 4.3. The purpose of studying two different transparencies of PV modules is to understand their effects on the electrical and thermal performance of the BIPV/T system. It has been observed that a decrease in packing factor leads to a decrease in the temperature of the PV module, thus increasing its electrical efficiency (Vats et al., 2012). It is expected that the 66-

cell modules will produce a higher thermal efficiency since more radiation will reach the back absorber sheet, increasing the air temperature inside of the channel.

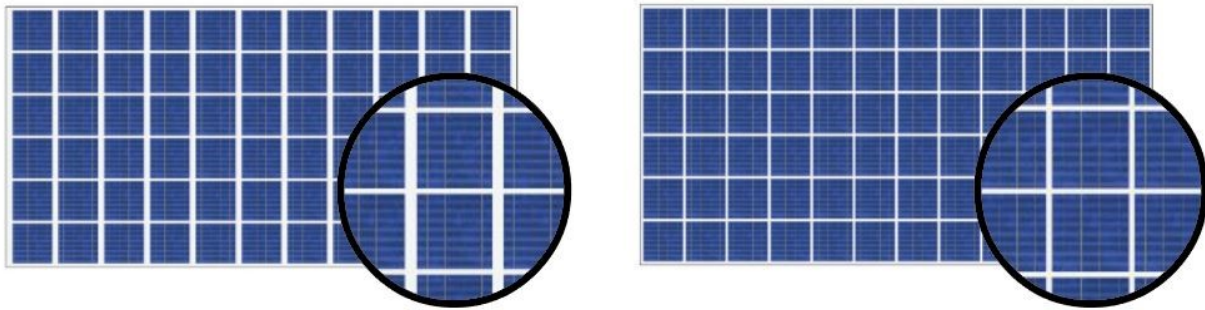


Figure 4.3: 66-cell module with a 20% transparency (left) and 72-cell module with a 12% transparency (right)

4.2 Construction

Once the architectural drawings for the prototype were finalized, the framing was fabricated and partially assembled at the shop of a local curtain wall manufacturer. Collaboration with the manufacturer allowed for adjustments throughout the design and construction processes as improvements and constraints were discovered. The dimensions of the prototype are 2.07 m in width and 2.12 meters in height, covering a total area of 4.39m². This covers the structural framing, inlets and PV modules. The PV modules are fastened to the side and top mullions with pressure plates. A center mullion provided support against deflection, along with two extra point supports. This is critical to supporting the dead load of the modules in the vertical position. The center mullion measures 45 mm across and protrudes into the air channel a depth of 45 mm.

4.2.1 Air channel

The air channel has a depth of 9.5 cm and a hydraulic diameter of 0.18 m, with a total flow path length of 2.09 m. Initially, it was desired to have an air channel of varying depth for more experimental options, but this was limited to one height due to construction constraints. For a length of one to two storeys, the intended application of this design, this channel depth would not result in high frictional losses even with the addition of an air director that would reduce the depth at its location. This is a solution to maintaining less than 70% blockage to the air flow in the channel and an average velocity of 1 m/s (Rounis et al., 2017).

Two modules were oriented horizontally and placed with a gap of 3 cm between to form the second air inlet. Spacing at this inlet is maintained by the point support attached to the center mullion. The width of this inlet is approximately two thirds of the area of the bottom inlet and was chosen based on a previous study on multiple-inlet BIPV/T flow modeling by Rounis (Rounis et al., 2015).

4.2.2 Insulation and Back Pan

At the base of the air channel, there is 51 mm (2") of extruded polystyrene (XPS) insulation (R-1.76) covered with an aluminum sheet which acts as a secondary absorber panel as well as the secondary plane for incidental water shedding. This insulation was provided by the manufacturer, however for building application, insulation that is accepted by the fire code must be used. The metal has a black coating to increase radiation absorption. A metal back pan is attached at the interior side of the insulation and serves as the final air-vapor barrier. Adhesive insulation (tape) is used at the side walls of the air channel, namely the mullion interior surface, in order to minimize lateral heat losses. This was to create a well insulated air channel and minimize side losses from the prototype, although this is not a typical CW insulation feature.

Due to the large width of the prototype and in order to ensure uniform flow within the air channel (and to avoid flow convergence), four outlets of 25 cm x 5 cm were cut out on the top mullion, upon with a custom manifold was attached (Figure 4.4).

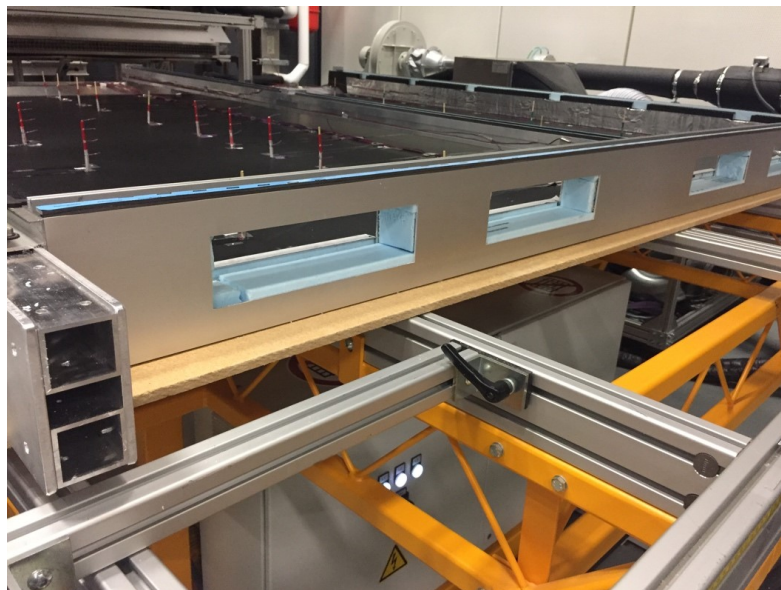


Figure 4.4: Openings for the manifold

Figure 4.5 shows, from left to right, the prototype assembled and with PV panels in place, the location where the CW framing was cut away to accommodate the junction boxes, openings in the top horizontal framing for the air flow manifold, and a sheet metal flashing at the base for water drainage. Photos in Appendix B show the details of the construction and instrument installation for the experiments. Appendix C includes the product specification sheets for the materials used.

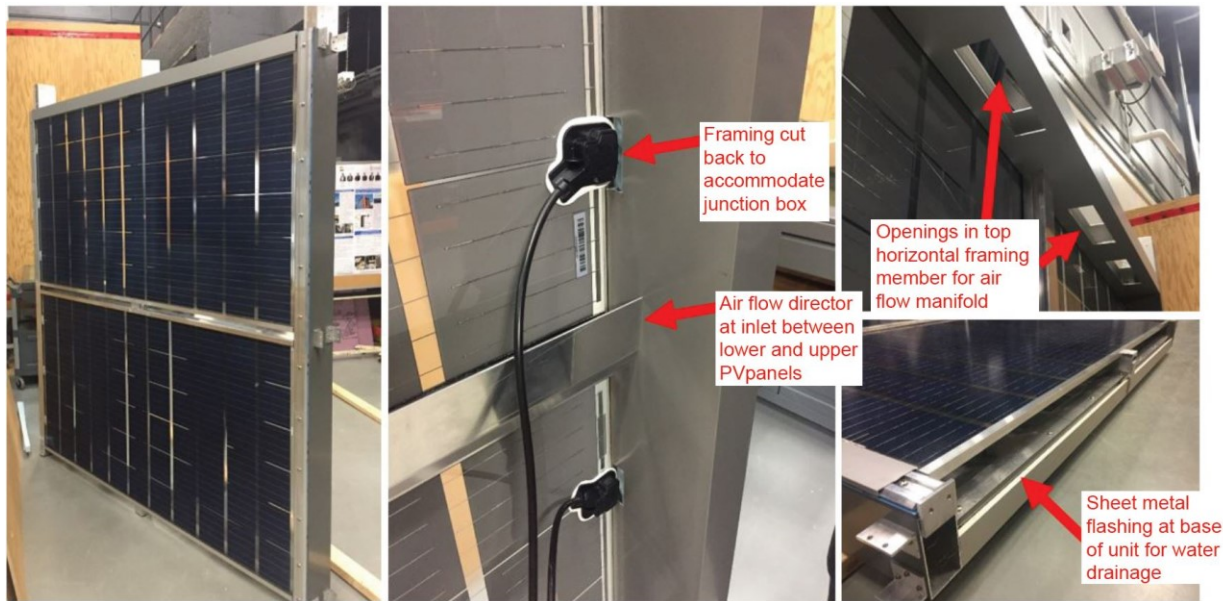


Figure 4.5: Details of constructed prototype

Although the prototype has the aforementioned adjustments for indoor laboratory testing, a number of resolutions were noted that would be required for a final product design. This includes a modified structural design based on system dimensions, PV wire management at the junction box, sealing of any additional penetrations and joints related to the PV wiring, type of air channel insulation and coating if aluminum backpans are not possible, and manifold location, orientation and penetration through the envelope.

Chapter 5

Experimental Testing In a Solar Simulator and Comparison with Model Predictions

The following chapter presents the methodology and results for the experiments performed on the BIPV/T prototype described in Chapter 4.

5.1 Experimental Setup

Experimental testing of the BIPV/T prototype was carried out at the Solar Simulator and Environmental Chamber laboratory of Concordia University in Montreal, Canada (Figure 5.1). This facility is used for laboratory testing of solar thermal collectors, PV modules, and hybrid PV/T systems under varying ambient temperatures, irradiation levels and wind speeds. The Solar Simulator contains eight metal halide lamps which simulate sunlight, along with a ventilated artificial sky, which is located in front of the lamps. The artificial sky maintains a surface temperature of $13^{\circ}\text{C} \pm 2^{\circ}\text{C}$ and helps to remove the long-wave infrared radiation that the high-temperature lamps emit. It consists of two low-iron glass panes with an anti-reflective coating. Cool air passes between the two panes to remove the infrared thermal effect and simulate the effect of the sky temperature. In this way, the lamps create a spectral distribution that complies with standards ISO 9806 and EN 12975 (CEN, 2006; ISO, 2017). The heat of the lamps can reach 27.6 kW, so a cooling unit, located in the mechanical room adjacent to the testing space, takes away this heat. The position of each of the lamps can be adjusted, and they can be dimmed to a variety of radiation levels, in the range of 500 W/m^2 to 1200 W/m^2 . The purpose of this is to allow for testing of a range of specimen sizes, thickness and to test at different radiation intensities. For the experiments conducted on the BIPV/T prototype, a radiation homogeneity of 94% was achieved, which is within the 15% deviation limit stated by ISO 9806 for solar thermal collectors, but not the 5% limit suggested by IEC 61215 for Class AAA solar simulators used for certification. Since the purpose of this work is experimental and is not certifying a product for performance characteristics, the homogeneity achieved is sufficient.

The platform for the specimen is 2.4 m wide by 3.2 m long and can rotate from 0° to 90° to allow for testing of different configurations of building envelope elements. Since the prototype

represents a vertical curtain wall facade assembly, all experiments were carried out with the test bed at a vertical position. A fan that is positioned at the rear end of the test platform is used to replicate the effect of wind to study the effects of wind driven convection. The fan blows ambient air parallel to the specimen at a velocity of up to 14 m/s, and has an adjustable height. An air collector test stand unit collects air from the specimen at flow rates adjustable up to 600 kg/h (0.17 kg/s). The ambient temperature of the facility is regulated at 21°C. A scanner is attached just over the test platform and can move across the surface on an x-y axis at 15 cm intervals. It is equipped with an anemometer for wind speed measurements and a pyranometer for radiation measurements.

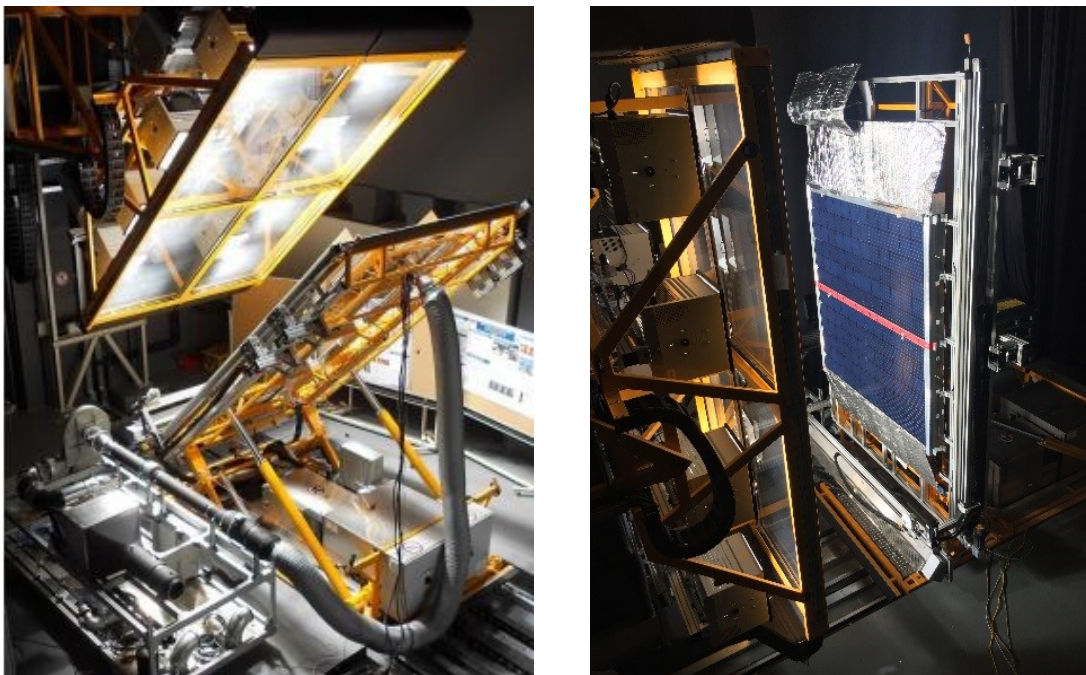


Figure 5.1: Solar simulation laboratory (Left) and vertical position of prototype during testing (right) (University, n.d.)

A total of 97 thermocouples were placed throughout the prototype to monitor the temperatures of the PV surfaces, the air channel and the black absorber sheet (metal back pan) covering the insulation (Figure 5.2 and Figure 5.3). Of these, 85 t-type thermocouples were used to measure temperatures at the insulation and back pan, throughout the air channel and at the surface of the PV modules. Although this resulted in a large number of sensors in the air channel, the dimensions are such that their presence would not interfere with the airflow in a significant way. The remaining thermocouples were used for measurements at 3.5 cm above the module surfaces at the air inlets, outer framing surfaces, underside of the prototype (back of the insulation)

to determine heat losses of the framing and insulation to the ambient environment. Three RTD sensors were placed into the manifold to measure outlet air temperatures.

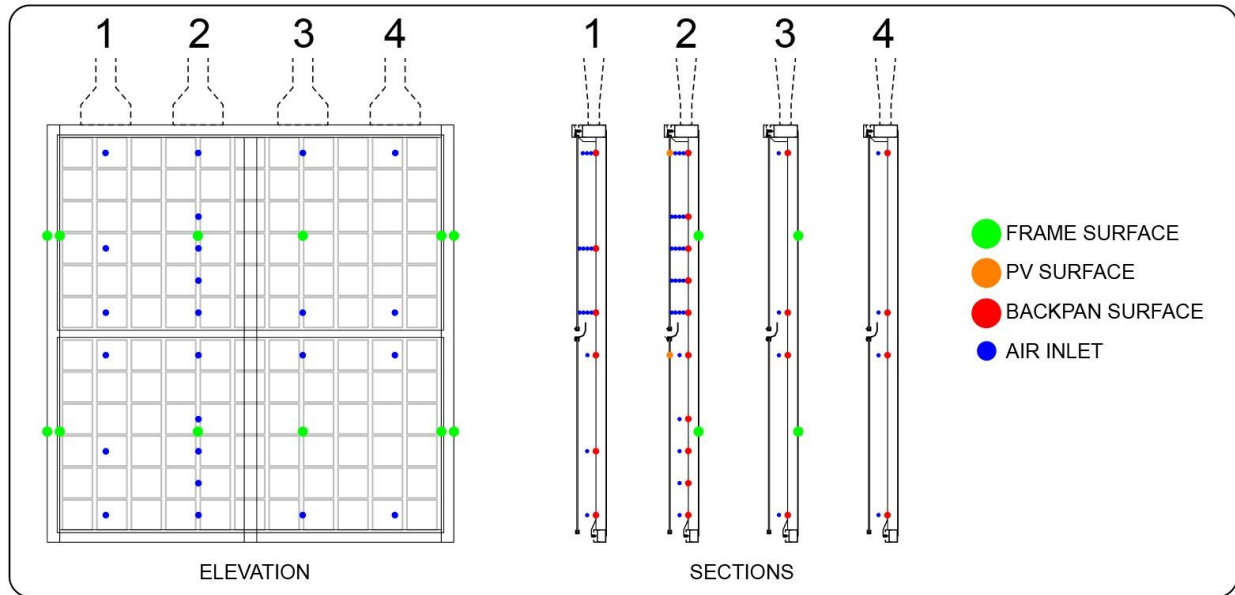


Figure 5.2: Location of thermocouples shown in elevation (left) and four sections (right)

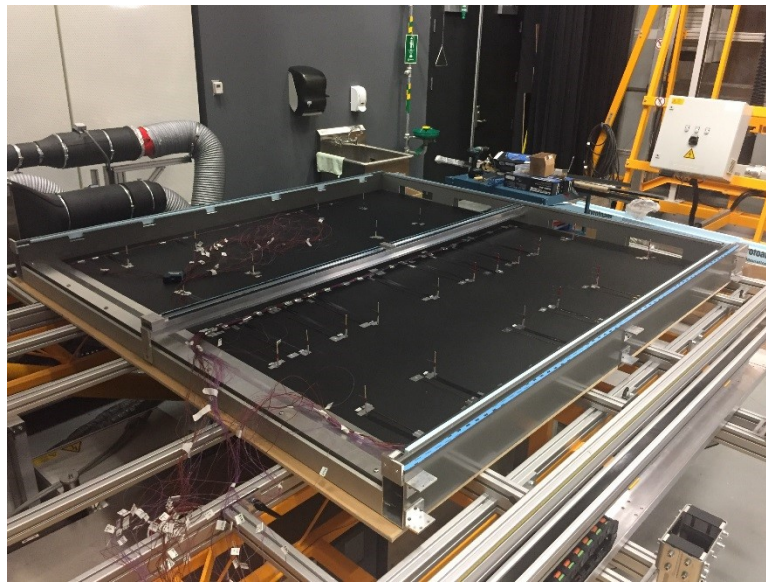


Figure 5.3: Thermocouple setup inside of BIPV/T air cavity

In each location, a rod was placed with 2 to 5 thermocouples along multiple heights (Figure 5.4, left). The reason for this is to have accurate measurements of the air temperatures across the channel in a particular location, which will assist with model verification of local heat transfer

phenomena in the two-inlet BIPV/T system. At the location of each rod, at least one thermocouple was placed directly on the surface of the black absorber sheet, and one thermocouple was suspended in the air channel (Figure 5.4, right).

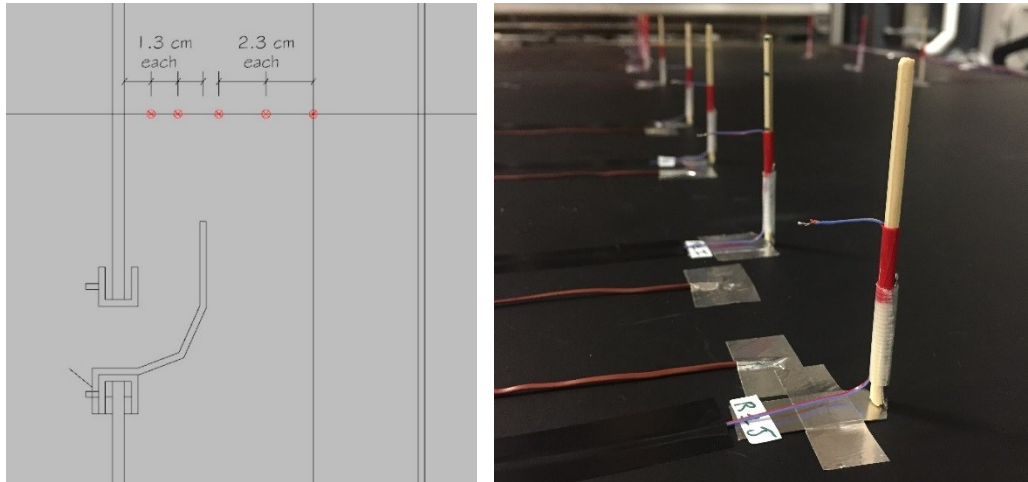


Figure 5.4: Thermocouple heights in channel (left) and attachment method (right)

This study discusses only the averages of air temperatures inside of the cavity (PV and center line air channel), since the values of most relevance are maximum PV module temperatures and the air temperatures at the outlet. Differences in the temperatures of the air layers along the cavity are more useful for specific modeling purposes. Finally, the manifold at the upper end of the prototype was connected to the air collector test stand unit, where flow rate of the air was adjusted and where final outlet air temperatures were measured. Table 5.1 presents additional information pertaining to the instruments used for measurements.

Table 5.1: Details of the Instruments Used for Measurements

Measurement	Instrument	Unit	Accuracy
Solar Irradiance	Pyranometer mounted on scanner over PSE test platform	W/m ²	+/-5%
Air temperature at outlet	RTD thermocouple	°C	+/-0.06°C
Air temperature at inlet	Type T thermocouple	°C	+/-0.5°C
PV surface temperature	Type T thermocouple	°C	+/-0.5°C

Air flow rate	PSE Air Collector Flow Meter	kg/hr	+2%
DC Voltage	DS-100C IV Curve Tracer by Daystar Inc.	V	+0.5%
DC Current	DS-100C IV Curve Tracer by Daystar Inc.	A	+0.5%
Wind speed	D12-65 Series hot film anemometer	m/s	+0.2 m/s

5.2 Scope of Experiments

The following section describes the specific objectives of the experimental work and presents the testing cases. Because this curtain wall BIPV/T system is intended for facade applications, all tests were carried out in the vertical position. Furthermore, the prototype that was constructed for the experimental work is meant to be part of a larger facade system, so the air gap of 9.5 cm thickness is not meant for an optimal stand alone unit of approximately 2 square meters with just two PV panels. The following physical configurations were studied to understand their effect on the electrical and thermal performances of the prototype. They are visually represented in Table .

- One inlet vs. two inlets for fresh air intake
- The addition of an air director at the top inlet
- 20% transparency vs. 12% transparency of the PV cells (66-cell vs. 72-cell modules, respectively. The 66-cell modules have a nominal output of 280 W and the 72-cell modules have a nominal output of 320 W.)

The following variations of fan flow rates and solar irradiation were applied to each of the physical configurations mentioned above. They are the environmental parameters:

- 3 different air flow rates (0.11 kg/s, 0.14 kg/s, and 0.17 kg/s. Respective air velocities are 0.5 m/s, 0.62 m/s, and 0.74 m/s). Lower flow rates were not used since they result in average air velocities of less than 0.5 m/s inside of the air channel and begin to resemble natural convection, which is not being studied in this BIPV/T design.
- 3 solar irradiation levels (839 W/m², 989 W/m², and 1109 W/m²)

In total, this resulted in 54 testing configurations. The reason for varying the fan flow rate and the radiation levels is for model verification purposes. The fan flow rates selected were limited by the air collector capabilities (maximum flow rate of 0.17 kg/s) and by rates at which natural convection occurs. The Reynolds number is a dimensionless ratio which describes the fluid flow regime inside a given geometry. It was calculated for all three flow rates to determine if flow was laminar or turbulent. In BIPV/T applications, turbulent flow is preferred to laminar flow because it enhances heat transfer between the fluid and the surrounding materials containing it. The equation for the Reynolds number is as follows (Hutcheon and Handegord, 1995):

$$Re = \frac{\text{Inertia forces}}{\text{Viscous forces}} = \frac{\rho v D_h}{\mu} \quad (5.1)$$

where

Re , Reynolds number;

ρ (kg/m³), density of the fluid medium, 1.2 kg/m³ for air;

v (m/s), average channel velocity, ranging from 0.5 m/s to 0.74 m/s;

D_h (m), hydraulic diameter of the channel, in this case 0.18 m and

μ (Pa * s), dynamic viscosity, 18.13 * 10⁻⁶ for air at 20°C.

The hydraulic diameter is defined as $D_h = 4 \cdot A_c / p$ where A_c (m²) is the channel cross-sectional area and p (m) is there perimeter. A Reynolds number less than 2300 indicates laminar flow in pipes and ducts (Owen and Kennedy, 2009). Taking into consideration that the geometry of the air channel in the prototype resembles two plane parallel surfaces, this value may be even lower. Table 5.2 shows the Reynolds numbers for the three flow rates selected for the experiments, suggesting that in all single-inlet cases, the flow is not laminar.

Table 5.2: Reynolds numbers for varying air flow rates inside of the channel

Mass flow rate (\dot{m})	Respective air velocity (v)	Reynolds number	Regime
0.11 kg/s	0.5 m/s	5957	Transitional/turbulent
0.14 kg/s	0.62 m/s	7387	Transitional/turbulent
0.17 kg/s	0.74 m/s	8816	Turbulent

Based on the experimental measurements, calculations were performed to obtain the values for the convective heat transfer coefficients (CHTC). A higher CHTC value is desired for an increase in heat transfer to the air. Table 5.3 shows average CHTC values for the entire collector operating at NOCT conditions, with 72-cell modules and a single inlet. The values were very similar for the other two radiation levels. There is not much change with varying flow, either. Combined convective and radiative top losses were approximately 18.5 to 20 W/m²K.

Table 5.3: CHTC values for varying air flow rates inside of the channel at NOCT, for the 72-cell single-inlet configuration

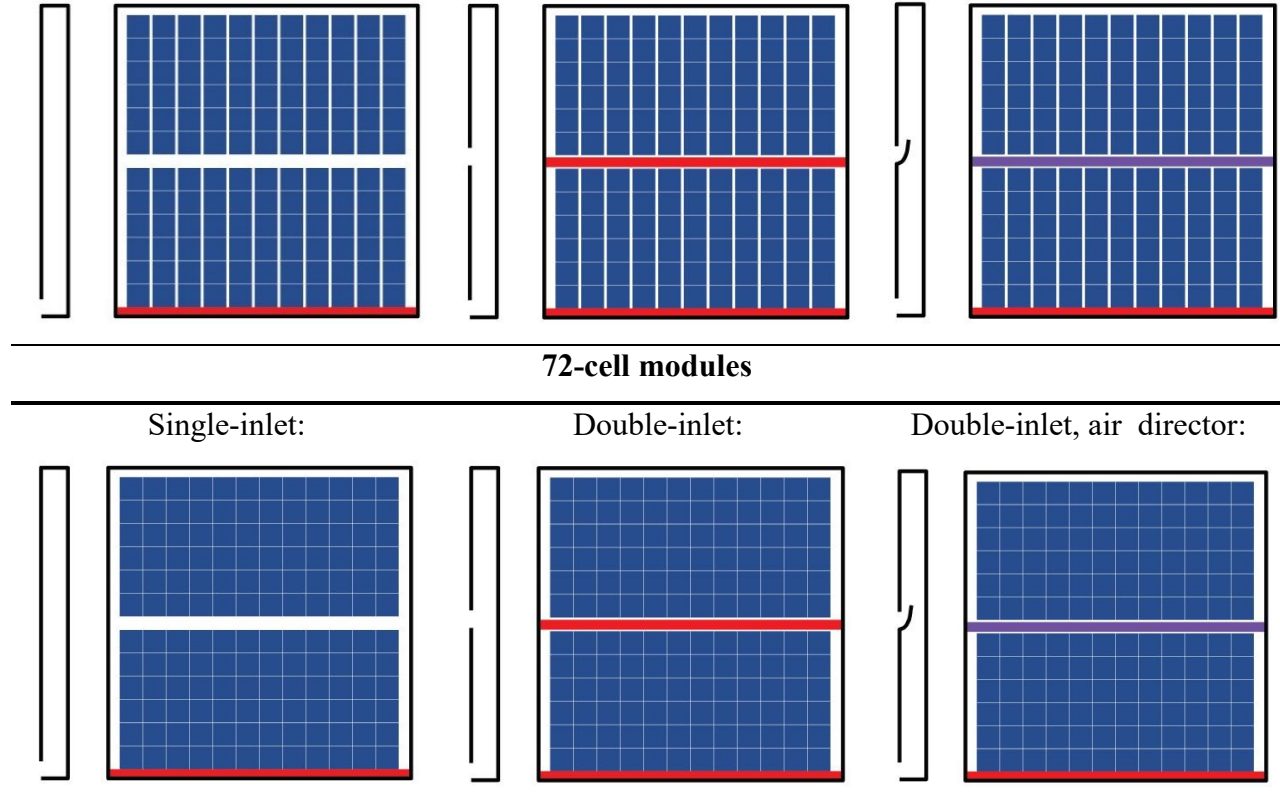
Mass flow rate (\dot{m})	h_{pv_surf} (W/m²K)	h_{back_surf} (W/m²K)
0.11 kg/s	3.82	6.71
0.14 kg/s	4.50	7.62
0.17 kg/s	5.29	8.53

From an air velocity of 1 m/s to 2 m/s, the CHTC generally increases (Yang and Athienitis, 2015). Ideally, the experiments would have included an air velocity of 2 m/s but setup limitations and prototype dimensions did not allow for this.

Given the practical application intent of this design, results described in the next section are only for nominal operating cell temperature (NOCT) conditions, which reflect how PV systems are tested in the industry. NOCT parameters define a standard reference environment and are mentioned in the IEC 61215 standards for outdoor measurements. NOCT conditions specify an irradiance of 800 W/m², an ambient temperature of 20°C and a wind speed of 1 m/s. The higher solar radiation levels approach standard testing conditions (STC), which represent more ideal settings, with an irradiance of 1000 W/m².

Table 5.4: Physical configurations of the prototype for testing

66-cell modules		
<i>Single-inlet:</i>	<i>Double-inlet:</i>	<i>Double-inlet, air director:</i>



5.3 Experimental Results

The following results show air temperature, PV surface temperature as well as electrical and thermal efficiency values for the prototype tested under conditions closest to NOCT, namely: 839 W/m² solar irradiation on the cell surface with an approximate uniformity of 94%, an ambient air temperature of 21°C ±1°C, and an average exterior wind speed of 1.1 m/s. This testing focused on the practical application of the system and does not include results for the other two solar irradiation values (989 W/m², and 1109 W/m²) which were used to collect data for model verification purposes.

To evaluate the conditions at steady state, the temperature values were plotted over the entire testing period. Only during the periods when steady state conditions were achieved were temperature values taken. The following points were considered during the analysis of the experimental data:

- After reaching steady state, temperatures were recorded for ten minutes and then averaged.
- The system is open-loop and the inlet temperature was equal to the ambient.

- The flow throughout the width of the air channel was assumed uniform based on flow velocity measurements
- Temperature distributions on an axis perpendicular to the flow, for each level of measurement, showed very small variations.
- Measurements taken with the RTD sensors placed in the manifold assume a fully mixed airflow

The results discussed in the next sections will compare thermal efficiency, outlet temperature, maximum PV surface temperature and electrical efficiency to highlight the improvements of certain physical configurations over others. Graphs summarizing the results are shown in Appendix D.

5.3.1 Thermal Efficiency

The total thermal energy extracted by the air flowing through the BIPV/T channel extracts heat from both front and back surfaces, where T_{out} is the air temperature as measured in the manifold and T_{in} the ambient temperature:

$$Q_{air} = \dot{m}c_p(T_o - T_i) \quad (5.2)$$

where

Q_{air} (W), thermal energy of the air exiting;

\dot{m} (kg/s), mass flow rate of the air;

c_p (J/kg°C), specific heat of the air;

T_o (°C), Temperature of the air at the outlet and

T_i (°C), Temperature of the air at the inlet.

Taking into account the solar radiation ($G = 839 \text{ W/m}^2$) and the area of the collector, which includes the entire surface area along with the frame ($A=4.39\text{m}^2$), thermal efficiency is then calculated:

$$\eta_{th} = \frac{Q_{air}}{G * A} \quad (5.3)$$

where

η_{th} (%), thermal efficiency of the collector;

Q_{air} (W), thermal energy of the air exiting the collector;

G (W/m²), solar radiation and

A (m²), total surface area of the collector.

For the 72-cell module system, the single inlet configuration shows the lowest thermal efficiency of 20.1% - 26.1% with varying flow rate. The double inlet configuration exhibited a thermal efficiency range of 22.6% - 29.8% and this increased to 24.5% - 30.3% when the air director was added. This means that a double-inlet system with an air director has an approximate thermal efficiency increase of 3.1% - 4.2% over the single-inlet configuration. For the 66-cell module system, the thermal efficiency increased by 0.7% - 2.3% as compared to the 72-cell modules. This is due to an increased transparency of the modules, allowing more radiation to be absorbed by the dark back pan. However, as discussed later in this section, this improvement comes with a decrease in electrical efficiency.

Based on the accuracy of the sensors used for the measurements, the calculations have a margin of error up to 0.64% for the electrical efficiency and 2.86% for the thermal efficiency (Appendix E).

Table 5.5: Thermal efficiency of the BIPV/T prototype

Configuration	66-cell			72-cell		
	<i>0.11kg/s</i>	<i>0.14kg/s</i>	<i>0.17kg/s</i>	<i>0.11kg/s</i>	<i>0.14kg/s</i>	<i>0.17kg/s</i>
Single-inlet	23.6%	24.7%	27.3%	21.4%	23.6%	26.1%
Double-inlet	23.4%	28.4%	31.9%	22.6%	26.3%	29.8%
Double-inlet, air director	25.7%	29.2%	32.3%	24.5%	27.8%	30.3%

5.3.2 Air Temperatures in Channel

The highest rise in air temperature (from inlet to outlet) was observed in the double-inlet configuration with the air director of the 72-cell module system. For this configuration, the lowest flow rate experienced a 6.7°C change while the highest flow rate produced a change of 8.2°C. The double-inlet configuration produced temperature rises in the range of 6.6°C – 7.5°C and the range for the single-inlet configuration was 5.8°C – 7.1°C. Similarly to the thermal efficiency results,

the 66-cell module system also showed higher outlet temperature for the air channel temperatures compared to the 72-cell modules.

Table 5.6: Air temperature rise within BIPV/T prototype air channel

Configuration	66-cell			72-cell		
Flow rates	0.11kg/s	0.14kg/s	0.17kg/s	0.11kg/s	0.14kg/s	0.17kg/s
Single-inlet	7.9°C	6.6°C	6.0°C	7.1°C	6.3°C	5.8°C
Double-inlet	7.8°C	7.6°C	7.1°C	7.5°C	7.0°C	6.6°C
Double-inlet, air director	8.5°C	7.8°C	7.2°C	8.2°C	7.4°C	6.7°C

5.3.3 PV Surface Temperatures

The single-inlet configuration showed results for highest peak PV surface temperatures. This was pronounced in the top row of cells of the top module. In Figure 5.5, the representative photograph (left), and the infrared images show steady state conditions for the 72-cell single-inlet configuration with a flow rate of 0.11 kg/s (middle) and for the 66-cell single-inlet configuration with a flow rate of 0.17 kg/s (right).

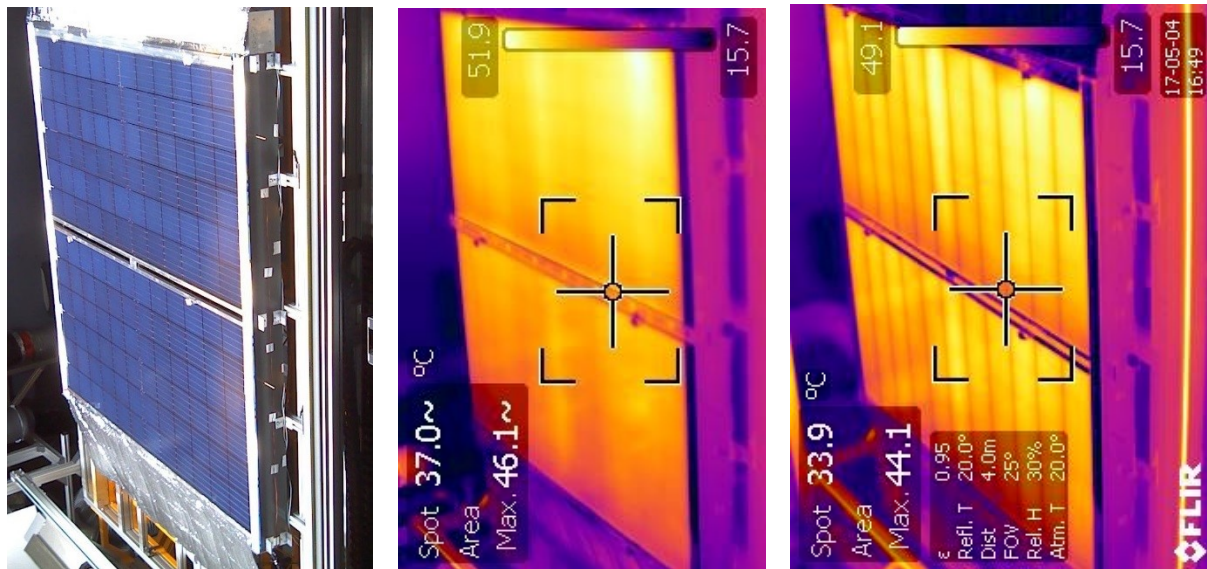


Figure 5.5: Photograph (left) and infrared images of prototype. The photo in the center shows a test in progress for the 72-cell, single-inlet configuration with a flow rate of 0.11 kg/s. The photo on the right shows a test in progress for the 66-cell, double-inlet configuration with a flow rate of 0.17 kg/s.

The difference between the single-inlet and double-inlet configurations here is that opening a second passage for air lowered the incoming flow of air at both locations, which means that the bottom PV panel in the single-inlet configuration experienced overall lower temperatures than the top panel as opposed to the double-inlet configurations. This temperature change is approximately 0.8°C.

The double-inlet configuration showed lower peak PV temperatures and the addition of the air director lowered these values even further. The best case is the double-inlet configuration with the air director at a flow rate of 0.17 kg/s, with an average maximum PV temperature of 52°C for the 66-cell modules. The worst case is the single-inlet configuration of the 72-cell modules, at a flow rate of 0.11 kg/s, with an average maximum PV temperature of 57°C.

Table 5.7: Maximum PV temperatures of the BIPV/T prototype

Configuration	66-cell			72-cell		
	0.11kg/s	0.14kg/s	0.17kg/s	0.11kg/s	0.14kg/s	0.17kg/s
Single-inlet	59.4°C	57.1°C	55.3°C	56.8°C	56.0°C	54.7°C
Double-inlet	58.1°C	56.1°C	53.4°C	56.6°C	55.6°C	53.7°C
Double-inlet, air director	55.6°C	54.3°C	52.1°C	55.4°C	54.2°C	53.0°C

5.3.4 Electrical Efficiency

Electrical efficiency was obtained by dividing the total electrical output of both PV panels by the radiation and prototype area:

$$\eta_{el} = \frac{E_{el}}{G * A} \quad (5.4)$$

where

η_{el} (%), electrical efficiency of the PVs;

E_{el} (W), electrical power produced by the PVs;

G (W/m²), solar radiation and

A (m²), total surface area of the collector.

Data from IV-curves taken for each individual PV module during steady state conditions was added to obtain the electrical output used in obtaining the electrical efficiency. The PV panels were connected in parallel but measured individually since the load used in the experiment could not take on the combined wattage.

Table 5.8: Electrical efficiency of the BIPV/T prototype

Configuration	66-cell			72-cell		
	<i>0.11kg/s</i>	<i>0.14kg/s</i>	<i>0.17kg/s</i>	<i>0.11kg/s</i>	<i>0.14kg/s</i>	<i>0.17kg/s</i>
Flow rates	<i>0.11kg/s</i>	<i>0.14kg/s</i>	<i>0.17kg/s</i>	<i>0.11kg/s</i>	<i>0.14kg/s</i>	<i>0.17kg/s</i>
Single-inlet	11.22%	11.36%	11.42%	12.62%	12.66%	12.74%
Double-inlet	11.34%	11.41%	11.47%	12.64%	12.66%	12.77%
Double-inlet, air director	11.38%	11.40%	11.48%	12.65%	12.70%	12.72%

5.3.5 Summary of results

Preliminary results for the NOCT testing conditions showed combined electrical and thermal efficiencies of up to 38.9% and 43.8% for the single and the double inlet configurations respectively. The double-inlet configurations performed best at all times, with 2% - 5% higher thermal efficiencies, 3°C – 4°C lower maximum PV temperatures, as well as marginally higher electrical efficiencies. Depending on the flow rate, the temperature rise inside the air channel varied from 6°C to 8.5°C for a 2 m long air channel, and it was approximately 1°C higher for the cases of the double-inlet configurations. The 66-cell modules had a slightly higher thermal efficiency due to the higher transparency, compared with the 72-cell modules. This thermal gain, however, was at a cost of the electrical efficiency.

It should be mentioned that the combined efficiencies mentioned previously, were calculated assigning the same value for relative electricity, which is high grade energy, and heat, which is low grade energy. In assessing the overall performance, or equivalent thermal efficiency, of a hybrid PV/T system, the value of electricity can be considered four times higher than that of heat (Athienitis et al., 2010).

The charts in Figure 5.6 summarizes the prototype’s performance at NOCT conditions with a channel flowrate of 0.14 m/s, as an example. The electrical efficiency of the 72-cell configuration is higher than the 66-cell configuration due to a larger coverage of the surface with solar cells, but has a slightly reduced thermal efficiency due to overall higher PV surface temperatures. In both

cases, it is observed that the addition of a second inlet improves the combined performance of the system. However, if the prototype was not limited in size to just two panels, the results would likely show more drastic changes between the single inlet and multiple inlet configurations for taller systems.

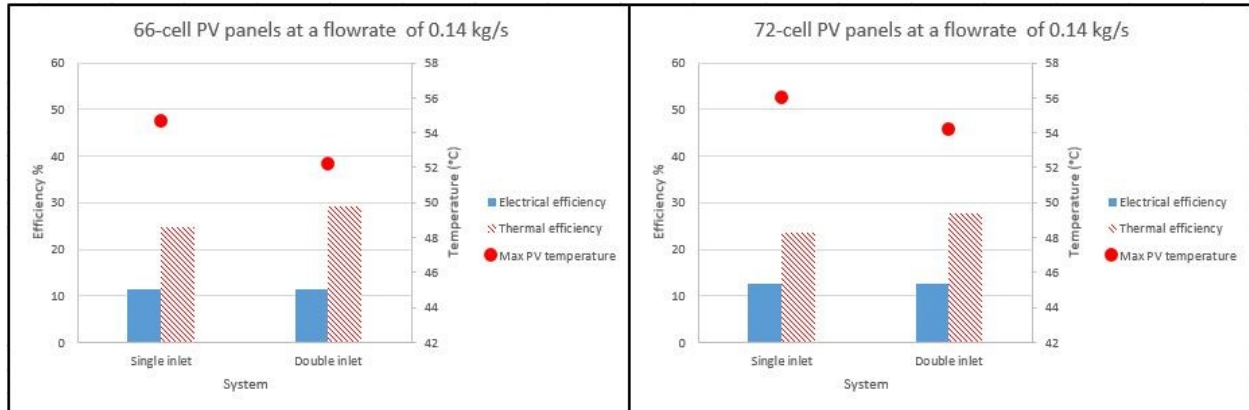


Figure 5.6: Summary results for 66-cell (left) and 72-cell (right) configurations at NOCT conditions

Chapter 6

Conclusion

This research presents the design considerations for an open-loop, air-based BIPV/T facade system based on requirements for building envelope performance and energy generation. While there have been advancements in optimizing the electrical and thermal performance of BIPV/T systems through comprehensive modeling and experimentation, the technology is not yet a viable cladding option, lacking design tools, comprehensive standards and established assembly methods. Information on installation and maintenance of BIPV and BIPV/T facades was gathered, and relevant standards from the electrical and building industries were listed.

Using the resulting data from literature in terms of BIPV/T performance and cladding design criteria, a curtain wall BIPV/T facade was conceived and developed through three novel case studies. Each case study focused on a different aspect of the design. The Courthouse project encouraged a careful look at which curtain wall features would complement the BIPV/T retrofit design, while the Solar Decathlon and IC-Impacts projects addressed system implementation on roofs, both new and existing. Guidelines for the development of a BIPV/T energy performance standard were also suggested in Section 3.6.3. Standards such as EN 61215, EN 61730 and UL 4703 for PV performance, EN 50583 (1 and 2) for BIPV performance, and ISO 9806 for solar thermal collectors were suggested for consideration in a BIPV/T standard.

Additionally, a prototype based on the curtain wall design was developed and constructed for characterization testing under NOCT conditions at an indoors solar simulator facility. The testing included a single and a double inlet configuration. The results showed a highly efficient BIPV/T envelope system with combined electrical and thermal efficiencies in the range of 40%. The double-inlet system performed better than the single in terms of electrical and thermal efficiency, as well as maximum PV temperatures. Initial testing indicated that thermal output increased by up to 18% with the addition of a second inlet in the prototype, while peak PV temperatures decreased by up to 3°C. Electrical output was marginally increased in the multiple inlet configuration (as opposed to the single-inlet system). These differences are expected to be greater in large scale applications, which is the intent of application for this system design.

The prototype shows the practical approach of a conventional cladding, while the case studies allow for the resolution of issues such as system sizing and layout, constructability, and integration with existing building components.

6.1 Contributions

This work combines architectural experience with engineering innovation to critically assess BIPV/T design needs from a building envelope, electrical and thermal performance aspect. Specifically, the following contributions are provided:

- A literature review of BIPV/T development and enhancements
- A review of existing standards for both the PV and building industry
- A summary of installation methods, maintenance techniques and potential challenges of initiating and keeping BIPV and BIPV/T systems
- Three novel case studies incorporating BIPV/T designs into potential of existing facades:
 - Courthouse Building with BIPV/T facade retrofit
 - Solar Decathlon – Deep Penetration Dwelling BIPV/T roof design
 - IC-Impacts – Modelling of BIPV/T roofs for low-rise residential buildings
- A summary and comparison of the case studies, including key parameters and constraints
- A proposal of a BIPV/T design methodology based on an analysis of the existing case studies and with the goal of moving from custom installations to standard and accessible assemblies
- Proposal of inclusion of certain standards into a BIPV/T performance standard
- Development of BIPV/T curtain wall prototype for construction and testing
- Experimental investigation of the prototype, including thermal enhancements, for base characterization

Two conference papers were published on this work:

- 1) Kruglov, O., Rounis, E.D., Athienitis, A.K., Ge, H., 2017. Experimental investigation and implementation of a multiple-inlet BIPV/T system in a curtain wall. Proceedings of the 15th Canadian Conference on Building Science and Technology (CCBST), Vancouver.
- 2) Kruglov, O., Rounis, E.D., Athienitis, A.K., Lee, B., Bagchi, A., Ge, H., Stathopoulos, T., 2018. Modular Rooftop Building-Integrated Photovoltaic/Thermal Systems for Low-Rise

6.2 Recommended future work

Prototype testing, which has been completed, up to this point provides some initial characterization information, but focuses primarily on the effects of changing the inlet configuration and the air flow. Constraints that would apply in actual construction should be included as parameters in the testing. Specifically, necessary installation changes that may be likely to occur and that may affect the air flow inside of the channel should be considered.

Additional parameters that should be studied in terms of their effect on the electrical and thermal efficiency of the system include:

- Installation of fins inside of the air channel
- The use of meshes at inlets (necessary for bird and insect protection)
- Varying the air channel depth while maintaining the full system thickness
- Configuration of the manifold due to potential limitations of floor height and space availability (Figure 6.1)
- The use of different types of insulations, such as mineral wool

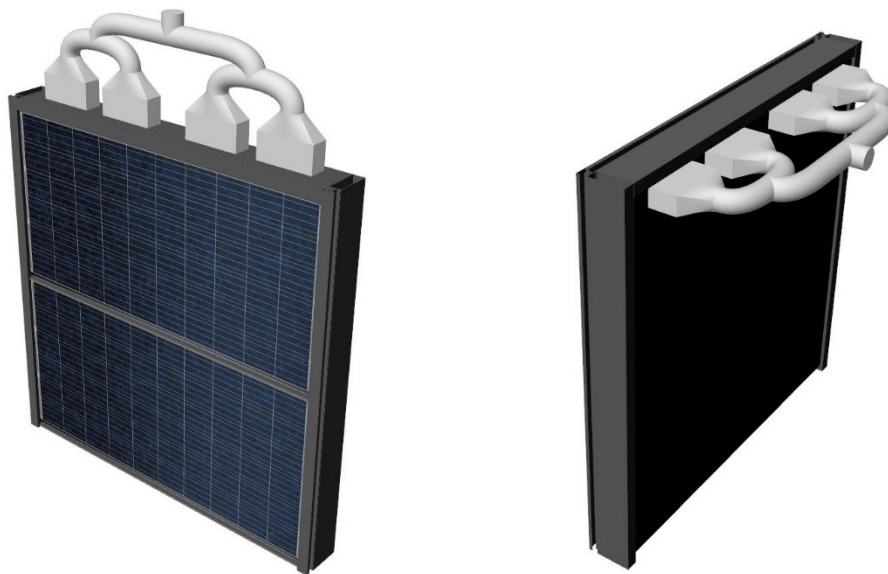


Figure 6.1: Vertical manifold configuration that was tested (left) and horizontal manifold configuration as a future testing option (right)

Future work that is not focused on the PV performance aspect of the prototype would include testing the prototype for water management per an existing standard such as the rain penetration test in ASTM E331. Diagnostic water testing to determine problem areas should be included along with this. Adding the prototype to a fully enclosed test hut which is located inside of an environmental chamber is currently ongoing (Figure 6.2). Possible testing for the passive thermal and moisture properties of the system as an envelope component is one option for this setup.

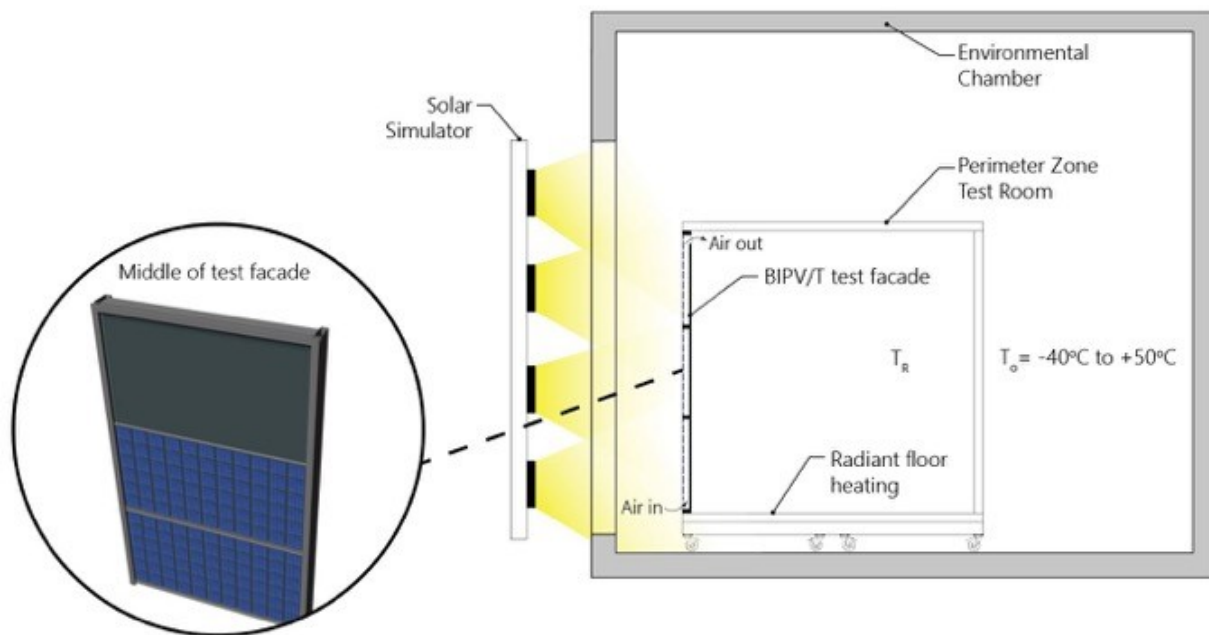


Figure 6.2: BIPV/T prototype as part of a facade on an enclosed test hut for thermal testing

Finally, further analysis of the data resulting from the electrical and thermal performance testing can be incorporated into a parametric modeling program for architects to be able to use this in conjunction with physical modeling in programs for early design stage analysis of building performance.

References

- Aste, N., Del Pero, C., Leonforte, F., 2016. The first Italian BIPV project: Case study and long-term performance analysis. *Sol. Energy* 134, 340–352. <https://doi.org/10.1016/j.solener.2016.05.010>
- Athienitis, A., Cellura, M., Chen, Y., Delisle, V., Bourdoukan, P., Kapsis, K., 2015. Modeling and Design of Net ZEBs as integrated energy systems, in: Athienitis, A., O'Brien, W. (Eds.), *Modeling, Design, and Optimization of Net-Zero Energy Buildings*. Wilhelm Ernst & Sohn, pp. 9–73.
- Athienitis, A.K., Bambara, J., O'Neill, B., Faille, J., 2010. A prototype photovoltaic/thermal system integrated with transpired collector. *Sol. Energy* 85, 139–153. <https://doi.org/10.1016/j.solener.2010.10.008>
- Athienitis, A.K., Barone, G., Buonomano, A., Palombo, A., 2018. Assessing active and passive effects of façade building integrated photovoltaics/thermal systems: Dynamic modelling and simulation. *Appl. Energy* 209, 355–382. <https://doi.org/10.1016/j.apenergy.2017.09.039>
- Baljit, S.S.S., Chan, H., Sopian, K., 2016. Review of building integrated applications of photovoltaic and solar thermal systems. *J. Clean. Prod.* 137, 677–689. <https://doi.org/10.1016/j.jclepro.2016.07.150>
- Bambara, J., 2012. *Experimental Study of a Façade-integrated Photovoltaic/thermal System with Unglazed Transpired Collector*. Concordia University.
- Bambook, S.M., Sproul, A.B., 2012. Maximising the energy output of a PVT air system. *Sol. Energy* 86, 1857–1871. <https://doi.org/10.1016/j.solener.2012.02.038>
- BEEP, 2016. *Design Guidelines for Energy-Efficient Multi-Storey Residential Buildings*.
- Bigaila, E., Rounis, E., Luk, P., Athienitis, A., 2015. A study of a BIPV/T collector prototype for building façade applications, in: *Energy Procedia*. Elsevier B.V., pp. 1931–1936. <https://doi.org/10.1016/j.egypro.2015.11.374>
- Blieske, U., Stollwerck, G., 2013. Glass and other encapsulation materials, Semiconductors and Semimetals. <https://doi.org/10.1016/B978-0-12-381343-5.00004-5>

- BSI, 2016a. BS EN 50583 Photovoltaics in Buildings - Part 1: BIPV Modules. 50583:1.
- BSI, 2016b. BS EN 50583 Photovoltaics in Buildings - Part 2: BIPV Systems. 50583:2.
- Candanedo, L.M., Athienitis, A.K., Candanedo, J.A., O'Brien, W., Chen, Y., 2010. Transient and steady state models for open-loop air-based BIPV / T systems. *ASHRAE Trans.* 600–612.
- CEN, 2006. EN 12975 - Thermal solar systems and components - Solar collectors.
- Chen, Y., Athienitis, A.K., Galal, K., 2010. Modeling, design and thermal performance of a BIPV/T system thermally coupled with a ventilated concrete slab in a low energy solar house: Part 1, BIPV/T system and house energy concept. *Sol. Energy* 84, 1892–1907. <https://doi.org/10.1016/j.solener.2010.06.013>
- Chow, T.T., 2010. A review on photovoltaic/thermal hybrid solar technology. *Appl. Energy* 87, 365–379. <https://doi.org/10.1016/j.apenergy.2009.06.037>
- Chow, T.T., He, W., Ji, J., 2007. An experimental study of façade-integrated photovoltaic/water-heating system. *Appl. Therm. Eng.* 27, 37–45. <https://doi.org/10.1016/j.applthermaleng.2006.05.015>
- Dermardiros, V., n.d. Energy Performance, Comfort and Lessons Learned from a Net-Zero Energy Library.
- Dominguez, A., Kleissl, J., Luvall, J.C., 2011. Effects of solar photovoltaic panels on roof heat transfer. *Sol. Energy* 85, 2244–2255. <https://doi.org/10.1016/j.solener.2011.06.010>
- Eicker, U., Demir, E., Gürlich, D., 2015. Strategies for cost efficient refurbishment and solar energy integration in European Case Study buildings. *Energy Build.* 102, 237–249. <https://doi.org/10.1016/j.enbuild.2015.05.032>
- Eiffert, P., 2003. Guidelines for the Economic Evaluation of Building Integrated Photovoltaic Power Systems 1–52. <https://doi.org/NREL/TP-550-31977>
- Eiffert, P., Kiss, G.J., 2000. Building-Integrated Photovoltaic Designs for Commercial and Institutional Structures A Sourcebook for Architects 92.
- Farkas, K., Grete, A., Andresen, I., 2009. ARCHITECTURAL INTEGRATION OF PHOTOVOLTAIC CELLS OVERVIEW OF MATERIALS AND PRODUCTS FROM AN

ARCHITECTURAL POINT OF VIEW.

- Goodrich, A., James, T., Woodhouse, M., 2012. Residential, Commercial, and Utility-Scale Photovoltaic (PV) System Prices in the United States: Current Drivers and Cost-Reduction Opportunities. <https://doi.org/10.2172/1036048>
- Hailu, G., Dash, P., Fung, A.S., 2015. Performance evaluation of an air source heat pump coupled with a building-integrated photovoltaic/thermal (BIPV/T) System under cold climatic conditions. *Energy Procedia* 78, 1913–1918. <https://doi.org/10.1016/j.egypro.2015.11.370>
- Hegazy, A.A., 2000. Comparative study of the performances of four photovoltaic / thermal solar air collectors. *Energy Convers. Manag.* 41.
- Hill, J., 2018. IHS Markit Predicts 2018 Global Solar Demand To Hit Record 113 Gigawatts | CleanTechnica [WWW Document]. Clean Tech. URL <https://cleantechnica.com/2018/04/09/ihs-markit-predicts-2018-global-solar-demand-to-hit-record-113-gigawatts/> (accessed 5.10.18).
- Hussain, F., Othman, M.Y.H., Yatim, B., Ruslan, H., Sopian, K., Anuar, Z., Khairuddin, S., 2015. An improved design of photovoltaic/thermal solar collector. *Sol. Energy* 122, 885–891. <https://doi.org/10.1016/j.solener.2015.10.008>
- Hutcheon, N.B., Handegord, G.O.P., 1995. Fluids in Motion, in: *Building Science for a Cold Climate*. National Research Council of Canada, pp. 127–158.
- ICC-ES, 2015. AC 365 Acceptance Criteria for Building-Integrated Photovoltaic (BIPV) Roof Covering Systems. 365.
- IEA, 2018. Task 15: Enabling Framework for the Acceleration of BIPV.
- IEA, 2017. Tracking Clean Energy Progress 2017.
- IEC, 2018. IEC - TC 82 Projects and Publications [WWW Document]. *Int. Electrotech. Comm.* URL https://www.iec.ch/dyn/www/f?p=103:23:15144662289726:::FSP_ORG_ID,FSP_LANG_ID:1276,25 (accessed 10.8.18).
- IEC, 2016a. IEC 61215 Crystalline silicon terrestrial photovoltaic (PV) modules - Design

- qualification and type approval. 61215.
- IEC, 2016b. IEC 61730 Photovoltaic (PV) module safety qualification. 61730.
- IEC, 2006. IEC 60904 Photovoltaic Devices Part 1: Measurement of Photovoltaic Current-Voltage Characteristics. 60904.
- IRENA, 2018. Renewable Power Generation Costs in 2017, International Renewable Energy Agency. https://doi.org/10.1007/SpringerReference_7300
- ISO/TC 180 - Solar energy [WWW Document], 1980. . Int. Organ. Stand. URL <https://www.iso.org/committee/54018.html> (accessed 10.8.18).
- ISO, 2018. ISO/TS 18178 - Glass in building -- Laminated solar photovoltaic glass for use in buildings.
- ISO, 2017. ISO 9806 - Solar energy - Solar thermal collectors - test methods.
- Jelle, B.P., Breivik, C., Drolsum Røkenes, H., 2012. Building integrated photovoltaic products: A state-of-the-art review and future research opportunities. *Sol. Energy Mater. Sol. Cells* 100, 69–96. <https://doi.org/10.1016/j.solmat.2011.12.016>
- Kaiser, A.S., Zamora, B., Mazo'n, R., Garcí'a, J.R., Vera, F., 2014. Experimental study of cooling BIPV modules by forced convection in the air channel. *Appl. Energy* 135, 88–97. <https://doi.org/10.1016/j.apenergy.2014.08.079>
- Kapsis, K., 2016. Modelling, Design and Experimental Study of Semi-Transparent Photovoltaic Windows for Commercial Building Applications.
- Kumar, R., Rosen, M.A., 2011. Performance evaluation of a double pass PV/T solar air heater with and without fins. *Appl. Therm. Eng.* 31, 1402–1410. <https://doi.org/10.1016/j.applthermaleng.2010.12.037>
- Lstiburek, J.W., 2017. Great Fire of London: Rain Screens, Claddings and Continuous Insulation. BSI Insight 1–10.
- Melrose, J., Perroy, R., Careas, S., 2015. Planning and Installation Photovoltaic Systems: A guide for installers, architects and engineers (2nd Edition), Statewide Agricultural Land Use Baseline 2015. <https://doi.org/10.1017/CBO9781107415324.004>

- Mike Carter, C.E.T. and Roman Stangl, C.E.T., 2016. Considerations for Building Design in Cold Climates | WBDG Whole Building Design Guide 1–6.
- National Disaster Management Authority, 2013. Seismic Vulnerability Assessment of Building Types in India.
- NFPA, 2012. NFPA 285 Standard Fire Test Method for Evaluation of Fire Propagation Characteristics of Exterior Non-Load-Bearing Wall Assemblies Containing Combustible Components.
- Owen, M.S., Kennedy, H.E. (Eds.), 2009. Fluid Flow, in: ASHRAE Handbook - Fundamentals. American Society of Heating, Refrigeration and Air-Conditioning Engineers, Inc., p. 3.1-3.14.
- Pe, M., 2012. Performance analysis and neural modelling of a greenhouse integrated photovoltaic system 16, 4675–4685. <https://doi.org/10.1016/j.rser.2012.04.002>
- Peng, C., Huang, Y., Wu, Z., 2011. Building-integrated photovoltaics (BIPV) in architectural design in China. *Energy Build.* 43, 3592–3598. <https://doi.org/10.1016/j.enbuild.2011.09.032>
- Peng, J., Lu, L., Yang, H., Han, J., 2013. Investigation on the annual thermal performance of a photovoltaic wall mounted on a multi-layer façade. *Appl. Energy* 112, 646–656. <https://doi.org/10.1016/j.apenergy.2012.12.026>
- Products: 2500 UT Unitwall System - Kawneer North America [WWW Document], n.d. URL https://www.kawneer.com/kawneer/north_america/en/products/2500_UT_unitwall.asp (accessed 10.1.18).
- Quesada, G., Rousse, D., Dutil, Y., Badache, M., Hallé, S., 2012. A comprehensive review of solar facades. Opaque solar facades. *Renew. Sustain. Energy Rev.* 16, 2820–2832. <https://doi.org/10.1016/j.rser.2012.01.078>
- Reinhart, C., 2014. The Source, in: Stein, R. (Ed.), *Daylighting Handbook I*. pp. 39–61.
- Roberts, S., Guariento, N., 2015. Building Integrated Photovoltaics: A Handbook. Statew. Agric. L. Use Baseline 2015 1. <https://doi.org/10.1017/CBO9781107415324.004>
- Rounis, E.D., Athienitis, A.K., Stathopoulos, T., 2016. Multiple-inlet Building Integrated

- Photovoltaic/Thermal system modelling under varying wind and temperature conditions. *Sol. Energy* 139, 157–170. <https://doi.org/10.1016/j.solener.2016.09.023>
- Rounis, E.D., Bigaila, E., Luk, P., Athienitis, A., Stathopoulos, T., 2015. Multiple-inlet BIPV/T modeling: Wind effects and fan induced suction. *Energy Procedia* 78, 1950–1955. <https://doi.org/10.1016/j.egypro.2015.11.379>
- Rounis, E.D., Ioannidis, Z., Dumoulin, R., Kruglov, O., Athienitis, A.K., Stathopoulos, T., 2017. Design and Performance Assessment of a Prefabricated BIPV/T Roof System Coupled with a Heat Pump, in: 12th International Conference on Solar Energy for Buildings and Industry. Rapperswil.
- Rounis, E.D., Kruglov, O., Ioannidis, Z., Athienitis, A.K., Stathopoulos, T., 2017. Experimental Investigation and Characterization of Building Integrated Photovoltaic / Thermal Envelope System With Thermal Enhancements for Roof, in: 33rd European Photovoltaic Solar Energy Conference and Exhibition. EU PVSEC, Brussels, pp. 2553–2559.
- Safa, A.A., Fung, A.S., Kumar, R., 2015. Comparative thermal performances of a ground source heat pump and a variable capacity air source heat pump systems for sustainable houses. *Appl. Therm. Eng.* 81, 279–287. <https://doi.org/10.1016/j.applthermaleng.2015.02.039>
- Scognamiglio, A., 2017. Building-Integrated Photovoltaics (BIPV) for Cost-Effective Energy-Efficient Retrofitting, *Cost-Effective Energy Efficient Building Retrofitting: Materials, Technologies, Optimization and Case Studies*. Elsevier Ltd. <https://doi.org/10.1016/B978-0-08-101128-7.00006-X>
- Scott, K., Zielnik, A., 2009. Developing Codes and Standards for BIPV and Integrated Systems.
- Shankleman, J., Warren, H., 2017. Solar Power Will Kill Coal Faster Than You Think [WWW Document]. Bloomberg. URL <https://www.bloomberg.com/news/articles/2017-06-15/solar-power-will-kill-coal-sooner-than-you-think> (accessed 5.10.18).
- Shukla, A.K., Sudhakar, K., Baredar, P., Mamat, R., 2018. Solar PV and BIPV system: Barrier, challenges and policy recommendation in India. *Renew. Sustain. Energy Rev.* 82, 3314–3322. <https://doi.org/10.1016/j.rser.2017.10.013>
- Skylight with Transparent Photovoltaic Glass [WWW Document], n.d. URL

<https://www.onyx-solar.com/product-services/photovoltaic-glass-solutions/pv-skylight>
(accessed 9.29.18).

Solar Panel CS6X-P - Canadian Solar [WWW Document], n.d. URL
<https://www.canadiansolar.com/solar-panels/dymond.html> (accessed 10.1.18).

The World Bank, 2017. India Transforms Market for Rooftop Solar. World Bank - Featur. Story.

The World Bank, n.d. Global Solar Atlas [WWW Document]. World Bank Gr. URL
<http://globalsolaratlas.info/?c=19.890723,81.452637,5&s=13.09,80.27&m=sg:ghi> (accessed
4.3.18).

Tian, W., Wang, Y., Ren, J., Zhu, L., 2007. Effect of urban climate on building integrated
photovoltaics performance. *Energy Convers. Manag.* 48, 1–8.
<https://doi.org/10.1016/j.enconman.2006.05.015>

Tiwari, A., Sodha, M.S., Chandra, A., Joshi, J.C., 2006. Performance evaluation of photovoltaic
thermal solar air collector for composite climate of India. *Sol. Energy Mater. Sol. Cells* 90,
175–189. <https://doi.org/10.1016/j.solmat.2005.03.002>

Tonui, J.K., Tripanagnostopoulos, Y., 2006. Improved PV/T solar collectors with heat extraction
by forced or natural air circulation. *Int. J. Hydrogen Energy* 31, 2137–2146.
<https://doi.org/10.1016/j.ijhydene.2006.02.009>

Un, S., 2017. Rooftop solar is the fastest-growing segment in India's renewables market. *Quartz*.

Unicel Architectural | Manufacturers of aluminum and glazing products [WWW Document], n.d.
URL <http://www.unicelarchitectural.com/en/index.html> (accessed 10.1.18).

University, C., n.d. Centre for Zero Energy Building Studies [WWW Document]. Concordia Univ.
URL <https://www.concordia.ca/research/zero-energy-building/facilities/labs-equipment.html#solar> (accessed 10.6.18).

Vats, K., Tomar, V., Tiwari, G.N., 2012. Effect of packing factor on the performance of a building
integrated semitransparent photovoltaic thermal (BISPVT) system with air duct. *Energy
Build.* 53, 159–165. <https://doi.org/10.1016/j.enbuild.2012.07.004>

Wang, Y., Ke, S., Liu, F., Li, J., Pei, G., 2017. Performance of a building-integrated

- photovoltaic/thermal system under frame shadows. *Energy Build.* 134, 71–79.
<https://doi.org/10.1016/j.enbuild.2016.10.012>
- Weller, B., Hemmerle, C., Jakubetz, S., Unnewehr, S., 2010. Detail Practice: Photovoltaics.
<https://doi.org/10.11129/detail.9783034615709>
- Yang, R.J., 2015. Overcoming technical barriers and risks in the application of building integrated photovoltaics (BIPV): Hardware and software strategies. *Autom. Constr.* 51, 92–102.
<https://doi.org/10.1016/j.autcon.2014.12.005>
- Yang, T., Athienitis, A.K., 2016a. A review of research and developments of building-integrated photovoltaic/thermal (BIPV/T) systems. *Renew. Sustain. Energy Rev.* 66, 886–912.
<https://doi.org/10.1016/j.rser.2016.07.011>
- Yang, T., Athienitis, A.K., 2016b. A review of research and developments of building-integrated photovoltaic/thermal (BIPV/T) systems. *Renew. Sustain. Energy Rev.* 66, 886–912.
<https://doi.org/10.1016/j.rser.2016.07.011>
- Yang, T., Athienitis, A.K., 2015. Experimental investigation of a two-inlet air-based building integrated photovoltaic/thermal (BIPV/T) system. *Appl. Energy* 159, 70–79.
<https://doi.org/10.1016/j.apenergy.2015.08.048>
- Yang, T., Athienitis, A.K., 2014a. A study of design options for a building integrated photovoltaic/thermal (BIPV/T) system with glazed air collector and multiple inlets. *Sol. Energy* 104, 82–92. <https://doi.org/10.1016/j.solener.2014.01.049>
- Yang, T., Athienitis, A.K., 2014b. A study of design options for a building integrated photovoltaic/thermal (BIPV/T) system with glazed air collector and multiple inlets. *Sol. Energy* 104, 82–92. <https://doi.org/10.1016/j.solener.2014.01.049>
- Yang, T., Athienitis, A.K., 2012. Investigation of performance enhancement of a building integrated photovoltaic thermal system, in: *The Canadian Conference on Building Simulation*. pp. 122–135.
- Yang, Y., 2015. Why Millions of Chinese-Made Solar Panels Sat Unused In Southern California Warehouses for Years [WWW Document]. URL <https://psmag.com/environment/why-millions-of-chinese-made-solar-panels-sat-unused-in-southern-california-warehouses-for->

years (accessed 6.20.18).

- Yano, A., Kadowaki, M., Furue, A., Tamaki, N., Tanaka, T., Hiraki, E., Kato, Y., Ishizu, F., Noda, S., 2010. Shading and electrical features of a photovoltaic array mounted inside the roof of an east e west oriented greenhouse. *Biosyst. Eng.* 106, 367–377. <https://doi.org/10.1016/j.biosystemseng.2010.04.007>
- Zanetti, I., Bonomo, P., Frontini, F., Saretta, E., Donker, M. van den, Vossen, F., Folkerts, W., 2017. BIPV- Product overview for solar building skins- Status Report 2017 76.
- Zhang, X., Shen, J., Lu, Y., He, W., Xu, P., Zhao, X., Qiu, Z., Zhu, Z., Zhou, J., Dong, X., 2015. Active Solar Thermal Facades (ASTFs): From concept, application to research questions. *Renew. Sustain. Energy Rev.* 50, 32–63. <https://doi.org/10.1016/j.rser.2015.04.108>
- Zogou, O., Stapountzis, H., 2012. Flow and heat transfer inside a PV/T collector for building application. *Appl. Energy* 91, 103–115. <https://doi.org/10.1016/j.apenergy.2011.09.019>

Appendix A: Electrical, Solar Thermal and Building Standards

* Indicates that the standard is referenced in EN 50583.

**Indicates that the standard is referenced in AC 365.

Table A.1: PV/Electrical standards by issuing committee

Issuing Committee	Name	Description
IEC	IEC 61215 (EN 61215)*	Crystalline silicon terrestrial photovoltaic (PV) modules: Design qualification and type approval
	IEC 61277	Terrestrial Photovoltaic (PV) Power Generating Systems
	IEC 61345	UV Test for Photovoltaic (PV) Modules
	IEC 61701	Salt mist corrosion testing of photovoltaic (PV) modules
	IEC 62759	Photovoltaic (PV) modules – Transportation testing
	IEC 62782	Photovoltaic (PV) modules – Cyclic (dynamic) mechanical load testing
	IEC 62716	Photovoltaic (PV) modules – Ammonia corrosion testing
	IEC 62804	Photovoltaic (PV) modules – Test methods for the detection of potential-induced degradation
	IEC 62109	Safety of power converters for use in PV power systems
	IEC 61730*	Standard for PV module safety and mechanical resistance
	IEC 61853 (1, 2, 3, 4)	Photovoltaic (PV) module performance testing and energy rating
	IEC 62116	Test of anti-islanding protections
	IEC 60904	Photovoltaic Devices Part 1: Measurement of Photovoltaic Current-Voltage Characteristics
	IEC 62108	Concentrator PV modules and assemblies
IEC Installation Codes	IEC 62234	Safety Guidelines for Grid Connection PV Systems Mounted on Buildings
	IEC 60364-7-712	Electrical Installations, amended to include PV install
	IEC 61727	Characteristics of the utility interface
	IEC 61724	PV system performance monitoring
UL	UL 1703**	Flat plate PV modules and panels *Note: updated standard published in Oct. 2014 treats PV modules and roofing materials as integrated building elements, change is expected to be in the newer versions of the IBC

	UL 1741	Inverters, Converters, Controllers and Interconnection System Equipment for Use with Distributed Energy Resources
	UL 4703	Standard for Photovoltaic Wire
<i>EN</i>	EN 50380*	Datasheet and nameplate information for PV modules
	EN 61082*	Preparation of documents used in electrotechnology
	EN 62446*	Grid connected PV systems
<i>CSA</i>	CSA 107.1	Power conversion equipment (Sections added to “General Use Power Supplies” for PV inverters)
<i>Inverter standard</i>		
<i>IEEE Monitoring performance</i>	IEEE P 1547.3	Standard for Interconnecting Distributed Resources with Electric Power Systems

Table A.2: Solar thermal standards by issuing committee

Issuing Committee	Name	Description
<i>ISO</i>	ISO 9806	Solar thermal collectors – test methods
	ISO 9553	Methods of testing preformed rubber seals and sealing compounds used in collectors
	ISO 9459	Solar heating – Domestic water heating systems

Table A.3: Building standards by issuing committee

Issuing Committee	Name	Description
<i>EN</i>	EN 12179*	Curtain walling – Resistance to wind load – test method
	EN 13830*	Curtain walling – product standard
	EN 13501-1*	Fire safety
	EN 13116*	Curtain walling – resistance to wind load
	EN 15601*	Rain penetration testing
	EN 13022*	Glass in Building: Structural Sealant Glazing
	EN 12600*	Glass in Building: Pendulum test
	EN 12758*	Protection against noise
	EN 410*	Glass in Building: Determination of luminous and solar characteristics of glazing

EN 356	Glass in Building: Security glazing – Testing and classification of resistance against manual attack
EN 673*	Glass in Building: Determination of thermal transmittance (U Value) – Calculation method
EN 571 (1, 2, 5, 8, 9)	Glass in Building: Basic soda lime silicate glass products
EN 1748 (1, 2)	Glass in Building: Special basic products
EN 13024 (1, 2)	Glass in Building: Thermally toughened borosilicate safety glass
EN 1279*	Glass in Building: Insulating Glass Units
EN 1288 (1, 2, 3, 4, 5)	Glass in Building: Determination of the bending strength of glass
EN 12488*	Glass in Building: Glazing recommendations – Assembly principles for vertical and sloping glazing
EN 12578*	Glass in Building: Glazing and airborne sound insulation
EN 12600*	Glass in Building: Pendulum test – Impact test method and classification for flat glass
EN 16002*	Flexible sheets for waterproofing – Determination of the resistance to wind load of mechanically fastened flexible sheets for roof waterproofing
EN 13956*	Flexible sheets for waterproofing – plastic and rubber sheets for roof waterproofing
EN 14449*	Glass in Building: Laminated glass and laminated safety glass
EN 14782*	Self-supporting metal sheet for roofing, external cladding and internal lining. Product specification and requirements
EN 14783*	Fully supported metal sheet and strip for roofing, external cladding and internal lining. Product specification and requirements
EN 12519*	Windows and pedestrian doors - Terminology
EN 15804*	Sustainability of construction works - Environmental product declarations
EN 15978*	Sustainability of construction works – Assessment of environmental performance of buildings
EN 13363*	Solar protection devices combined with glazing – Calculation of solar and light transmittance
ISO	ISO 3585 Borosilicate glass 3.3 – Properties

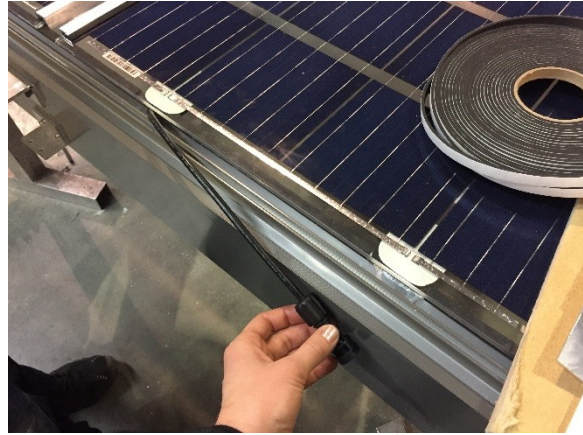
	ISO 52016	Energy performance in buildings – Energy needs for heating and cooling, internal temperatures and sensible and latent heat loads
	ISO 12631*	Thermal performance of curtain walling – Calculation of thermal transmittance
	ISO 16293	Glass in building: Basic soda lime silicate glass
	ISO 12543 *	Glass in building: Laminated glass and laminated safety glass (1,2,3,4,5,6)
AAMA	AAMA 501	Test methods for exterior walls
	AAMA 501.4	Recommended static test method for evaluating curtain wall and storefront systems subjected to seismic and wind induced interstory drifts
	AAMA 501.6	Recommended dynamic method test method for determining a seismic drift causing glass fallout from a wall system
	AAMA 502	Voluntary specification for field testing of windows and sliding glass doors
	AAMA 503	Voluntary specification for field testing of metal storefronts, curtain walls and sloped glazing systems
	AAMA 850	Fenestration Sealants Guide Manual
	AAMA 1503	Voluntary test method for thermal transmittance and condensation resistance of windows, doors and glazed wall sections
	AAMA 1504	Voluntary standard for thermal performance of windows, doors and glazed wall sections
	AAMA CW-11	Design wind loads and boundary layer wind tunnel testing
	AAMA CW-RS-1	The rainscreen principle and pressure equalized wall design
ASTM	ASTM C1172	Standard Specification for Laminated Architectural Flat Glass
	ASTM D3161**	Test method for wind resistance of asphalt shingles
	ASTM D3746**	Test method for impact resistance of bituminous roofing systems
	ASTM E84	Test method for surface burning characteristics of building materials
	ASTM E108**	Test methods for fire tests of roof coverings
	ASTM E283	Standard test method for determining rate of air leakage through exterior windows, curtain walls, and doors under specified pressure differences across the specimen

	ASTM E330	Standard test method for structural performance of exterior windows, curtain walls, and doors by uniform static air pressure difference
	ASTM E331	Standard test method for water penetration of exterior windows, skylights, doors and curtain walls by uniform static air pressure difference
	ASTM E547	Standard test method for water penetration of exterior windows, skylights, doors and curtain walls by cyclic static air pressure difference
	ASTM E1105	Standard test method for water penetration of installed exterior windows, curtain walls, and doors by uniform or cyclic static air pressure difference
	ASTM E1233	Standard test method for structural performance of exterior windows, curtain walls and doors by cyclic static air pressure differential
	ASTM E1887	Standard test method for performance of exterior windows, curtain walls, doors and storm shutters impacted by missiles and exposed to cycle pressure differentials
	ASTM E1996	Standard specification for performance of exterior windows, curtain walls, doors and storm shutters impacted by windborne debris in hurricanes
	ASTM E2010	Standard test method for positive pressure fire test for window assemblies
	ASTM E2188	Standard test method for insulating glass unit performance
	ASTM E2190	Standard specification for insulating glass unit performance and evaluation
	ASTM F1233	Standard Test Method for Security Glazing Materials and Systems
NFRC	NFRC 100	Procedure for determining fenestration product U-factors
	NFRC 400	Procedure for determining fenestration product air leakage
	NFRC 500	Procedure for determining fenestration product condensation resistance values
NFPA	NFPA 285	Standard fire test method for evaluation of fire propagation characteristics of exterior non-load-bearing wall assemblies containing combustible components
CAN/CSA	CAN/CSA A440	Fenestration energy performance
UL	UL 790**	Standard test methods for fire test of roof coverage
	UL 580**	Test for uplift resistance of roof assemblies
	UL 1897**	Uplift tests for roof covering systems

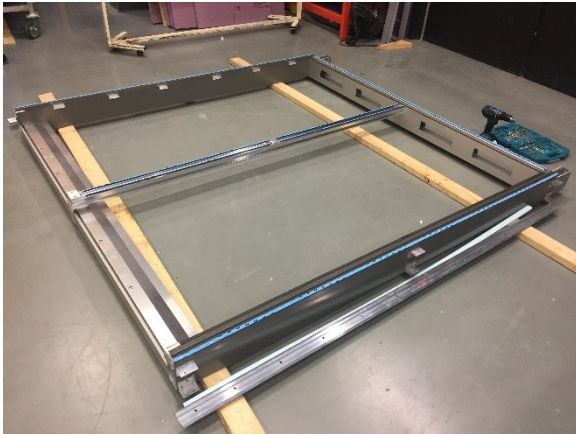
Appendix B: Photographs of Prototype Construction



Framing assembly at Unicel shop



Wiring from junction-box exiting mullion channel



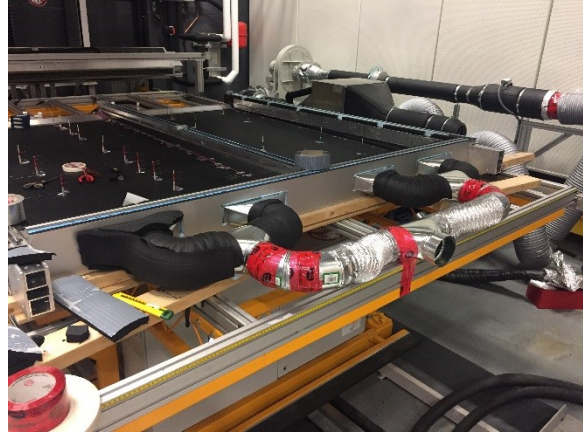
Framing without insulation PV modules



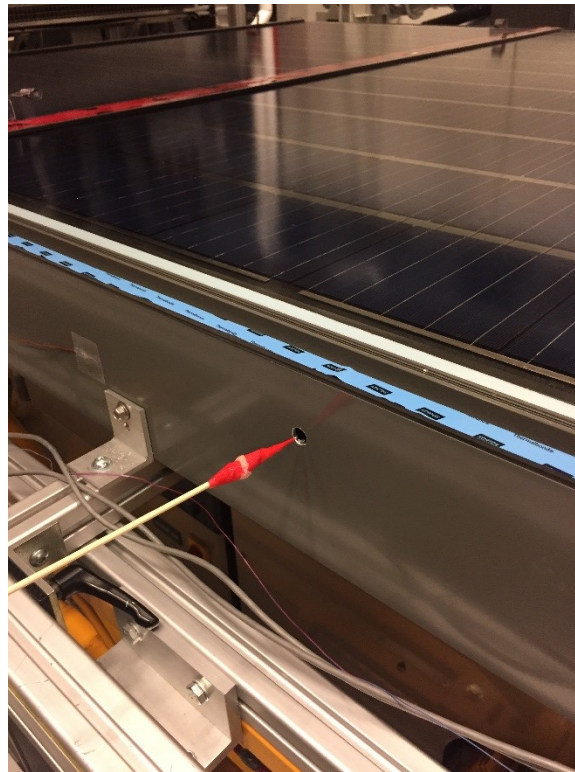
Prototype without insulation and backpan, seen from interior side



Thermocouples installed over insulation and absorber in channel



Assembly of the manifold



Opening made in frame for anemometer measurements

Appendix C: Product Specification Sheets

Canadian Solar Module Specifications:









DOUBLE-GLASS MODULE

DIAMOND CS6X-310/315/320P-FG

Canadian Solar's Diamond CS6X-P-FG module is a 72 cell double-glass module. By replacing the traditional polymer backsheet with heat-strengthened glass, the Diamond module has a lower annual power degradation than a traditional module and better protection against the elements, making it more reliable and durable during its lifetime.

KEY FEATURES

-  **Anti-PID module**
 - Anti-PID cell technology
 - Anti-PID encapsulation technology
-  **Lower annual power degradation & more system power yield over lifetime**
 - First year annual degradation 2.5%, each subsequent year 0.5%
 - 85.5% power output at year 25
 - 83% power output at year 30
-  **Better fire protecting performance**
 - Fire class A certified according to fire test IEC 61730-2 / MST 23
 - Certified for fire type 3 according to UL 1703
-  **Designed for high voltage systems of up to 1500 V_{DC}, saving BoS costs**
-  **Sea/waterside PV system installation**
 - Glass backside blocks moisture permeability
 - No module-level corrosion
-  **5400 Pa snow load, 2400 Pa wind load**

 **CanadianSolar**



MANAGEMENT SYSTEM CERTIFICATES*

ISO 9001:2008 / Quality management system
ISO/TS 16949:2009 / The automotive industry quality management system
ISO 14001:2004 / Standards for environmental management system
OHSAS 18001:2007 / International standards for occupational health & safety

PRODUCT CERTIFICATES*

IEC 61215 / IEC 61730: VDE / CE
UL 1703: CSA / PV CYCLE (EU)



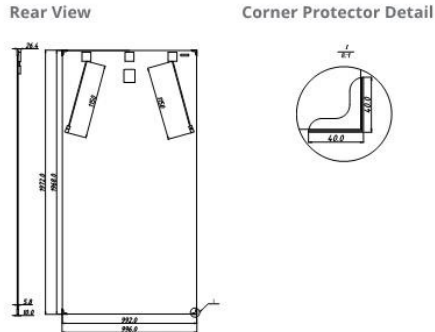
* As there are different certification requirements in different markets, please contact your local Canadian Solar sales representative for the specific certificates applicable to the products in the region in which the products are to be used.

CANADIAN SOLAR INC. is committed to providing high quality solar products, solar system solutions and services to customers around the world. As a leading manufacturer of solar modules and PV project developer with about 10 GW of premium quality modules deployed around the world since 2001, Canadian Solar Inc. (NASDAQ: CSIQ) is one of the most bankable solar companies worldwide.

CANADIAN SOLAR (USA) INC.

2420 Camino Ramon, Suite 125 San Ramon, CA, USA 94583-4385, www.canadiansolar.com, sales.us@canadiansolar.com

MODULE / ENGINEERING DRAWING (mm)



ELECTRICAL DATA / STC*

Electrical Data CS6X	310P-FG	315P-FG	320P-FG
Nominal Max. Power (Pmax)	310 W	315 W	320 W
Opt. Operating Voltage (Vmp)	36.4 V	36.6 V	36.8 V
Opt. Operating Current (Imp)	8.52 A	8.61 A	8.69 A
Open Circuit Voltage (Voc)	44.9 V	45.1 V	45.3 V
Short Circuit Current (Isc)	9.08 A	9.18 A	9.26 A
Module Efficiency	15.88%	16.14%	16.39%
Operating Temperature	-40°C ~ +85°C		
Max. System Voltage	1500 (IEC) or 1000 V (UL)		
Module Fire Performance	Type 3 (UL 1703) or CLASS A (IEC 61730)		
Max. Series Fuse Rating	15 A		
Application Classification	Class A		
Power Tolerance	0 ~ + 5 W		

* Under Standard Test Conditions (STC) of irradiance of 1000 W/m², spectrum AM 1.5 and cell temperature of 25°C.

ELECTRICAL DATA / NOCT*

Electrical Data CS6X	310P-FG	315P-FG	320P-FG
Nominal Max. Power (Pmax)	225 W	228 W	232 W
Opt. Operating Voltage (Vmp)	33.2 V	33.4 V	33.6 V
Opt. Operating Current (Imp)	6.77 A	6.84 A	6.91 A
Open Circuit Voltage (Voc)	41.3 V	41.5 V	41.6 V
Short Circuit Current (Isc)	7.36 A	7.44 A	7.50 A

* Under Nominal Operating Cell Temperature (NOCT), irradiance of 800 W/m², spectrum AM 1.5, ambient temperature 20°C, wind speed 1 m/s.

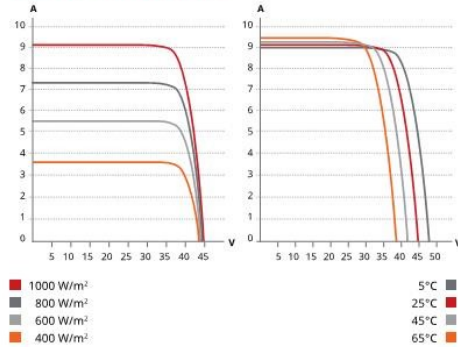
PERFORMANCE AT LOW IRRADIANCE

Industry leading performance at low irradiance, average 96.0% relative efficiency from an irradiance of 1000 W/m² to 200 W/m² (AM 1.5, 25°C).

The specification and key features described in this datasheet may deviate slightly and are not guaranteed. Due to on-going innovation, research and product enhancement, Canadian Solar Inc. reserves the right to make any adjustment to the information described herein at any time without notice. Please always obtain the most recent version of the datasheet which shall be duly incorporated into the binding contract made by the parties governing all transactions related to the purchase and sale of the products described herein.

Caution: For professional use only. The installation and handling of PV modules requires professional skills and should only be performed by qualified professionals. Please read the safety and installation instructions before using the modules.

CS6X-310P-FG / I-V CURVES



MODULE / MECHANICAL DATA

Specification	Data
Cell Type	Poly-crystalline, 6 inch
Cell Arrangement	72 (6×12)
Dimensions	1968×992×5.8mm (77.5×39.1×0.23 in) without J-Box and corner protector
(Incl. corner protector)	1972×996×10 mm (77.6×39.2×0.39 in) without J-Box
Weight	27.5 kg (60.6 lbs)
Front Cover	2.5 mm heat strengthened glass
Back Glass	2.5 mm heat strengthened glass
Frame	Frameless
J-Box	Split J-Box, IP67, 3 diodes
Cable	4 mm ² (IEC) or 4 mm ² & 12 AWG 1000 V (UL)
Cable Length	1150 mm (45.3 in), 500 mm (19.7 in) (+) and 350 mm (13.8 in) (-) is optional for portrait installation*
Connectors	Amphenol H4 UTX (IEC), Renhe 05-6 (UL)
Standard Packaging	30 pieces
Module Pieces per Container	660 pieces (40' HQ)

* The application of this short length cable can only be used in portrait installation (clamping mounting method) systems in which the distance between modules should be less than or equal to 50 mm. In the event the distance between the PV modules to be installed is more than 50 mm, please make sure to consult our technical team for evaluation and advice.

TEMPERATURE CHARACTERISTICS

Specification	Data
Temperature Coefficient (Pmax)	-0.41% / °C
Temperature Coefficient (Voc)	-0.31% / °C
Temperature Coefficient (Isc)	0.053% / °C
Nominal Operating Cell Temperature	45±2°C

PARTNER SECTION



Insulation specification sheet:



STYROFOAM™ Brand SM Extruded Polystyrene Foam Insulation

1. PRODUCT NAME

STYROFOAM™ Brand SM Extruded Polystyrene Foam Insulation

2. MANUFACTURER

Dow Chemical Canada ULC
Dow Building Solutions
450-1st St. SW, Suite 2100
Calgary, AB T2P 5H1
1-866-583-BLUE (2583) (English)
1-800-363-6210 (French)

dowbuildingsolutions.com

3. PRODUCT DESCRIPTION

STYROFOAM™ Brand SM Extruded Polystyrene Foam Insulation is a multi-purpose extruded polystyrene board that helps to meet the needs of the commercial and residential foundation and slab market. The closed-cell structure of STYROFOAM™ Brand SM Insulation resists water absorption, enabling it to retain a high R-value (RSI)* over time – a necessary property in below-grade residential foundation applications.

STYROFOAM™ Brand SM Insulation helps to protect foundation dampproofing and waterproofing, especially during backfilling. It also provides a secondary barrier against groundwater leakage. With STYROFOAM™ Brand SM Insulation, the freeze-thaw cycling of the foundation wall is minimized, reducing the possibility of cracking. And a warmer foundation wall reduces the potential for condensation and adds to the thermal mass of the building.

Basic Use

STYROFOAM™ Brand SM Insulation can be used against almost any commercial or residential foundation wall in above- and below-grade applications.

*R means resistance to heat flow. The higher the R-value or RSI, the greater the insulating power.

4. TECHNICAL DATA

Applicable Standards

ASTM International

- ASTM C518 – Standard Test Method for Steady-State Thermal Transmission Properties by wMeans of the Heat Flow Meter Apparatus
- ASTM D1621 – Standard Test Method for Compressive Properties of Rigid Cellular Plastics
- ASTM E96 – Standard Test Methods for Water Vapour Transmission of Materials

- ASTM D696 – Standard Test Method for Coefficient of Linear Thermal Expansion of Plastics Between -30° and 30°C with a Vitreous Silica Dilatometer
- ASTM D2842 – Standard Test Method for Water Absorption of Rigid Cellular Plastics
- CAN/ULC S701 Type 4
- CCMC 04888-L

Physical Properties

STYROFOAM™ Brand SM Insulation exhibits physical properties as indicated in Table 2 when tested as represented.

TABLE 1: Sizes, R-values and Edge Treatments for STYROFOAM™ Brand SM Extruded Polystyrene Foam Insulation

Standard Size (Imperial) ¹			
Board Thickness ⁽¹⁾ , Inches (mm)	R-Value	Board Size (Inches)	Edge Treatment
1.0	5.0	24 × 96	Butt Edge & Shiplap
1.5	7.5	24 × 96	Butt Edge & Shiplap
2.0**	10.0	24 × 96	Butt Edge & Shiplap
2.4	12.0	24 × 96	Shiplap
2.5	12.5	24 × 96	Shiplap
3.0	15.0	24 × 96	Butt Edge & Shiplap
4.0	20.0	24 × 96	Butt Edge & Shiplap
Standard Size (Metric) ¹			
Board Thickness ⁽¹⁾ , Millimeters	RSI	Board Size (mm)	Edge Treatment
50	1.73	600 × 2400	Butt Edge & Shiplap
75	2.61	600 × 2400	Butt Edge & Shiplap

(1) Not all product sizes are available in all regions.

** Also available in 4x8 Shiplap

Additional sizes may be stocked on a regional basis. Contact your local Dow seller for additional information.

TABLE 2: Physical Properties of STYROFOAM™ Brand SM Extruded Polystyrene Foam Insulation

Property And Test Method	Value
Thermal R resistance per inch (25 mm), ASTM C518 @ 75°F (24°C) mean temp., ft ² •h•°F/Btu (m ² •°C/W) min., R -value (RSI)	5.0 (.88)
Compressive Strength ⁽¹⁾ , ASTM D1621, psi (kPa), min.	30 (207)
Water Absorption, ASTM D2842, % by volume, max.	0.7
Water Absorption, ASTM C272, % by volume, max	0.3
Water Vapour Permeance, ASTM E96, perm (ng/Pa•s•m ²), max. ⁽²⁾	1.5 (90)
Maximum Use Temperature, °F (°C)	165 (74)
Coefficient of Linear Thermal Expansion, ASTM D696, in/in•°F (mm/m•°C)	3.5 × 10 ⁻⁵ (6.3 × 10 ⁻²)

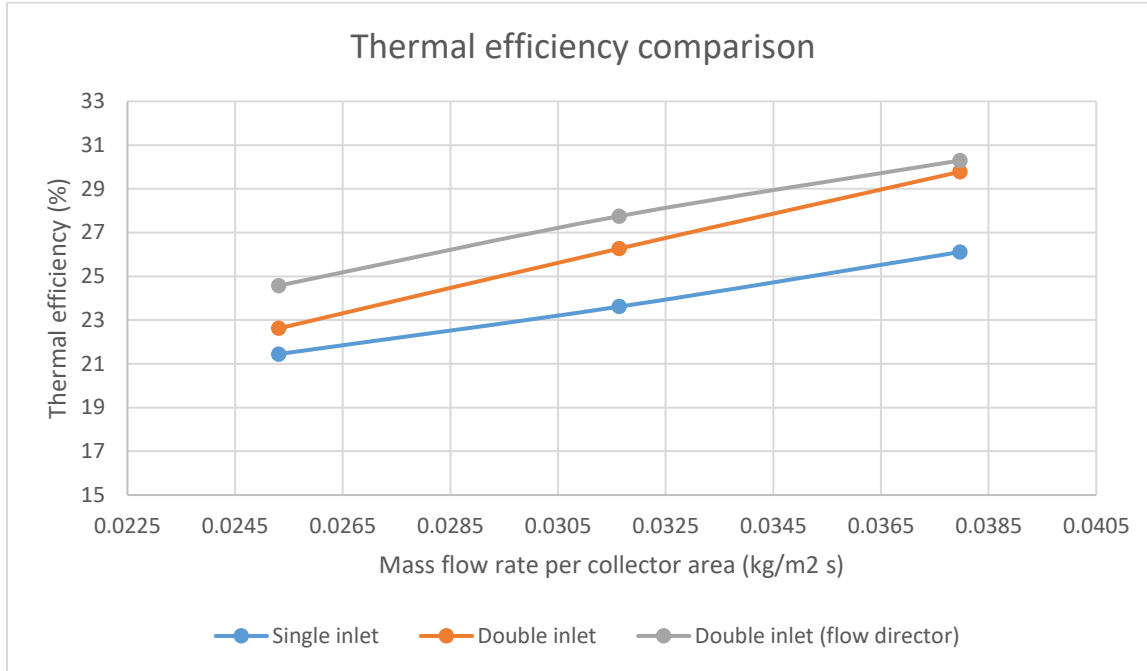
(1) Vertical compressive strength is measured at 10 percent deformation or at yield, whichever occurs first.

(2) Based on 1" (25 mm) thickness.

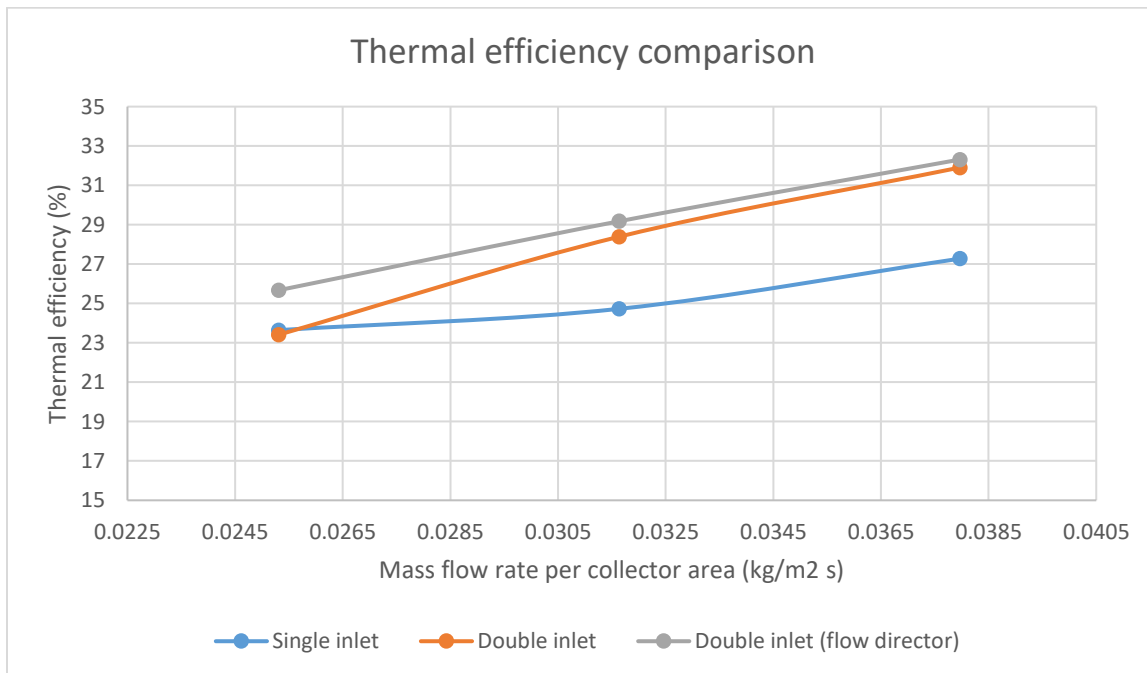
PRODUCT INFORMATION | Canada | COMMERCIAL/RESIDENTIAL

Appendix D: Results of Experimental Work

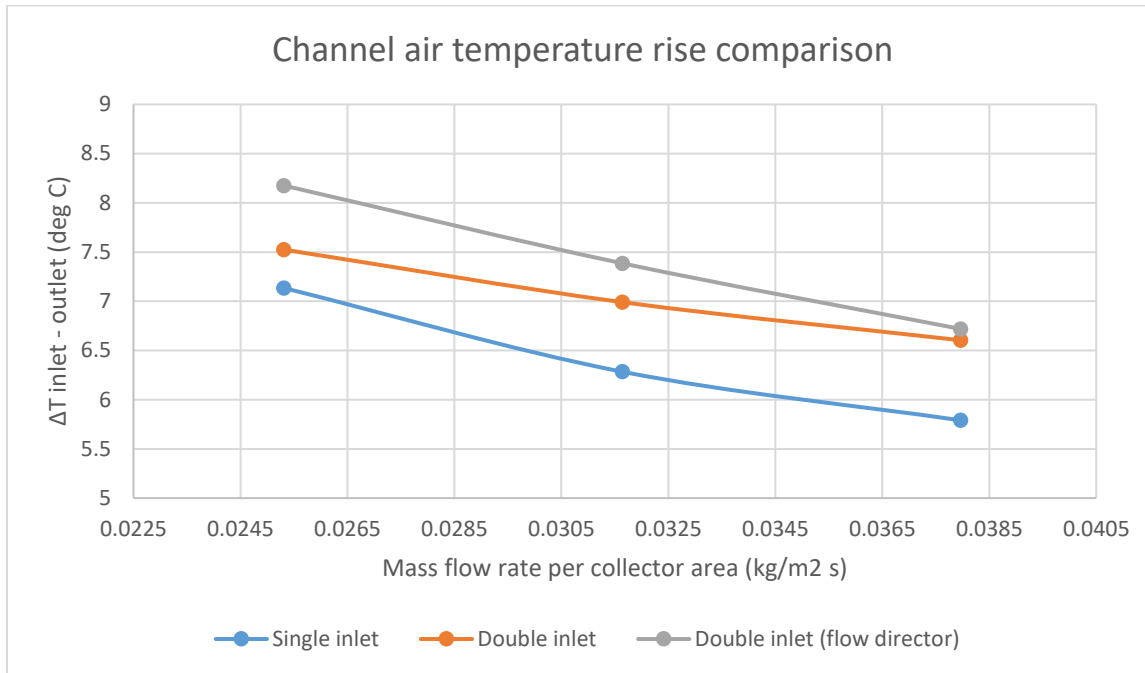
Thermal efficiency results - 72-cell configuration:



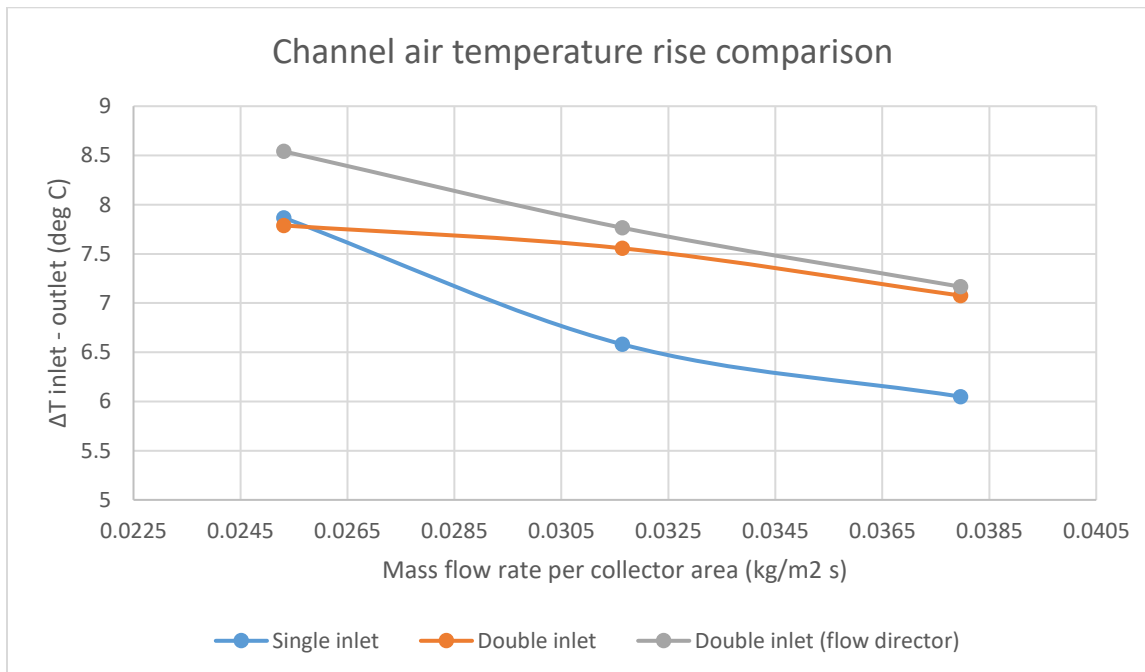
Thermal efficiency results - 66-cell configuration:



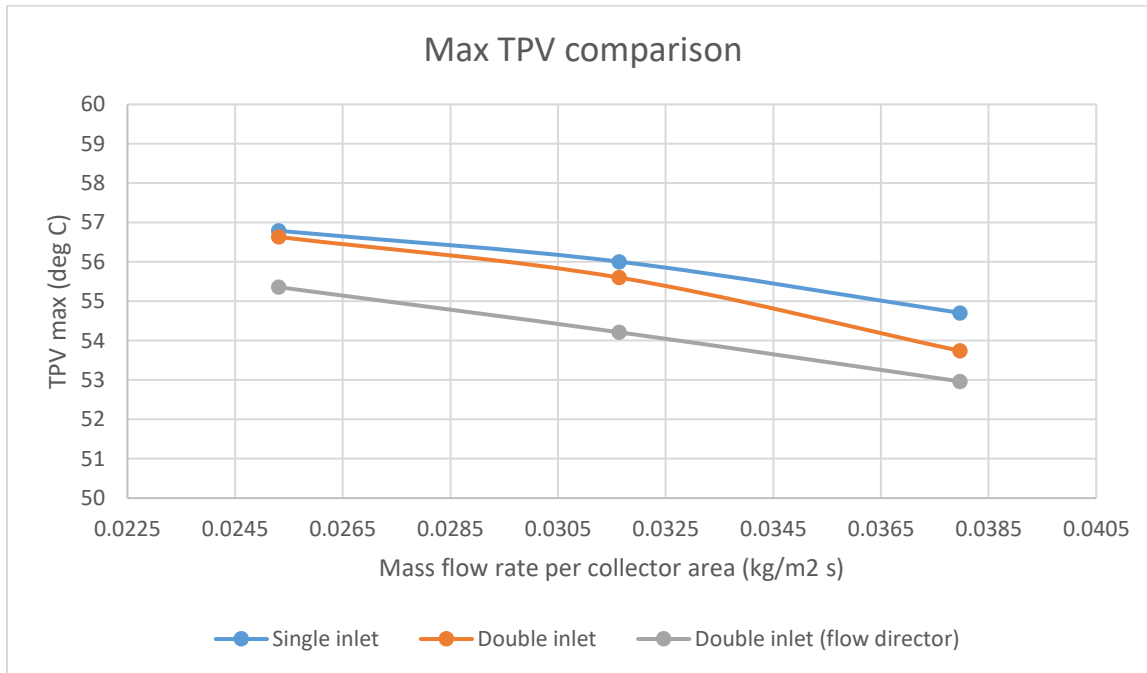
Air temperatures in channel - 72-cell configuration:



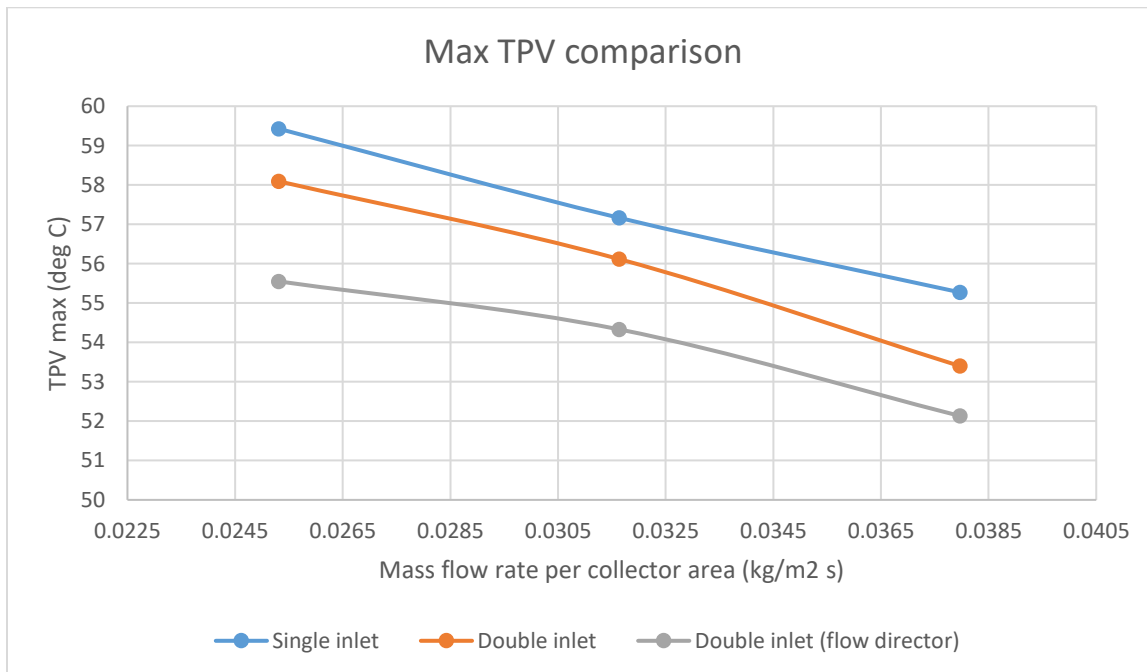
Air temperatures in channel - 66-cell configuration:



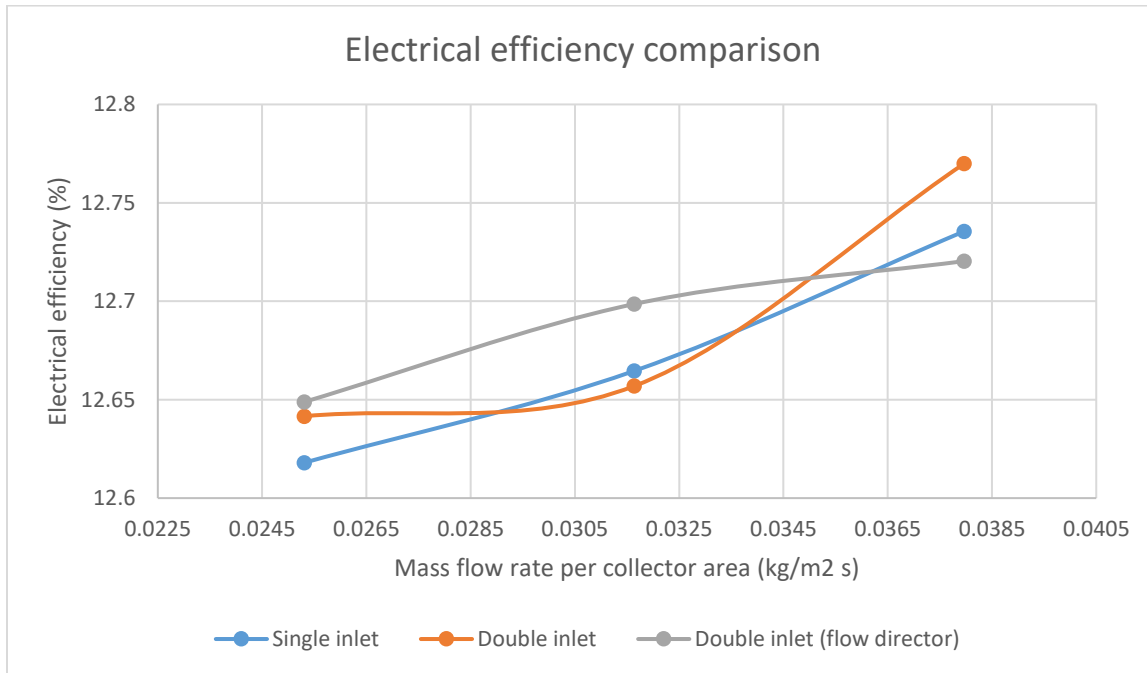
Maximum PV temperatures - 72-cell configuration:



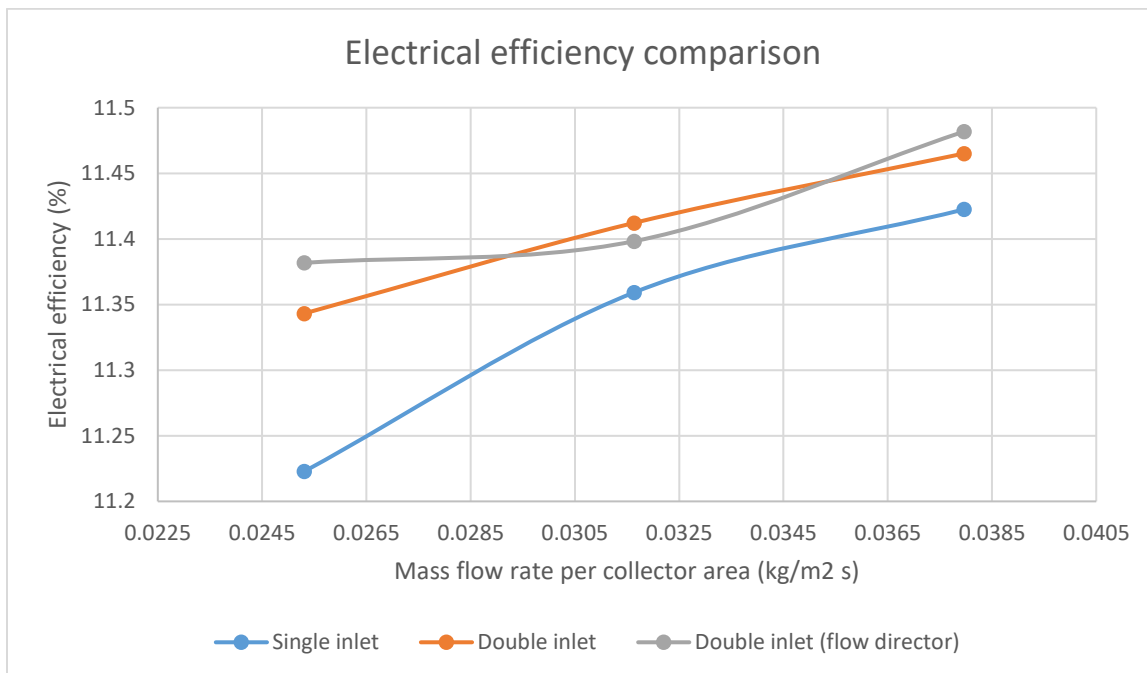
Maximum PV temperatures - 66-cell configuration:



Electrical efficiency results - 72-cell configuration:



Electrical efficiency results - 66-cell configuration:



Appendix E: Measurement Uncertainties

The uncertainty for electrical efficiency is affected by the voltage and current measurements, and is calculated using

$$\Delta\eta_{el} = \sqrt{\left(\frac{I_U}{G \cdot A}\right)^2 \cdot (V_U \cdot 0.005)^2 + \left(\frac{V_U}{G \cdot A}\right)^2 \cdot (I_U \cdot 0.005)^2 + \left(\frac{I_L}{G \cdot A}\right)^2 \cdot (V_L \cdot 0.005)^2 + \left(\frac{V_L}{G \cdot A}\right)^2 \cdot (I_L \cdot 0.005)^2 + \left(\frac{-V_U \cdot I_U - V_L \cdot I_L}{A \cdot G^2}\right)^2 \cdot (G \cdot 0.05)^2}$$

The uncertainty for thermal efficiency is affected by the air mass flow rate, inlet and outlet air temperatures. This uncertainty is calculated using

$$\Delta\eta_{th} = \sqrt{\left(\frac{C_p(T_o - T_i)}{G \cdot A}\right)^2 \cdot (\dot{m} \cdot 0.02)^2 + \left(\frac{\dot{m} \cdot C_p}{G \cdot A}\right)^2 \cdot (T_o \cdot 0.06)^2 + \left(\frac{-\dot{m} \cdot C_p}{G \cdot A}\right)^2 \cdot (T_i \cdot 0.5)^2 + \left(\frac{-\dot{m} \cdot C_p(T_o - T_i)}{G \cdot A}\right)^2 \cdot (G \cdot 0.05)^2}$$

The table below shows uncertainty values for the different module configurations and varying flow rates. The highest electrical efficiency uncertainty is 0.64% and the highest thermal efficiency uncertainty is 2.86%.

66-cell				72-cell			
	Air flow rate	η_{el}	η_{th}		Air flow rate	η_{el}	η_{th}
Single	400	0.56%	1.98%	Single	400	0.63%	1.90%
	500	0.57%	2.31%		500	0.64%	2.28%
	600	0.57%	2.71%		600	0.64%	2.67%
Double	400	0.57%	1.97%	Double	400	0.64%	1.94%
	500	0.57%	2.43%		500	0.64%	2.36%
	600	0.58%	2.85%		600	0.64%	2.78%
Double w/ director	400	0.57%	2.05%	Double w/ director	400	0.64%	2.01%
	500	0.57%	2.46%		500	0.64%	2.41%
	600	0.50%	2.86%		600	0.64%	2.80%